

**THE OPPOSING EFFECTS OF HDL METABOLISM
ON PROSTATE CANCER**

by

CYNTHIA ALICIA TRAUGHBER

Submitted in partial fulfillment of the
requirements for the degree of Doctor of Philosophy

Dissertation Advisor: Jonathan D. Smith, Ph.D.

Department of Molecular Medicine

CASE WESTERN RESERVE UNIVERSITY

AUGUST 2020

CASE WESTERN RESERVE UNIVERSITY
SCHOOL OF GRADUATE STUDIES

We hereby approve the dissertation of

Cynthia Alicia Traugher

Candidate for the degree of **Doctor of Philosophy**

Angela Ting, PhD
Committee Chair

Jonathan D. Smith, PhD
Committee Member

W.H. Wilson Tang, MD
Committee Member

J. Mark Brown, PhD
Committee Member

Nima Sharifi, MD
Committee Member

Date of Defense 29 April 2020

*We also certify that written approval has been obtained for any
proprietary material contained therein

Dedication

I dedicate this to my mama,

Mrs. Betty Jo "Jody" Brooks.

Thank you for ALWAYS being my biggest supporter throughout my entire life.

I'm confident that any success I've had would not have been possible

without your unconditional love and continually prayers for me,

Thanks for always loving me through all the mistakes that I've made,

the hardships I've put myself through, and every obstacle that I've had to overcome.

YOU ARE MY ROCK AND MY HERO!

Table of Contents

Lists of Tables	iii
List of Figures.....	iv
Acknowledgements.....	1
Abstract.....	3
I. Introduction	5
I.1 Prostate Cancer.....	5
I.2 Cholesterol Regulation.....	10
I.3 High-density Lipoprotein	13
I.4 Scavenger receptor class B, type I (SR-B1).....	16
I.5 ATP-binding cassette, subfamily A, member 1 (ABCA1).....	19
II. CRISPR/Cas9	22
II.1 Genome Editing	22
III. Uptake of high-density lipoprotein by scavenger receptor class B type 1 is associated with prostate cancer proliferation and tumor progression in mice.....	29
III.1 Introduction.....	29
III.2 Material and Methods	30
III.3 Results	36
III.4 Discussion	49
III.5 Supplemental Information	54
IV. CRISPR use for additional projects	64
IV.1 Gene Editing Work Flow and Example of Knockout.....	64
IV.2 Generation of Gpnmb KO for manuscript resubmission	72

IV.3 Preliminary work the anti-proliferative effects of ABCA1 in prostate cancer	76
V. Conclusions and future directions	85
VI. Appendix.....	89
VII. Bibliography.....	90

List of Tables

1.1 Prostate Cancer Statistics from NCI SEERS Program	6
3.1 sgRNA and screening primers for mouse and human <i>SCARB1</i>	33
4.1 sgRNA and Screening primers for human <i>SCARB1</i>	66
4.2 sgRNA for mouse <i>Gpnmb</i>	72
4.3 cloning primers for human <i>ABCA1</i>	78

List of Figures

Abstract.....	4
2.1 DNA Binding and Editing Strategy by ZFNs and TALENs.....	23
2.2 Bacterial CRISPR/Cas.....	25
2.3 CRISPR/Cas9 editing of DNA.....	27
3.1 Expression of lipoprotein metabolism genes in normal prostate and prostate tumor tissue.....	37
3.2 HDL effects on total cholesterol levels in prostate cancer cells.....	39
3.3 HDL effects on cell accumulation and proliferation of prostate cancer cells.....	40
3.4 HDL effects in WT and SR-B1 KO cells.....	43
3.5 HDL uptake and impact on statin treated cells.....	45
3.6 Tumor progression study in vivo.....	48
3.7 HDL and LDL effects on total cholesterol levels in prostate cancer cells.....	58
3.8 Prostate cancer cell number and lipid uptake upon SR-B1 inhibition.....	59
3.9 HDL lipid uptake upon with SR-B1 KO.....	60
3.10 Cell accumulation assay for DU145 WT and SR-B1 KO.....	61
3.11 Characterization of WT and apoA1-KO mice.....	62
3.12 Histology of subcutaneous tumors from study arms.....	63
4.1 SCARB1 Expression in Renal Tissue.....	67
4.2 CRISPR design and editing of human SCARB1 gene exon 4.....	69
4.3 SR-B1 KO in Caki-1 Cell Accumulation.....	71
4.4 Editing of GPNMB and Use in Lysosomal Function Assay.....	75
4.5 LXR effects on ABCA1 expression and cell number in prostate cancer cells.....	80
4.6 Cholesterol efflux to apoA1 in LXR treated prostate cancer cells.....	82

4.7 LXR activation reduces AKT activity in prostate cancer cells	82
4.8 CRISPRa of ABCA1 in DU145 cells.....	84
5.1 Combinatorial treatment for ABCA1 induction, SR-B1 inhibition, and PI3K inhibition additively decrease prostate cancer cell growth.....	85
5.2 HDL-PIP2 in DU145 cells.	86

ACKNOWLEDGEMENTS

First, I'd like to thank God for the individuals that he has put in my life to strengthen me and carry me throughout every professional and personal experience I've had in the course of pursuing this degree. I can truly attest that I have been pressed, perplexed, persecuted, and put down at times, BUT not destroyed.

I want to thank my advisor Dr. Jonathan Smith for accepting me into his lab and never giving up on me. You have been my biggest supporter from day one to the very end, even when others doubted me, I doubted myself, and when I was misunderstood. Thanks for fighting for me and sticking it out. I will always be grateful for your patience, optimism, and unwavering support. To Dr. Driscoll, thanks for taking the initiative to speak to me. When I first started the program I was extremely shy and overwhelmed. As I've developed in ways that have puzzled many people, I appreciated you for always seeking to understand, acknowledging that I had some value, being progressive, and not putting labels on me. I would also like to thank my thesis committee for showing up to all my committee meetings, handling my shortcomings with care, and being optimistic, especially during times I had great experimental challenges. I would like to thank my labmates past and present who have been supportive. I especially want to thank Jen, who helped me overcome some major technical hurdles (no pun intended), Emmanuel as we struggled getting the mouse studies correct, and lastly Kailash who saw me from the beginning and still believes in me til now.

To my closest girlfriends, you all are like sisters to me. I'm glad to have you all. You all know me through and through. You've celebrated with me during the highs, but you all were also there during my darkest times. I'm grateful that I've met such amazing women who are able to empathize and sympathize through all of the struggles that I've

faced as a minority female in a corporate science space. Thanks for seeing me how and when I needed to be seen. Thanks for helping me feel normal. To my other friends in grad school, medical school, or in the Cleveland area, thanks for all the fun time and the community that we've been able to build as many of us don't have family here. To my cousins, aunts, uncles, and home church family, thanks for your many prayers, letters, and messages. It meant so much to know I was loved. I especially want to thank James and Angela Traugher. You two are like a second set of parents to me. Thank you for your calls and opening up your home when I was in town to visit. I've missed you all so much.

To my sister and brother, Ashley and Frankie, I love you two for only being a phone call away and coming to visit me. Thanks for always seeing the best version of me and encouraging me. Keep following your dreams and pursuing your goals.

Lastly, I want to thank mom for being my everything. You still see a version of myself that I don't feel that I have lived up to as of yet. I thank you for your continual support and for the countless hour of conversations and wisdom that you've given me. I hope that I can at least become a fraction of what an awesome person you have been to me and others. I thank you for the many sacrifices you've made and mountains you climbed for me and my siblings. I love you.

The Opposing Effects of HDL Metabolism on Prostate Cancer

Abstract

by

CYNTHIA ALICIA TRAUGHER

Objective – Prostate cancer is the second leading cause of cancer-related deaths among men in the US. Although some reports show high concentrations of HDL-cholesterol increase risk for prostate cancer, this association has not been consistent. High density lipoprotein (HDL) metabolism, is facilitated largely by scavenger receptor class B, type 1 (SR-B1) that mediates its uptake into cells, and ABCA1 that mediates its generation. SR-B1 is upregulated in prostate cancer tissue, whereas some evidence suggests that ABCA1 is downregulated in the disease. Our efforts were to determine if SR-B1-dependent HDL uptake and/or HDL biogenesis by ABCA1 export of lipids to apoA1 promotes prostate cancer cell proliferation and disease progression.

Hypothesis – HDL uptake by SR-B1 drives prostate cancer proliferation and disease progression, whereas ABCA1 mediated lipid efflux decreases prostate cancer proliferation and disease progression (**Fig. Abstract**)

Methods and Results – Here, we report that knockout (KO) of SR-B1 via CRISPR/Cas9 editing led to reduced HDL uptake into prostate cancer cells, and reduced their proliferation in response to HDL. *In vivo* studies using syngeneic SR-B1 wildtype (SR-B1^{+/+}) and SR-B1 KO (SR-B1^{-/-}) prostate cancer cells in WT and apolipoprotein-AI KO (apoA1-KO) C57BL/6J mice showed that WT hosts, containing higher levels of total and HDL-cholesterol, grew larger tumors than apoA1-KO hosts with lower levels of total and

HDL-cholesterol. Furthermore, SR-B1^{-/-} prostate cancer cells formed smaller tumors in WT hosts, than SR-B1^{+/+} cells in same host model. Tumor volume data was overall consistent survival data.

Conclusion – The results suggest that HDL through tumoral SR-B1 significantly influences the proliferation of prostate cancer cells and is a driver of the disease. Further investigation is needed to conclusively determine how HDL metabolism by ABCA1 influences prostate cancer cells and its impact on disease progression.

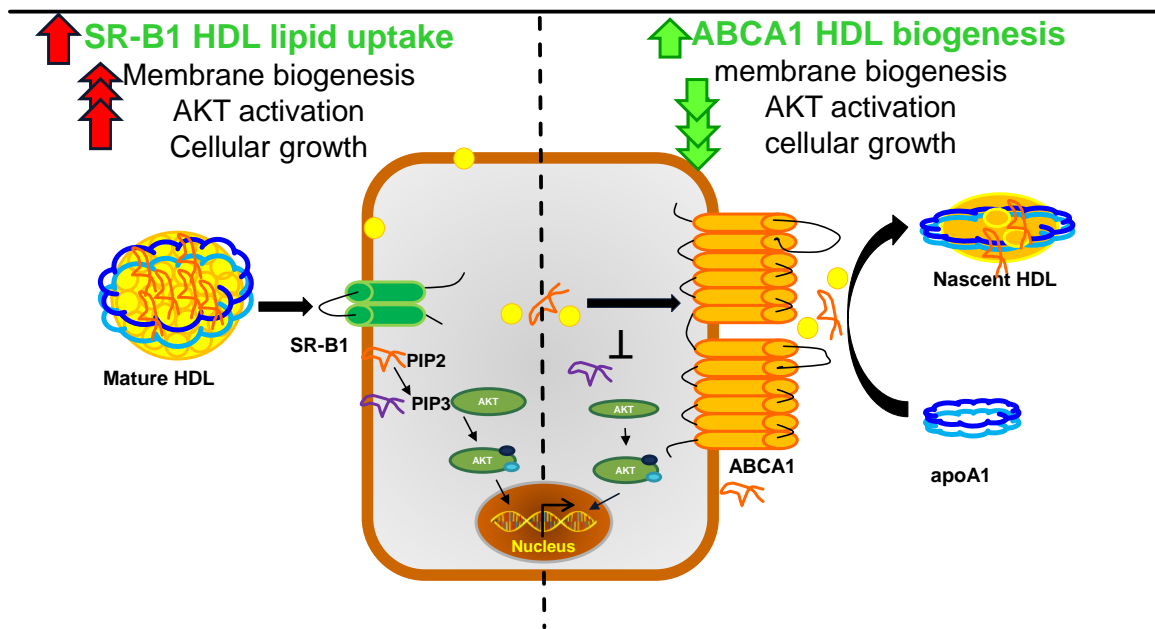


Figure Abstract. SR-B1 uptake of HDL provides lipids to support cell growth and tumor progression, whereas ABCA1 export of lipids onto apoA1, generating HDL, will blunt processes that drive prostate cancer cell growth and tumor progression

CHAPTER I

Introduction

I.1 Prostate Cancer

The prostate is the walnut sized organ that sits below the bladder to produce semen that nourishes and protects sperm (1). Prostate cancer has been described as overgrowth of epithelial cells (2). Prostate cancer is the most commonly diagnosed cancer and second leading cause of cancer-related death among men in the US. In 2018 nearly 1.3 million new cases of prostate cancer were reported worldwide, with an estimated ~192,000 new cases and ~33,000 deaths in the US in 2020. Additionally it is estimated that 1 in 9 men will develop prostate cancer in their lifetime.(3).

There are several risk factors for prostate cancer including age, ethnicity (4), family history (5,6), and environmental factors such as diet (7-9). Lifetime risk of men developing prostate cancer is 11.6%, whereas the median age of prostate cancer patients is 66, with the age of death at 80 years of age. These ages are 63 and 76, respectively for the black population, which is disproportionately affected by this disease. Here, prostate cancer risk, incidence, and death are higher in African-American populations as opposed to other ethnicities as seen in **Table 1.1** (3,4,7,10).

Environmental factors have also been implicated in development of this disease. For example, incidences of prostate cancer were shown to be more than 4-fold higher in Japanese migrants in the Western world as opposed to those living in Japan (7,8). Mortality rates for prostate cancer are 3-fold higher in the US, where there is up to 17 times more total fat consumption than in Asian countries (9). In addition to environmental factors several studies have confirmed that genetics play a major role in risk for the

disease. Studies in a Chinese population showed that a family history of prostate cancer increased prostate cancer risk for those patients by 2.1-fold (5). These findings have been recapitulated in a diverse ethnic cohorts (96-97% Caucasian; 3-4% African American, Asian, and other race) in which men with a family history of prostate cancer had 68% increased risk for the disease and a 72% increased risk for a lethal form of the disease compared to groups that lacked a family history of prostate cancer (6).

PROSTATE CANCER STATISTICS						
Ethnicity	ALL	WHITE	BLACK	ASIAN	HISPANIC	
years of age						
Median Age Diagnosis	66	66	64	NA	NA	
Median Age Death	80	80	76	NA	NA	
%						
Lifetime Risk Diagnosis	11.6	10.82	15.78	7.37	10.82	
Lifetime Risk Dying	2.44	2.29	3.94	2.18	2.76	
Risk of dying	Age	%	%	%	%	
	40	2.57	2.4	4.25	2.23	2.87
	50	2.65	2.48	4.44	2.26	2.93
	60	2.79	2.62	4.8	2.32	3.05
	70	2.95	2.77	5.27	2.39	3.18
	80	3.03	2.86	5.59	2.46	3.19
incidence / 100,000 persons						
Incidence	109.5	101.9	176.7	55.6	93.4	
rate / 100,000 persons						
Death Rate	7.8	7.4	14.3	3.5	6.4	

Table 1.1 Prostate Cancer Statistics from NCI Surveillance, Epidemiology, and End Results (SEERS) Program. Median ages at diagnosis and death (2012-2016), lifetime risk for prostate cancer diagnosis and dying from prostate cancer (2014-2016), prostate cancer incidences (2012-2016), and prostate cancer death rates (2012-2016) for All, White, Black, Asian, and Hispanic ethnicities. NA; not available

Prostate cancer is a disease typically driven by male hormones known as androgens (2,11); however male development is dependent upon them. Testosterone (T) and dihydrotestosterone (DHT) are the main androgens that activate the androgen receptor (AR) needed for the development external male genitalia. The hypothalamus, pituitary, adrenals, and testes are the major organs that are involved in androgen production (12). In brief, the hypothalamus releases gonadotropin releasing hormone (GnRH) that

stimulates the pituitary to produce luteinizing hormone (LH), that prompt leydig cells of the testes to produce the majority of testosterone needed to support the male reproductive system and define male characteristics (13). A minor pathway for testosterone production is by the hypothalamic-pituitary-adrenal axis. Here, the hypothalamus secretes corticotropin-releasing hormone (CRH), which stimulates the pituitary to secrete adrenocorticotrophic hormone (ACTH) that then prompts the adrenals to produce dehydroepiandrosterone (DHEA). DHEA can be converted to testosterone. This testosterone can be converted to a more active form, DHT, by the enzyme 5- α -reductase.

Some of the earliest studies investigating prostate cancer and hormone were performed by Huggins and Hodges. They demonstrated that serum levels of acid and alkaline phosphatases were increased in men with prostate cancer. They additionally demonstrated that castration ultimately reduced these levels of serum phosphatase (11), and that castration also lead to regression of prostate cancer size in most of their subjects, demonstrating for the first time that, androgens play a role in the disease (2). As seen in the Huggins and Hodges study, prostate cancer usually responds to androgen deprivation therapies such as castration, however some prostate cancers become resistant. Notable mutations that promote resistance to therapies include, mutations and amplification of the androgen receptor (AR) as well as PTEN mutations or deletions (14).

Androgen signaling is facilitated by the androgen receptor (AR), which has a higher affinity for DHT than testosterone (15). When the AR is not binding its ligands, it is sequestered in the cytoplasm by heat-shock proteins to prevent translocation to nucleus. Binding of DHT or testosterone facilitates translocation to the nucleus and promote proliferation (16). Some studies have shown that 25-51% of prostate cancer patients have amplification of the AR, or patients have increased copy number of the AR gene and increased expression of AR (17,18). In the cancer genome atlas (TCGA), of the 1,738

samples that have some form of AR alteration, 32% have amplification of the AR (19). In spite of androgen deprivation therapies (ADT), which seek to lower androgens that activate AR, it is known that serum and tissue hormones, like DHT are reduced, yet not depleted (20). It is plausible that this residual androgen pool activates amplified AR to drive the disease (14).

PTEN, the phosphatase and tensin homolog, is a phosphatase that remove the 3' phosphate from phosphatidylinositol 3,4,5-trisphosphate (PIP3) to generate phosphatidylinositol 4,5-bisphosphate (PIP2). PIP2 is a phospholipid primarily sequestered on the inner leaflet of the plasma membrane, where it can be converted to PIP3 with subsequent recruitment and activation of AKT (21). PTEN mutations are common in several human cancers including, but not limited to prostate cancer, breast cancer, endometrial cancer (22). Loss of PTEN, leaves the PI3-kinase unchecked (converting PIP2 to PIP3), resulting in accumulation of PIP3 and subsequent activation of AKT driving processes such as cell proliferation, angiogenesis, and reduced apoptosis (14,23). Knockout of *Pten* in mice results in upregulated Akt activation and metastatic prostate cancer (24). Furthermore, In the transgenic adenocarcinoma of the mouse prostate (TRAMP) mouse model, heterozygous and homozygous deletions of *Pten* results in an increased rate of disease progression and reduced survival compared to *Pten* WT TRAMP mice (25). In TCGA, of the 1,107 prostate cancer samples that have an alteration in PTEN, 72% of the alterations were due to PTEN deletion (19). Another study showed that 43% of the patients had *PTEN* loss (17) a meta-analysis of patients with prostate cancer showed that patients with *PTEN* deletion has a higher risk for relapse after having a radical prostatectomy (26).

Depending on ethnicity and family history, the earliest an individual should be tested for prostate cancer is at age 40 (8,27). Prostate cancer greatly impacts the genitourinary

and musculoskeletal systems with common issues such as erectile dysfunction, urination dysfunction, as well as pain or stiffness in lower back and legs (28). Initial examination of the prostate for cancer is performed by digital rectal exam (DRE) or trans-rectal ultrasound (TRUS). Though Huggins et al. made initial breakthroughs in controlling androgens as a form of countering prostate cancer progression, it was speculated that this form of androgen deprivation may not be sustainable for decreasing disease burden (2). In connection with their prior study with serum phosphatase, it was also shown that though upon initial lowering of the phosphatases, at some time the serum phosphatases would become elevated in spite of the castration (11). Since the serum phosphatase study in which these phosphatases served as biomarkers of prostate cancer, better biomarkers have been identified, such as prostate specific antigen (PSA) became a more reliable biomarker based on patient status post radical prostatectomy (29).

Normal levels of PSA are considered to be less than 4 ng/ml blood, whereas individuals with levels greater than the accepted standard are recommended to have prostate biopsy performed (30). PSA levels have been correlated to prostate cancer onset (31), however, other underlying conditions such as benign prostate hyperplasia and prostatitis also promote elevated levels of PSA (27). Over screening with PSA tests increases over diagnosis of prostate cancer by as much as 50%, with increasing lifetime risk for the disease from 6.4% to 10.6% (32). Alternative approaches for screening and treatment plans are thus recommended because it has been shown that most men diagnosed with prostate cancer, will not die from the disease. More specifically, if an individual has a Gleason 2-4 grade tumor, the chance of death as a result of prostate cancer is 4-7% in within a 15 years of diagnosis (33).

Prostate cancer is characterized by its location and pathological grade. There are four main stages of prostate cancer; T1 to T4. Stages T1 and T2 are stages in which the cancer

is localized only to the prostate, whereas in stage T3, the cancer has spread just outside of the prostate, up to the seminal vesicles. Lastly, stage T4 indicates that prostate cancer has metastasized to other organs (34). With respect to prostate cancer grade, there are Gleason patterns 1 to 5, in which 1 denotes a least aggressive form in which cells are well differentiated, whereas pattern 5 indicates a more aggressive cancer, corresponding to cells being poorly differentiated. Two Gleason patterns are assigned to the tumor which make up the Gleason score (2-10), an indicator of how advanced the tumor is (34,35).

There are several approaches to treating prostate cancer. Factors such as patient age, prostate cancer stage, and risk for progression play important roles in the course of treatment. Options include active surveillance (watchful waiting), prostatectomy, chemical castration, chemo- and radiation therapy (30).

I.2 Cholesterol Regulation

The backbone of all steroid hormones, like testosterone and DHT, is cholesterol (36). It is also the precursor to oxysterols, bile acids, and vitamin D (37). Cholesterol has four hydrocarbon rings in which a hydroxyl group is linked to the third carbon in the ring structures and an additional carbon chain is connected to 17th carbon of its ringed structure. It is an essential lipid that plays a roles in many aspects of the cells including membrane fluidity, signaling transduction, and membrane trafficking (36).

It is estimated that 20-25% of the lipid fraction in the plasma membrane is cholesterol, in which lipids such as phospholipids, sphingolipids, and glycolipids make up the remaining fraction (36,38). The term lipid rafts is designated to a clustering of cholesterol and these lipids that function to support protein induced cell signaling kinases. Among these include a host of receptor tyrosine kinases as well as g-protein coupled receptor kinases, in which cholesterol depletion or supplementation can modulate their activation (39). Therefore the cell must have a tightly regulated process for cholesterol sensing, synthesis, and regulation.

Cholesterol can be synthesized by cells or it can be acquired by dietary intake. The mevalonate pathway is responsible for producing cellular cholesterol and other sterols from acetyl-CoA. This process primarily takes place in the endoplasmic reticulum (ER) in which the rate-limiting enzyme of this pathway is hydroxymethylglutaryl CoA reductase (HMGCR). HMGCR is the target of cholesterol lowering drugs known as statins (40,41). HMGCR is an ER membrane protein that is transcriptionally controlled by sterol regulatory element-binding protein 2 (SREBP2) (42). During times when cells do not need to generate cholesterol, SREBP2 remains complexed to the SREBP cleavage activating protein (Scap) and INSIG1/2 proteins in the ER. Scap and INSIG proteins are sterol sensing proteins in which cholesterol and 25-hydroxycholesterol are sensed, respectively.

When cholesterol levels are low, the Scap-SREBP2 complex dissociates from INSIG1/2 and is transported to the golgi by COPII vesicles (36,43,44). Subsequently, S1P and S2P proteins cleave SREBP, in which its helix-loop-helix domain travels to the nucleus where it acts a transcription factor to upregulate cholesterol synthesizing genes such as HMGCR (36,43). Synthesized cholesterol and sterols are subsequently distributed through the cell to the plasma membrane, endosomes, ER, or stored in lipid droplets (36).

When cellular cholesterol levels are elevated the cell must remove or store the excess cholesterol. The liver x receptors (LXR) and retinoid x receptors (RXR) can act as transcription factors to upregulation several proteins that aid in cholesterol removal and storage. Among these includes a group of proteins known as the ATP-binding cassette (ABC) transporters (45,46). ABCA1 and ABCG1 are heavily involved in cholesterol and phospholipid efflux from cell to high-density lipoprotein (HDL) (46). During this process lipid-poor apolipoprotein-AI (apoA1) accepts cholesterol and phospholipids effluxed by ABCA1 generating nascent HDL particles. Maturation of the HDL is dependent upon further cellular cholesterol efflux mediated by ABCG1 and upon esterification of cholesterol by the enzyme lethicin:cholesterol acyltransferase (LCAT) that produces the hydrophobic core and spherical form of HDL (47). Within cells, the enzyme known as acyl CoA cholesterol acyltransferase (ACAT), aids in esterifying cholesterol so that it may be stored inside cells as harmless lipid droplets when there is excess cholesterol. This stored cholesterol ester (CE) can be hydrolyzed by cholesterol ester hydrolases (CEH) or lysosomal acid lipases to convert cellular CE back into free cholesterol that can be distributed through the cells or effluxed from cells through the ABC transporters (36,47). Alternative to cellular biogenesis of cholesterol, cholesterol can be acquired from lipoproteins such as low-density lipoprotein (LDL) and high-density lipoprotein (HDL). Lipoproteins are characterized by their major protein components (apolipoprotein(s)), the

type of lipid(s) they carry, and the density of their particle as a whole. The types of lipoproteins that exist, ranging from the least to most dense, include: chylomicrons, very low-density lipoprotein (VLDL), low-density lipoprotein (LDL), and high-density lipoprotein (HDL) (48). Due to being water-insoluble, cholesterol can only circulate through the body in the form of lipoproteins. Cell acquisition of LDL cholesterol, involves the LDL particle being endocytosed by cells. Subsequently the particle is taken through a series of endocytic compartments in where its receptor (LDLR) is recycled or degraded, and then the cholesterol is hydrolyzed so that proteins (Neimann-Pick 1 and Neimann-Pick2) can move the cholesterol out of endosomes so that it can be distributed throughout or exported from the cell (36).

Similar to LDL uptake, there is holo-particle uptake of HDL by pinocytosis(49) and through SR-B1-mediated endocytosis (50). Additionally, HDL lipids can be delivered to cells independent of whole these processes by using selective cholesterol uptake (51,52). Here, SR-B1 facilitates uptake of HDL without internalization of the whole particle, but through uptake of its lipids including free cholesterol (53-57), cholesterol ester (51,52,55), and phospholipids (58,59).

1.3 High-density Lipoprotein (HDL)

HDL is the smallest and densest lipoprotein, ranging from 5-12 nm in size and densities from 1.063 to 1.21 g/ml. Although apolipoprotein-A1 (apoA1) is the largest protein component of HDL, apolipoproteins A2, C, and E (apoA2, apoC, and apoE) are also associated with HDL in smaller quantities(48). ApoA1 is synthesized by the liver and the intestine(60), in its lipid-poor form where it can travel through the blood to peripheral tissues to generate HDL and facilitate reverse cholesterol transport (RCT). In this process apoA1 interact with ABCA1 on peripheral cells to extract cholesterol and phospholipids. These nascent HDL particles can then move back into circulation in which the cholesterol

can become esterified through the enzyme Lecithin cholesterol acyltransferase (LCAT), which helps the HDL mature and further be lipidated by ABCG1. While HDL is in circulation it can transport some of its cholesterol ester to other lipoproteins such as VLDL and LDL, through the cholesterol ester transfer protein (CETP). HDL, via its receptor SR-B1, and LDL/VLD, via LDLR and related receptors, can then deliver their cholesterol and lipids to the liver where the cholesterol can be processed and secreted into the bile via ABCG5 and ABCG8, and subsequently transported to the small intestine where it is ultimately removed from the body in through fecal matter(61).

HDL-cholesterol levels differ between men and women. Epidemiologic studies of men and women from ages 45-54 across multiple countries consistently revealed that women have higher levels of HDL-cholesterol compared to men(62). This difference is close to 10 mg/dL (63), and is thought to be due to changes in hormone levels. It has been demonstrated that prior to puberty females and males have similar levels of HDL. However at puberty female HDL levels do not change, but males HDL levels drop and are lower than female HDL levels (64). It has been reported that as males advance towards puberty that not only do HDL levels decrease, but testosterone levels increase. With males that had delayed puberty, testosterone injections were given that also led to lower HDL and apoA1 levels (65). Thus, it is androgens that regulates HDL physiologically, not estrogens.

Cholesterol has been a topic for interest in prostate cancer for several years. Many studies have been performed to assess the cholesterol and risk for prostate cancer, showing that total cholesterol is positively associated with increased risk for prostate cancer (66-69). Thus the idea of lowering cholesterol to reduce risk is plausible. Therefore statins, which lower cholesterol by inhibiting the mevalonate pathway and subsequent upregulation of hepatic LDLR, have been studied to evaluate influence in prostate cancer. A number of studies showed that statin usage decreased risk for prostate cancer (70-78).

However, there were a similar number of studies that conclude that statin use is not associated with risk for prostate cancer (79-86).

To examine HDL effects on prostate cancer, nearly 5,000 men were analyzed from the REDUCE Trial that were select by excluding individuals with missing baseline cholesterol levels or having used statins. Comparing baseline HDL levels to 2-year post treatment (placebo vs. dutasteride). It was shown that increased HDL, regardless of treatment, tracked with overall prostate cancer as well as with advanced prostate cancer (66). A similar study was performed with roughly half as many subjects as in the previous study, and without the use of dutasteride. This study confirmed increased HDL was associated with increased risk for low-grade prostate cancer (87). In contrast to these studies, the AMORIS study found that low HDL was associated with increased risk for the disease. However, some patients had used statins, and the study could not discriminate between high- or low-grad prostate cancer with respect to HDL and prostate cancer risk. Additionally, in the REDUCE trial, men enrolled were greater than 50 years of age, whereas in the AMORIS study, individuals younger than 20 were also included and the study did not control for individuals who previously used statins (88). Some studies showed that higher HDL levels were associated with increased risk for prostate cancer (66,69) while others suggested that lower levels of HDL or apoA1 were associated with increased risk for prostate cancer (67,68,88). Conflicts such as these has led to assessments of HDL and prostate cancer risk across multiple studies. Yupeng, et al, performed a meta-analysis on 14 studies looking at the relationship between total and/or sub fractions of cholesterol and prostate cancer risk. Here, six studies combined showed that HDL did not have a significant association with the risk of developing prostate cancer. However, analysis of three studies that looked at prostate cancer progression revealed that higher HDL was associated with 21% increased risk for progression to high-grade

prostate cancer; but, this result failed to reach statistical significance, due in part to the small sample size (89). In addition, factors such as statin use and duration of statin use could possibly influence the inconsistencies between these studies.

Pre-clinical studies in mice have demonstrated that higher apoA1/HDL levels decrease lung cancer and melanoma burden (90). However, in the TRAMP mouse model, that spontaneously forms prostatic tumors, it was observed that a western type diet, which increased HDL levels also correlated with more prostate tumors and metastasis. Though total cholesterol levels were elevated in mice on western type diet, TRAMP mice vs non-TRAMP mice had significantly lower total cholesterol on the western type diet (91). These studies show conflicting roles of HDL levels on cancer. We have proposed that within prostate cancer, alone, the discrepancies may be linked to HDL, but more specifically to metabolism of HDL through scavenger receptor class B, type I (SR-B1) and ATP-binding cassette transporter A1 (ABCA1).

I.4 Scavenger Receptor class B type 1

The *SCARB1* gene encodes scavenger receptor class B, type 1 (SR-B1), which is a 509 amino acid, two transmembrane domain protein. The estimated molecular weight of SR-B1 is 57 kilo Daltons (kDa), however, due to glycosylation, it is usually observed in Western blot as roughly an 82 kDa protein (92,93). The majority of the protein structure exists as an extracellular loop, whereas its N- and C-terminal domains of 10 and 40 residues, respectively, are intracellular (94). SR-B1 binds HDL (51,95,96), however it is a multi-ligand receptor and has been shown to bind other lipoproteins including LDL and its modified forms (96,97) as well as VLDL (96). SR-B1 is expressed by several tissues including the liver and steroidogenic tissues such as the adrenals, testes, and ovaries

where it mediates cholesterol uptake, to promote cholesterol ester (CE) storage used for steroid hormone synthesis (51,94,95,98).

SR-B1 expression is regulated pre- and post- transcriptionally by many hormones and regulatory factors. Expression of SR-B1 has been shown to regulate protein kinases such as ERK and PI3K/AKT. For example, SR-B1 expressing breast cancer cells have increased activation of ERK and/or AKT when treated with HDL, whereas SR-B1 knockdown attenuated the signaling (99). Additionally, SR-B1 has been implicated as anti-atherogenic due to its ability to activate the endothelial nitric oxide synthase (eNOS) and subsequent production of nitric oxide (NO) (100). ApoE KO mice that expressed SR-B1, formed smaller aortic lesions compared to double ApoE/SR-B1 KO mice (101).

Hormonal regulation is highly similar in steroidogenic tissue. In adrenal cells, SR-B1 expression has been shown to be regulated steroidogenic factor 1 (SF-1) that binds to the SR-B1 promoter to induce its transcription(102) as well as by the adrenocorticotrophic hormone (ACTH), naturally produced the pituitary gland, demonstrated in both human and mice induces adrenal SR-B1 expression (98,103,104). ACTH is likely facilitated through the activation and signaling of cAMP/protein kinase A transduction (103). In the rat liver, activation of peroxisome proliferation-activation receptor gamma (PPAR γ) promoted expression of SR-B1 due to binding of SR-B1 promoter (105). Furthermore, human and mouse SR-B1 is inducible by oxysterol activated nuclear receptors such as liver x receptor alpha LXR α , LXR β , and retinoic x receptor (RXR) (106).

Unlike the LXR and RXR, the nuclear receptors, DAX-1 (dosage-sensitive sex adrenal hypoplasia congenital critical region on the X chromosome, gene-1) and pregnane X receptor (PXR) are suppressors of SR-B1. DAX-1 negative regulates SR-B1 in mouse adrenal cells and human hepatocytes by prevent SREBP from binding to response elements on SR-B1 (107). PXR also effected promoter activity of SR-B1 in human and rat

hepatocytes decreasing SR-B1 expression (108). In addition to transcriptional regulation of SR-B1, microRNAs (miRs) suppress rat and human SR-B1 by binding to the 3' untranslated regions (UTR) of SR-B1 (109,110). These studies demonstrated that miR-96, miR-185, and miR-223 repressed SR-B1 leading to reduce HDL uptake by hepatocytes (110). Additionally, miR125a and miR-455 reduced HDL uptake by rat and mouse Leydig tumor cells (109), where it led to decreased steroidogenesis (109). Due to the impact of SR-B1 expression on signal transduction, HDL uptake, and steroidogenesis in cancer cells and steroidogenic tissues, it is not surprising to delve into how SR-B1 impacts prostate cancer. Recent studies have indicated that SR-B1 is upregulated in prostate cancer tissue (111,112), which has also been seen in clear cell renal cell carcinoma (113,114).

In prostate cancer, Schörghofer et al. showed that SR-B1 was elevated in high-grade and metastatic prostate cancer compared to low-grade and localized prostate cancer. Additionally, this upregulated SR-B1 correlated with decreases in disease free survival compared to lower SR-B1 expressing tumors. LDLR expression was unchanged for these same parameters and did not influence disease free survival (112). Similar findings were found by Gordon et al. who showed that SR-B1 was upregulated in prostate cancer tissue and more so in metastatic prostate cancer. Surprisingly, LDLR expression was decreased in their study (111). Upregulation of SR-B1 is not exclusive in prostate cancer but has been demonstrated in clear cell renal cell carcinoma (115) and breast cancer (116). In addition to decreasing disease free survival, additional consequences of upregulated SR-B1 include increased uptake of HDL, increase in testosterone and DHT synthesis (111), reducing progression-free survival (114), and increasing cellular proliferation (111,114,116).

These functions of SR-B1 in the context of prostate are important because an earlier study attributed that progression of this disease is heavily driven by accumulation of lipids due to uptake of LDL via the LDLR (117). This lipid accumulation was also demonstrated in breast cancer cells, which had upregulation of both SR-B1 and LDLR (116). Thus it is plausible that the upregulated SR-B1 functions to drive or progress prostate cancer.

Studies have investigated the role of SR-B1 in prostate cancer progression by using RNA interference or chemical inhibition of the receptor. In the Gordon study, RNA interference or chemical inhibition of SR-B1 resulted in reduced HDL uptake and cell growth, increased cell death, and reduced testosterone, DHT, and PSA secretion of C4-2 cells. Most of these findings were mirrored in the human PC3 prostate cancer cell line, in which xenograft tumors grew slower in response to SR-B1 inhibition by BLT-1 (111). Some of the effects were shown in an additional study in which SR-B1 was inhibited by the drug ITX5061. Here SR-B1 reduced HDL uptake in prostate cancer cells. They further demonstrated that resistance to androgen deprivation therapy was overcome by inhibiting SR-B1. This resulted not only in smaller tumors, but also in tumor regression, decreased tumoral testosterone, and decreased metastasis of the disease (118).

I.5 ATP-binding cassette, subfamily A, member 1 (ABCA1)

ABCA1 is a 2,261 amino acid protein that has twelve transmembrane domains. It has a major role in efflux cholesterol from cells to apoA1 to generate nascent HDL particles. ABCA1 has been demonstrated to transport not only cholesterol out of the cell, but other primary roles include transport of phospholipids such as phosphatidylserine, phosphatidylcholine, phosphatidylethanolamine, and sphingomyelin, across the lipid bilayer (47). More recently, ABCA1 was identified as a phosphatidylinositol 4,5-bisphosphate (PIP₂) transporter, in which assists in apoA1 binding to cells to facilitate

cholesterol efflux. The transport of PIP2 has also been demonstrated to be carried on HDL in circulation and has the capacity to be delivered to cells via SR-B1 (58).

Similar to SR-B1, ABCA1 is also regulated by LXR activation by compound T0901317 and hydroxycholesterols in both macrophages and prostate cancer cell lines (119,120). Studies have confirmed the significance of this pathway in not only cellular proliferation but tumor progression as well. For example, Dufour et al, demonstrated that the prostate epithelial cells from *Lxr*-deleted mice have increased cellular proliferation compared to WT prostate epithelial cells (121). With respect to tumor progression, mice treated T0901317 had delayed LNCaP prostate cancer cell tumor progression over non-treated wildtype mice after castration (122). This is interesting because in another xenograft model, these castration resistant prostate cancer cells not only had an increase in ABCA1, but also increased SR-B1 expression. This event corresponded with increased tumoral cholesterol and DHT synthesis, suggesting a profound role in balancing cholesterol (HDL) in this disease (123).

In contrast to SR-B1, ABCA1 is suppressed by androgens (124) as well as by statins (125) and by hypermethylation of its promoter (126). Lee et al demonstrated that ABCA1 is decreased, as prostate cancer advances. Furthermore, suppression was linked to hypermethylation showing that LNCaP prostate cancer cells were not expressing ABCA1 as in DU145 cells. Upon using a demethylating agent (5-aza-2'-deoxycytidine) and T0901317, LNCaP cells expressed ABCA1. ABCA1 induction in both cell lines promoted cholesterol efflux to apoA1 and HDL. In addition, induced ABCA1 expression also resulted in decrease in total cellular cholesterol levels in both lines (126). The ability of DU145, LNCaP, and even PC3 prostate cancer cell to promote an increase in cholesterol efflux was recapitulated by Sekine et al. However, treatment with HDL in the cells promoted increase in cell numbers, but did not ultimately impact cellular cholesterol levels.

Interestingly, HDL mediated impacts on cell number were not due to SR-B1 expression as determined by knockdown. However, knockdown of ABCA1 reduced proliferation as well as ERK and Akt signaling in PC3 cells. Overexpression of ABCA1 however, induced the processes in LNCaP cells (125).

Taking into account work on correlative studies on HDL and prostate cancer risk as well as differential regulation of HDL receptors SR-B1 and ABCA1, we decided to investigate the roles of HDL and its receptor, SR-B1, in prostate cancer proliferation and disease progression. Here we will take advantage of the widely used human DU145 prostate cancer cell line and the mouse TRAMP-C2 cell line as well as WT and apoA1 KO mice with significant difference in HDL levels to address the hypothesis that SR-B1 mediated HDL uptake drives prostate cancer proliferation.

CHAPTER II

CRISPR/Cas9

II.1 Genome Editing

Over the past several decades, attempts to understand how genetic alterations influence disease has been of interest. Techniques have been developed to challenge multiple aspects of the central dogma of biology in order to understand more about genomes and the consequences thereof. Since the early 2000s, attention has been focused on nucleases to aid in genome editing (127). Included in this group are zinc-finger nucleases (ZFNs), transcription activator-like effector nucleases (TALENs), and clustered regulatory interspaced short palindromic repeats (CRISPR)/Cas9 nuclease. The most basic function of each of these systems is inducing breaks at a specified sequence in genomic DNA and relying on cellular machinery to repair the break, known as non-homologous end joining (NHEJ) or donating exogenous genetic material in a process known as homology directed repair (HDR), ultimately leading to alteration in a targeted gene.

Zinc-finger nucleases (ZFNs) and transcription activator-like effector nucleases (TALENs) both operate by the proteins binding to a specific sequence in the genome and using a fusion to a bacterial type II restriction enzyme, *fokI*, that must dimerize to induce double strand DNA breaks in a DNA-sequence-independent manner (128,129). ZFNs and TALENs both have a DNA binding element; however, the major difference between their mechanisms is that the DNA binding domain must recognize 3 base pairs (bp) at time, whereas in the TALENs system, one TALE specifically binds to only 1 bp (**Figure 2.1**). Multiple ZFN proteins or TALEs can be combined to increase specificity of the editing

system. The advantages of using ZFNs and TALENs is that they are able to target multiple genes in many widely used model organisms. However, their benefits do not outweigh those of the CRISPR/Cas9 system due to being less efficient, less specific, more expensive, harder to engineer, and extended time to edit (128,129).

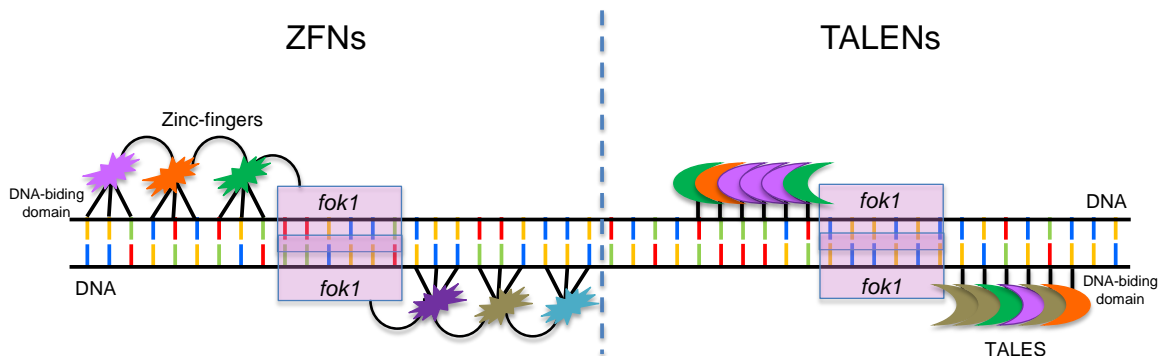


Figure 2.1 DNA Binding and Editing Strategy by ZFNs and TALENs. ZFN and TALEN proteins contain DNA binding domains that recognize specific base pair(s). One ZFN protein recognizes 3 base pairs. Up to 6 zinc-finger proteins can be combined with the fok1 nuclease to create a ZFNs system. TALEs (transcription activator-like effectors) recognizes only one base pair. As many as 20 TALEs can be combined with fok1 to create a TALENs system. Fok1 nuclease in each system must homodimerize to induce double-strand DNA breaks. Repairs can be made by NHEJ or HDR.

The clustered regulated interspaced palindromic repeats (CRISPR) / CRISPR associated (Cas) 9 protein has been widely used as a research tool since 2013 (130). The CRISPR/Cas system was first identified as a natural process that occurs in bacteria as an adaptive host-defense immune mechanism to remove viral (phage) DNA that had integrated into their genome (131). CRISPRs were first identified just over 30 years ago in the *iap* gene in *E. coli* (132). These short interspaced fragments of DNA (protospacers) between the palindromic repeat is DNA that has been acquired from viral infection and are subsequently used to counter further infection. Palindromic sequences are DNA or RNA that reads identically in both 5'-3' (forward sense) and 3'-5' (reverse sense) directions. There are CRISPR associated (Cas) proteins that are involved in this editing system. CRISPR/Cas systems have been categorized into as many as 6 systems, with 3 systems

that are widely studied (133-135). Categorization of CRISPR/Cas systems are defined by their target molecules (DNA, RNA, both), the processing of their CRISPR RNA (crRNA), transcripts derived from viral DNA incorporated into bacterial DNA protospacer regions, and how many and which Cas proteins are needed to facilitate the editing. Within each system exists one of two classes of Cas proteins. These Cas proteins function as integrases, RNA processors, or excisors. In Class I, Cas protein types I, III, and IV must multiplex with other Cas proteins to carry out editing, whereas Class II Cas proteins (types II, V, VI), only need 1 Cas protein to facilitate the “effector” function of the CRISPR/Cas System(133). Most CRISPR/Cas systems function in the same way. There are two classes of CRISPR associated (Cas) proteins that are involved processing viral DNA to develop this immunity. Upon viral introduction into the bacterial cells, Cas proteins will scan the viral DNA for a nucleotide sequence (2-5bp) adjacent to the protospacer (136-138) which is called the protospacer adjacent motif (PAM). Other Cas proteins will excise these nucleotides from the viral genome and then integrate them into the CRISPR regions of the bacterial genetic code. The DNA will be processed to RNA known as pre-crRNA (CRISPR RNA), this will further be processed to mature crRNA which will then have the capacity to complex with Cas protein(s) to form this effector complex. When the bacteria is challenged again with viral DNA that was previously acquired and processed, the crRNA containing a protospacer motif complementary to the viral PAM site, form an effector complex with Cas protein, which then cleave the viral DNA leading to the degradation of the foreign material (**Fig. 2.2**) (133).

CRISPR/Cas9, a type II CRISPR/Cas system, differs from the other bacterial CRISPR/Cas systems for a number of reasons. Unlike some systems, the CRISPR/Cas9 system requires transcription of not only crRNA, but a trans-activating crRNA (tracrRNA). This tracrRNA is produced from transcribed repeat sequences in between integrated viral sequences. The tracrRNA will hybridize to transcribed CRISPR repeats of the crRNA that will facilitate its recruitment of Cas9, the sole Cas protein (a Class II Cas protein) leading to the effector function of this system, whereas other systems may require multiple Cas proteins or a different sole effector Cas protein (**Fig. 2.2**) (133-135,139).

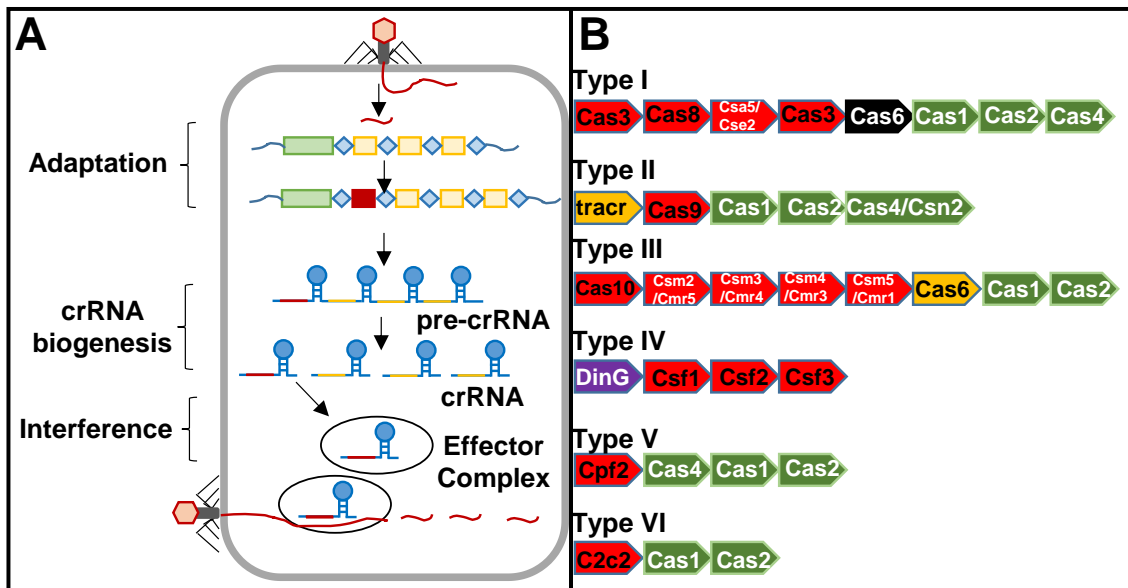


Figure 2.2 Bacterial CRISPR/Cas System A) Representation of CRISPR/Cas systems in bacteria. B) varying classes Cas proteins. Adaptation(integrase) Cas proteins (red), Effector (excisor) Cas proteins (green), crRNA processors (yellow).

The feasibility of using the CRISPR/Cas as a research tool was introduced in 2012 by Jinek et al, who developed an RNA guided system using Cas protein 9 (Cas9) derived from *Streptococcus pyogenes* (SpCas9) and a single-strand guide RNA, which is composed of a crRNA joined to a trans-activating crRNA (tracrRNA) (140). This differs slightly from bacterial CRISPR/Cas9 in that the single guide RNA is transcribed as a single unit, whereas in bacteria the crRNA and tracrRNA are transcribed separately (141). Cas9 is guided to the gene of interest, then scans the DNA for the PAM which has a sequence 5'-NGG-3' (142). PAM sequence and length are different for various Cas protein (136-138). Once there, the HNH domain facilitates the break in the DNA strand complementary to guide RNA, whereas the RuvC domain, facilitates the non-complementary strand DNA cleavage, 3-4 base pairs (143) upstream of the PAM. The double strand breaks can be addressed by two main repair mechanisms; Non-homologous end joining (NHEJ) or Homology directed repair (HDR) (**Fig 2.3**).

In NHEJ, a protein complex coordinates to repair the break. In brief, DNA-PKc proteins are recruited to quickly stabilize the DNA by allow short stretches of DNA to bind, while also recruiting and activating Artemis which helps in snipping away nucleotides that were not quickly paired. The XRCC4 dimer complexes with KU70/80 heterodimer to further stabilize the DNA and recruit DNA ligase IV and XLF proteins to facilitate joining of DNA by phosphodiester bonding (As reviewed in (144)). Due to re-sectioning of the DNA in NHEJ, it is likely to lead to small insertions and deletions (indels), which can cause frameshift mutations that lead to truncated, non-functional proteins or premature stop codons in which nonsense mediate decay proteins are recruited to degrade the mRNA before being translated into protein (145). These processes makes the CRISPR/Cas9 system advantageous for creating functional gene knockouts.

Homology directed repair (HDR) is another DNA repair mechanism that is facilitated by protein multiplexes. In contrast to NHEJ, HDR is used to foster precise genome edits. Efficiency of this system is generally low ranging from 1-50% efficiency, due low recombination and competing with the NHEJ repair process (141). However, it can be improved by enhancing HDR or inhibiting NHEJ through different small molecules including, RS-1 (146), SCR7, resveratrol (147), L755507 (147,148), and Brefeldin A (148).

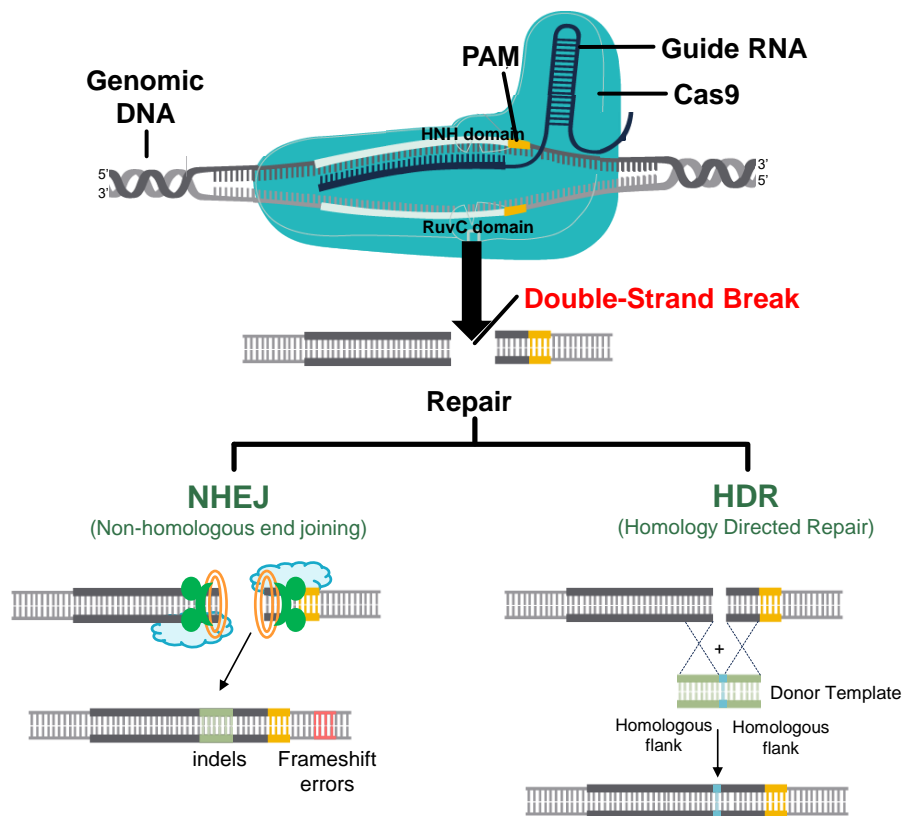


Figure 2.3 CRISPR/Cas9 editing of DNA. The guide RNA, which is composed of crRNA and tracrRNA (or synthetically determined scaffold repeat), guides Cas9 to a place in the genome. Cas9 recognized PAM in the genome and induces blunt double strand breaks in the DNA using its HNH and RuvC domain. The double strand break is unstable, and repair processes can occur. Non-homologous end joining (NHEJ) can be used in which a repair complex of proteins facilitates insertions and deletions (indels) into the break area. Improper number of nucleotides or improper synthesized nucleotide can result in downstream stop codons or nonsense mediated decay (NMD). Homology directed repair is another repair mechanism in which supplement DNA can be integrated in the break to edit the genome. *Permission for adaptation and usage from company Diagenode, Inc.*

After the introduction of CRISPR/Cas9 by Jinek et al, CRISPR/Cas9 was then utilized to edit mouse and human cell line genomes. This study confirmed the importance of the guide RNA to the target a specific genomic locus for assembly and recruitment of Cas9 to make DNA breaks, and demonstrated the potential for this system as an easy to use research tool (130). In addition to Cas9 being directed towards genes for editing, CRISPR/Cas9 has also been utilized for other reasons such as to enhance or repress gene expression. Jinek et al, in their landmark paper, revealed that introducing point mutation in the HNH and RuvC nuclease domains, prevented the ability of Cas9 to make cut DNA (140). Mutations in one or both domains has dubbed this type of cas9 as a nuclease deficient or “dead” Cas9 (dCas9). These dCas9s have been fused to different effector proteins such as transcriptional activators to enhance transcription, and thus subsequent gene expression. These CRISPR/dCas9 activators range in variety due to type of scaffolding of guide RNA as well as the number, type, and place of the transcriptional activators fused to dCas9(149). I have employed both CRISPR/Cas9 and CRISPR/dCas9 activation (CRISPRa) for gene alteration in mouse and human cell lines on multiple projects.

CHAPTER III

SR-B1 uptake of HDL promotes prostate cancer proliferation and tumor progression

This research was originally published in the Journal of Biological Chemistry. C. Alicia Traughber, Emmanuel Opoku, Gregory Brubaker, Jennifer Major, Hanxu Lu, Shuhui Wang Lorkowski, Chase Neumann, Aimalie Hardaway, Yoon-Mi Chung, Kailash Gulshan, Nima Sharifi, J. Mark Brown, Jonathan D. Smith. Uptake of High-Density Lipoprotein by Scavenger Receptor Class B Type 1 Is Associated With Prostate Cancer Proliferation and Tumor Progression in Mice. [published online ahead of print, 2020 May 1]. J Biol Chem. 2020;jbc.RA120.013694. doi:10.1074/jbc.RA120.013694

III.1 Introduction

Prostate cancer is the most common malignancy and second leading cause of cancer-related deaths among men in the United States (3). The association of HDL levels with prostate cancer risk has been inconsistent, with some studies showing a positive association (66,87) some showing an inverse association (88,150), and others showing no association (151,152). HDL biogenesis is mediated by ATP-binding cassette transporter A1 (ABCA1), which assembles cellular lipids with exogenous lipid-poor apolipoprotein A1 (apoA1) to generate nascent HDL (47). HDL uptake in tissues is facilitated by SR-B1 (94), which can also mediate bidirectional cholesterol transport between cells and HDL (51,153-155). SR-B1, encoded by the *SCARB1* gene, is highly expressed in the liver, and even more so in steroidogenic tissues, such as the adrenals, testes, and ovaries where it mediates cholesterol uptake, to promote cholesterol ester (CE) storage used for steroid hormone synthesis (95,98).

It has been reported that prostate cancer accumulates CE in lipid droplets that correlates with prostate cancer aggressiveness (117). This phenotype was attributed to PTEN deletion that ultimately resulted in upregulation of the LDL receptor (LDLR) and

subsequent uptake of LDL cholesterol (117). SR-B1 is inducible by androgens in human hepatoma cells and primary monocyte macrophage (156). Moreover, reports suggest that androgens during puberty are responsible for lower HDL levels in men vs. women, most likely due to higher hepatic SR-B1 levels (64,65,157,158). A prior study found that SR-B1 is upregulated in high grade vs. low grade prostate cancer, and in metastatic vs. primary prostate cancer, while the LDLR was not altered in high grade or metastatic prostate cancer (112). Furthermore it was shown that that high vs. low SR-B1 expression in prostatectomy specimens was associated with decreased progression-free survival (112). In a small study, SR-B1 mRNA levels were significantly higher in prostate cancer tissue vs. matched normal prostate tissue (111). In our study, we examined the effect of HDL on prostate cancer cell growth, proliferation, and tumor progression. We found that HDL, in an SR-B1-dependent manner, promoted increased prostate cancer cell growth *in vitro*. In a syngeneic mouse model, a high HDL environment promoted tumor progression in an SR-B1-dependent manner. These results suggest that SR-B1 and HDL uptake promote prostate cancer progression and that inhibiting HDL uptake may be a viable target for decreasing disease burden.

III.2 Materials and Methods

III.2.1 Cells and Chemicals

The human prostate cancer cell line DU145 and mouse prostate cancer cell line TRAMP-C2 were purchased from American Type Culture Collection (Manassas, VA). DU145 cell line was authenticated by Genetica cell line testing. DU145 was cultured in RPMI1640 (supplemented with 10 % FBS (Sigma) and TRAMP-C2 was cultured in DMEM supplemented with 10% FBS (Sigma) and 10 nM dihydrotestosterone (Sigma) at 37 °C in 5 % CO₂. Both cell lines were grown and treated with low-dose mycoplasma removal agent

(MP Biomedicals) as a preventative measure. Mycoplasma testing was performed regularly to confirm absence of mycoplasma contamination. SR-B1 rabbit polyclonal antibody (NB400-104) was purchased from Novus Biologicals. GAPDH rabbit polyclonal antibody (sc-25778) was purchased from Santa Cruz. Lipoprotein deficient serum (LPDS) was prepared as previously described (159). In brief, FBS was adjusted to 1.21 g/ml, then centrifuged to separate lipoprotein from sera. LPDS was collected and dialyzed against PBS (pH 7.4), and then sterilized using a 0.22 μ m filter. LPDS was adjusted to 30 mg/ml protein using PBS.

III.2.2 Isolation and labeling of lipoproteins

For lipoprotein isolation and labeling expired de-identified human plasma was collected from normal healthy volunteers was acquired from the Cleveland Clinic blood bank under an exempt Institutional Review Board protocol. LDL (1.019–1.063 g/mL) and HDL (1.063–1.21 g/mL) were isolated by potassium bromide density gradient centrifugation as described (159). Lipoproteins were dialyzed against PBS (pH 7.4), sterilized using a 0.22 μ m filter, and then protein concentration was determined by the Alkaline-Lowry method (160). HDL was labeled with Alexa568 by incubating 4.5 mg Human HDL in 90 μ l 1 M sodium bicarbonate with Alexa Fluor 568 succinimidyl ester (A20003, Thermo Fisher) for 1 hr at room temperature (8:1 dye:estimated apoA1 mole ratio). The reaction was stopped by incubating the conjugate with 0.1 ml of 1.5 M hydroxylamine (pH 8.5) for 1 hr at room temperature. The conjugate was purified by extensive dialysis with PBS. For murine lipoprotein isolation and quantification, blood from the retro-orbital venous sinus was collected and centrifuged at 12,000xg for 30 minutes.

III.2.3 Cell accumulation, proliferation, and cell cycle analysis of prostate cancer cells.

For cell accumulation, proliferation and cell cycle analysis, cells were seeded into a 24-well at densities of 10,000 and 20,000 cells/well for TRAMP-C2 and DU145 cells, respectively in 10% FBS containing media overnight, then incubated with serum free media for 30 minutes. Cells were then incubated in 10% LPDS with or without 300 µg/ml HDL in the absence or presence of 1 µM Lovastatin for 4 days. Thereafter, cells were lifted by trypsin and counted using the automated cell counter (Z series) by Beckman Coulter. For cell proliferation analysis, cells were labeled with 2×10^{-6} M PKH26 (Sigma) for 5 minutes, then plated in 10% FBS media overnight and subsequently treated with 300 µg/ml HDL in 10% LPDS media for 5 days and quantified by flow cytometry. For cell cycle analysis, cells were treated with or without 300 µg/ml HDL in 2% LPDS media for 1 day, ethanol fixed, stained with 50 µg/ml propidium iodide, and then subjected to flow cytometry.

III.2.4 Generation of SR-B1 KO cells.

In order to generate SR-B1 KO cell lines, TRAMP-C2 cells were transfected with the Cas9 expression plasmid, pSpCas9(BB)-2A-Puro (Addgene #48139) using Lipofectamine LTX & Plus Reagent (Invitrogen) according to manufacturer instructions, then treated with 5 µg/ml puromycin for 2 days to clonally select for Cas9 stably transfected TRAMP-C2 cells. Nucleofection (Amaxa), according to manufacturer, was used to transfect 1×10^6 Cas9 stable TRAMP-C2 cells with 0.6 nM mouse SR-B1 sgRNA targeting exon 4. Human DU145 cells (1×10^6) were co-transfected with 0.6 nM human SR-B1 sgRNA targeting exon 4 complexed with 0.07 nM Cas9 protein (Synthego) by nucleofection. Both sgRNAs were designed using CRISPOR online software (161) and synthesized by Synthego. sgRNA sequences can be found in **Table 3.1**. Transfected cells were plated in 96-well dishes to approximately 1 cell/well then clonally expanded and screened via PCR-Sanger

sequencing to detect targeted sequence disruptions, and then by Western blot for SR-B1.

PCR screening primers are in **Table 3.1**

sgRNAs	Sequence
<i>musg</i> SCARB1	UGCGGUUCAUAAAAGCACGC
<i>husg</i> SCARB1	CAUGAAGGCACGUUCGCCGA
PCR Screening Primers	Sequence
<i>musg</i> SCARB1-Fwd	GGTTCCATTTAGGCCTCAGGT
<i>musg</i> SCARB1-Rev	CTCTCTGAAGGGACAGAAGACAC
<i>husg</i> SCARB1-Fwd	CCAGTGGGTTCTGAGTTTCCA
<i>husg</i> SCARB1-Rev	GATCCCCAGCCAGCTACAAAGC

Table 3.1 sgRNAs and screening primers for mouse and human SCARB1

III.2.5 HDL uptake assay.

For HDL uptake assays, approximately 100,000 cells/well were seeded onto a 24-well plate and incubated overnight in 10% FBS containing media. Cells were then incubated with serum free media for 30 minutes and then treated with 20 µg/ml Alexa568-HDL, as described above, for 90 minutes. Cells were fixed, then counterstained with DAPI for microscopy, or stained first, then formalin fixed for flow cytometry.

III.2.6 Cholesterol Mass Assay

To evaluate cholesterol mass, cells were plated on a 6-well plate and incubated overnight in the medium, 10% FBS containing media. Cells were incubated in serum free media for 30 minutes and treated with or 200 µg/ml HDL for 2 days. Cholesterol concentrations were measured by an enzymatic fluorescent assay and normalized to protein as described by (162).

III.2.7 Western blot assay

For protein expression via Western blot, cell lysates were prepared in RIPA buffer (Pierce), containing 1 mM phenylmethylsulfonyl fluoride and 10% protease inhibitor cocktail (Sigma). Equal amounts of proteins were electrophoresed on 4–20 % SDS–PAGE and transferred to polyvinylidene difluoride membranes. Each membrane was incubated with a 1:2000 dilution of primary antibodies described above. Blots were developed with a 1:5000 dilution of the HRP-conjugated secondary antibody (BioRad). Proteins were visualized, using Amersham Hyperfilm ECL (GE Healthcare).

III.2.8 Syngeneic *in vivo* studies

Our *in vivo* studies used 20–22-Week-old, age-matched, apoA1-KO on and WT C57BL/6J male mice were subcutaneously injected in both flanks with 2×10^6 SR-B1 KO or WT TRAMP-C2 (syngeneic) prostate cancer tumor cells per site. Tumor progression and body weights were assessed three times per week for eight weeks or until reaching an experimental endpoint of tumor reaching 15 mm in diameter, tumor ulcerations, impaired mobility, or 20% loss in body weight. Tumor volume, based on caliper measurements, was calculated according to the ellipsoid volume formula, tumor volume = (the shortest diameter)² × the largest diameter × 0.525. After a mouse reached its endpoint, its final tumor volumes were included in the analysis up to the day that all mice from that group reached its endpoint, after which data were no longer plotted. All experiments and procedures were approved by Institutional Animal Care and Use Committee (IACUC) of the Cleveland Clinic, Cleveland, OH, USA (Protocol No. 2016-1722).

III.2.9 Bioinformatics

Bioinformatic information was acquired and viewed by The UCSC Xena browser (163) to visualize and extract expression data for *SCARB1*, *LDLR*, *ABCA1*, and *ABCG1* in normal and prostate cancer tissue from the TCGA PRAD dataset. The Genotype-Tissue

Expression (GTEx) Project (19) was supported by the Common Fund of the Office of the Director of the National Institutes of Health, and by NCI, NHGRI, NHLBI, NIDA, NIMH, and NINDS. The data used for the analyses described in this manuscript were obtained from the following independent searches [SCARB1], [rs4765623], [rs12582221], on the GTEx Portal on 01/08/2020; dbGaP accession number phs000424.v8.p2. LDlink (164) was used to evaluate the linkage disequilibrium of *SCARB1* SNPs [rs12582221] and [rs4765623] in the CEU population of the 1000 Genomes Project, with reference genome GRCh37/gh19 on 01/08/2020; LDlink phase 3, version 5.

III.2.10 Statistical Analysis

Statistical analysis of TCGA PRAD gene expression data from matched pairs of prostate cancer and normal adjacent tissue was analyzed by the Wilcoxon paired non-parametric signed rank test, and % changes were calculated from the antilog 2 of the median values. All *in vitro* data are expressed as the mean \pm SD of at least triplicates. Differences between the values were evaluated by either the Student T-test, with Bonferroni correction for multiple tests when appropriate, or one-way analysis of variance (one-way ANOVA) with Tukey's or Dunnett's post-hoc analysis, with $p < 0.05$ considered statistically significant. ANOVA annotation uses lettering (a, b, c, etc.), where groups not sharing the same letter indicates $p < 0.05$. All *in vivo* tumor volume data is expressed as mean \pm SEM Differences between the tumor volumes during the time course were evaluated two-way analysis of variance (two-way ANOVA). Survival curve data was evaluated by Mantel-Cox Log Rank analysis. Statistics were performed using GraphPad Prism V.8.1.1 software.

III.3 Results

III.3.1 *SCARB1* is upregulated in human prostate cancer

Previous studies have focused on lipoprotein receptors in prostate cancer, and how their changes may influence cholesterol transport in prostate cancer (111,112,117,126). Therefore, we evaluated expression of SR-B1, LDLR, ABCA1, and ABCG1 in RNA-seq data from a total of 52 normal prostate and 498 prostate cancer tumor tissues from the TCGA PRAD dataset (19). Since the LDLR expression levels in normal prostates were not normally distributed, non-parametric statistics were used for all gene expression data. The median log₂ expression levels of *SCARB1* mRNA in normal prostate and prostate cancer were 9.82 and 10.48, respectively, representing a 58% increase in SR-B1 mRNA in prostate cancer ($p < 0.0001$, **Fig. 3.1**). In contrast, LDLR mRNA was 31.5% lower ($p = 0.0006$; Fig. 1) in prostate cancer tissue, congruent with a previous report (111). The mRNA for the cholesterol efflux protein ABCA1 was unchanged between normal and prostate cancer tissue, whereas ABCG1 expression was 77% higher in prostate cancer ($p < 0.0001$; **Fig. 3.1**).

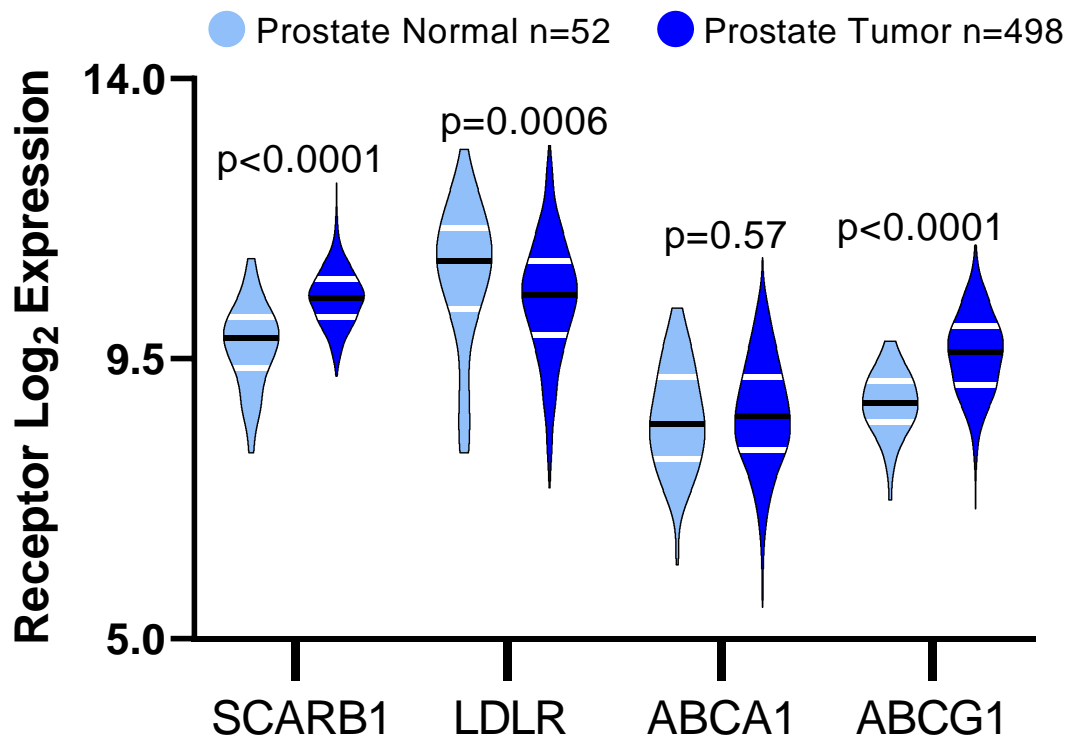


Figure 3.1. Expression of lipoprotein metabolism genes in normal prostate and prostate tumor tissue. mRNA expression of SCARB1, LDLR, ABCA1, and ABCG1 analyzed from TCGA PRAD RNA sequencing data (N=52 normal samples and N=498 tumor samples; median values shown (black line) and interquartiles (white lines); Mann-Whitney non-paired, non-parametric test p-values displayed).

III.3.2 HDL increased cell proliferation and cholesterol levels in prostate cancer cells

Since other studies (111,112) and our analysis of the TCGA data set showed upregulation of SR-B1 in prostate cancer (**Fig. 3.1**), we hypothesized that HDL may drive an increase of total cholesterol levels, similarly to what was previously illustrated for LDL (117). WT Human DU145 and mouse TRAMP-C2, expressing SR-B1 (SR-B1^{+/+}), prostate cancer cells were incubated with 200 µg/ml HDL for 2 days leading to 48% (p<0.01) and 15% (p<0.05) increases in total cellular cholesterol levels (**Fig. 3.2**), similar to that of LDL cholesterol (**Supplemental Figure 3.7**). We next determined if HDL could promote proliferation of prostate cancer cells by evaluating the impact on cell number. DU145 and TRAMP-C2 cells were treated with or without 300 µg/ml HDL in LPDS for 4 days. HDL induced 29% (p=0.0061) and 68% (p<0.0001) increases in cell number in DU145 and TRAMP-C2 cells, respectively (**Fig. 3.3**). To determine if this increase in cell number was due to increased cell proliferation, we performed a PKH26 dye-dilution assay in absence or presence of 300 µg/ml HDL. Flow cytometry analysis demonstrated that median fluorescence intensity (MFI) were significantly lower in HDL treated vs. untreated cells indicating more rounds of proliferation in both DU145 (26% decrease, p<0.001) and TRAMP-C2 (17% decrease, p<0.001) prostate cancer cells (**Fig. 3.3**).

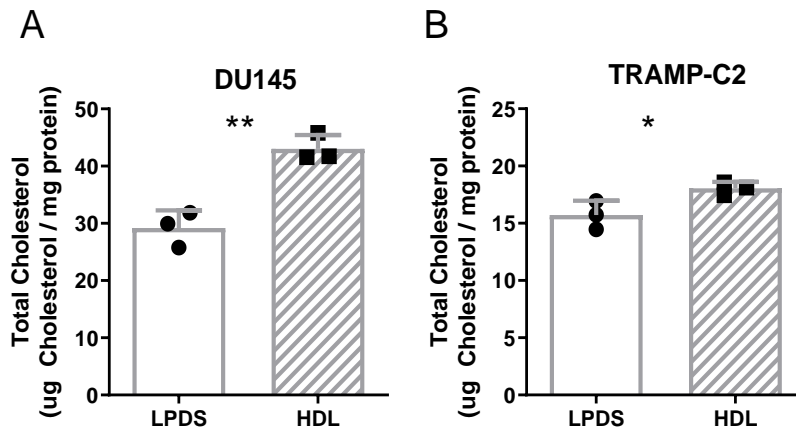


Figure 3.2. HDL effects on total cholesterol levels in prostate cancer cells. A) human DU145 and B) mouse TRAMP-C2 cells were incubated with \pm 200 μ g/ml HDL for 2 days in LPDS and total cholesterol levels normalized to cell protein determined (N=3; mean \pm SD; *, $p < 0.05$; **, $p < 0.01$, by t-test).

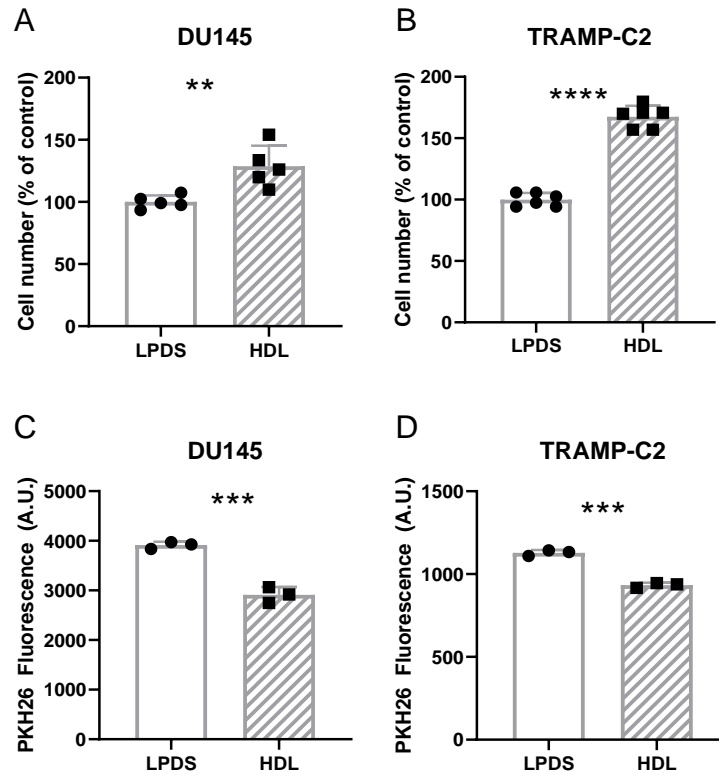


Figure 3.3. HDL effects on cell accumulation and proliferation of prostate cancer cells. A) human DU145 (N= 5 over 2 independent experiments) and B) mouse TRAMP-C2 (N=6 over 3 independent experiments) cells were treated ± 300 µg/ml HDL in LPDS media for 4 days and the final cell counts were normalized to the LPDS control. C, D) human DU145 and mouse TRAMP-C2 cells were labeled with the dye PKH26 and treated with ± 300 µg/ml HDL in LPDS media for 5 days and final dye dilution was analyzed by flow cytometry. Values are expressed as the mean ± SD; **p<0.01; ***, p<0.001. ****p<0.0001 by t-test.

III.3.3 SR-B1 is required for HDL-mediated prostate cancer growth *in vitro*

Due to the response of prostate cancer cells to HDL, we next determined if these HDL effects were mediated by SR-B1. BLT-1 inhibition of SR-B1 blunted HDL mediated effects on cell number (**Supplemental Fig. 3.8**) and reduced uptake of HDL-cholesterol (**Supplemental Fig 3.8**). To evaluate effects without off target effects by chemical inhibition, we knocked out SR-B1 in both the human and mouse prostate cancer cell lines using CRISPR/Cas9 targeting exon 4, an early coding exon of the *SCARB1* gene, to generate cell lines with complete knockout of SR-B1 expression. Western blot demonstrated successful SR-B1 KO clones (SR-B1^{-/-}) for both DU145 and TRAMP-C2 (**Fig. 3.4A**). Although HDL increased the relative cell number for both DU145 SR-B1^{+/+} (59.3% increase, p<0.0003) and SR-B1^{-/-} cells (23.4% increase, p=0.011), the increase in cell accumulation in response to a 4-day 200 µg/ml HDL treatment was significantly attenuated upon knockout of SR-B1 (**Fig. 3.4B**, p<0.0003, % control cell number in HDL-treated SR-B1^{+/+} vs. SR-B1^{-/-}). KO of SR-B1 in DU145 cells resulted in decreased HDL-cholesterol and HDL-cholesterol ester uptake (**Supplemental Fig. 3.9**). For the TRAMP-C2 line we isolated three independent SR-B1^{-/-} clonally-derived cell lines from edited TRAMP-C2 cells, and their cell accumulation in LPDS was evaluated, showing that the SR-B1^{-/-} #5 line accumulated the least cells (p=0.02 vs. TRAMP-C2 SR-B1^{+/+}), the SR-B1^{-/-} #10 line accumulated the most cells (NS vs. TRAMP-C2 SR-B1^{+/+}), and the SR-B1^{-/-} #17 line was most similar in cell number to SR-B1^{+/+} TRAMP-C2 cells (NS, **Fig. 3.4C**). The response of these cell lines to HDL was evaluated, normalized to the LPDS control for each of these lines. HDL significantly increased cell accumulation in WT cells (98% increase p=0.011), but not in any of the three SR-B1^{-/-} lines (**Fig. 3.4D**). Thus, we chose to further utilize and characterize HDL treatment on cellular processes in the SR-B1^{-/-} #17

cell line, as its basal growth levels in LPDS were the most similar to that of the TRAMP-C2 SR-B1^{+/+} cells (**Fig. 3.4C**).

We next investigated if absence of SR-B1 impacts cell cycling upon HDL treatment by treating TRAMP-C2 SR-B1^{+/+} and SR-B1^{-/-} cells with or without 300 µg/ml HDL in LPDS for 1 day, then assessing the fraction of cycling cells in G₂+S phase via propidium iodide content. We demonstrated that HDL increased the proportion of SR-B1^{+/+} cells cycling by 38% vs. the LPDS control (p=0.002), whereas in SR-B1^{-/-} cells there was only a 17.5% increase cycling cells in response to HDL (p=0.012, **Fig. 3.4E**). The HDL effect on cell cycling was significantly greater in SR-B1^{+/+} vs. SR-B1^{-/-} cells (p=0.001, **Fig. 3.4E**).

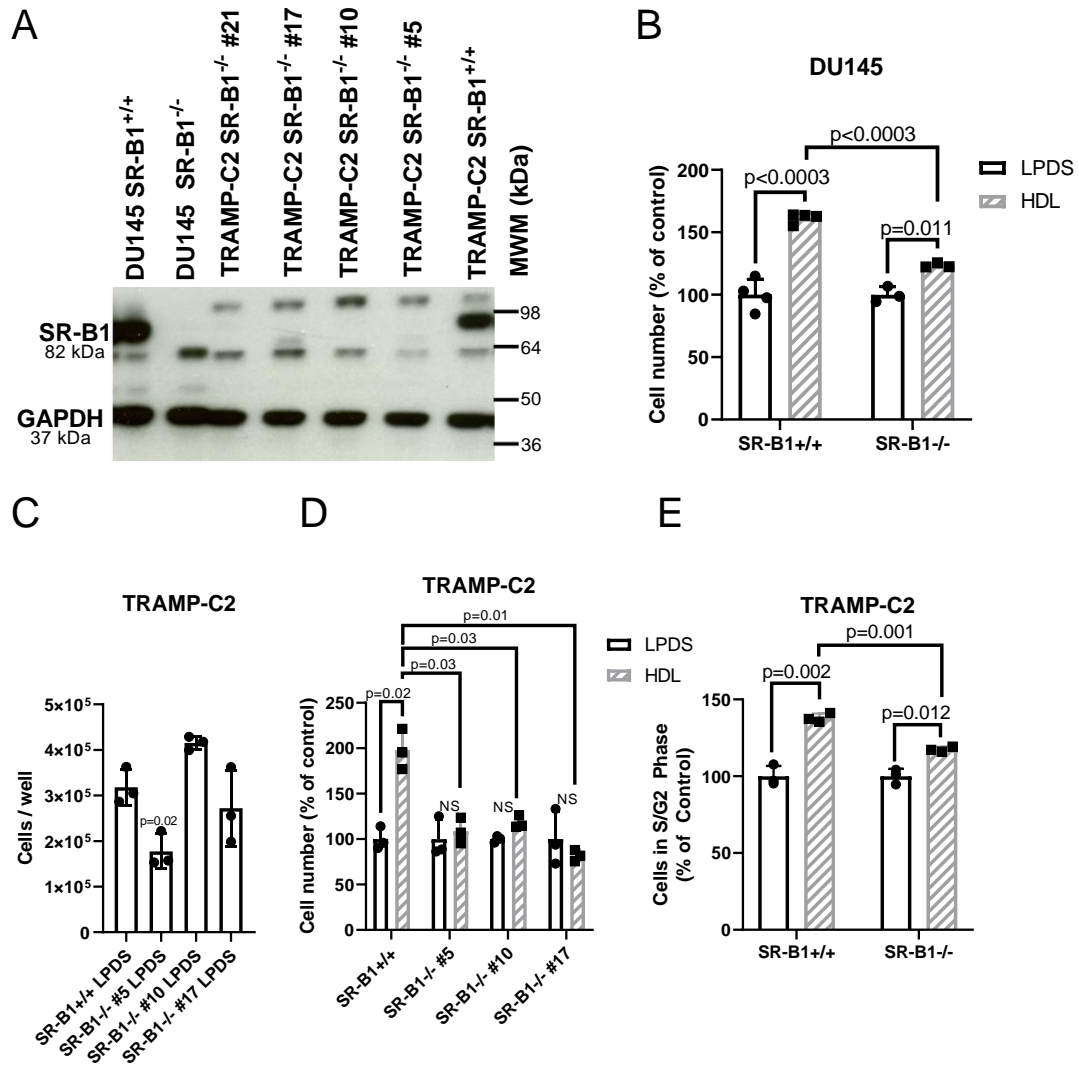


Figure 3.4. HDL effects in WT and SR-B1 KO cells. A) Western blot for SR-B1 in WT and SR-B1 KO DU145 and TRAMP-C2 cells. B) Cell accumulation assay for DU145 WT and SR-B1 KO cells incubated \pm 300 μ g/ml HDL in LPDS for 3 days (N=3-4; mean \pm SD; t-test with Bonferroni correction for 3 tests; p-values displayed). C) Cell number of SR-B1^{+/+} TRAMP-C2 cells and three independent SR-B1^{-/-} clonally derived cell lines after incubation in 10% LPDS for 3 days (N=3; mean \pm SD; ANOVA with Dunnett's post-test comparing to SR-B1^{+/+} cells; p-value displayed). D) Cell accumulation in TRAMP-C2 SR-B1^{+/+} and three SR-B1^{-/-} clones incubated \pm 200 μ g/ml HDL for 3 days normalized to each cell lines LPDS control (N=3; mean \pm SD; t-test with Bonferroni correction for 7 tests (4 tests \pm HDL for each line and 3 tests of HDL treated SR-B1^{+/+} vs. SR-B1^{-/-} clones), significant p-values displayed). E) Cell cycle analysis in TRAMP-C2 SR-B1^{+/+} and SR-B1^{-/-} cells treated \pm 300 μ g/ml HDL in LPDS media for 1 day (% of cells in S+G₂ phases; N=3; mean \pm SD; t-test with Bonferroni correction for 3 tests, p-values displayed).

To confirm that HDL-uptake was impacted upon KO of SR-B1, we incubated TRAMP-C2 SR-B1^{+/+} and SR-B1^{-/-} cells with Alexa568-HDL. Fluorescent microscopy showed that SR-B1^{+/+} cells took up more Alexa568-HDL as compared to SR-B1^{-/-} cells (**Fig. 3.5A**). This was further confirmed by flow cytometry, where the cells were treated with 20 µg/ml Alexa568-HDL with or without 2 mg/ml unlabeled-HDL competitor. The cellular uptake of Alexa568-HDL was determined by median fluorescence intensity (MFI) showing that the SR-B1^{-/-} cells had reduced total and specific Alexa568-HDL uptake compared to the SR-B1^{+/+} cells by 44.1% (p=0.002) and 59.6%(p=0.007), respectively (**Fig. 3.5B**). To investigate if cholesterol is involved in the HDL effect on cell accumulation, we treated SR-B1^{+/+} or SR-B1^{-/-} cells with or without 1 µM lovastatin to reduce endogenous cholesterol biosynthesis, which significantly decreased cell accumulation in both cell lines (p<0.05, **Fig. 3.5C**). HDL treatment for 4 days added to the lovastatin significantly rescued the cell accumulation only in the SR-B1^{+/+} cells (p<0.05 vs. lovastatin alone, **Fig. 3.5C**). These findings were partially recapitulated in the DU145 WT and KO lines (**Supplemental Fig. 3.10**). This suggests that HDL provides cholesterol, in an SR-B1-dependent manner, to help cells grow when de novo cholesterol was reduced by statin treatment (**Fig 3.5C**).

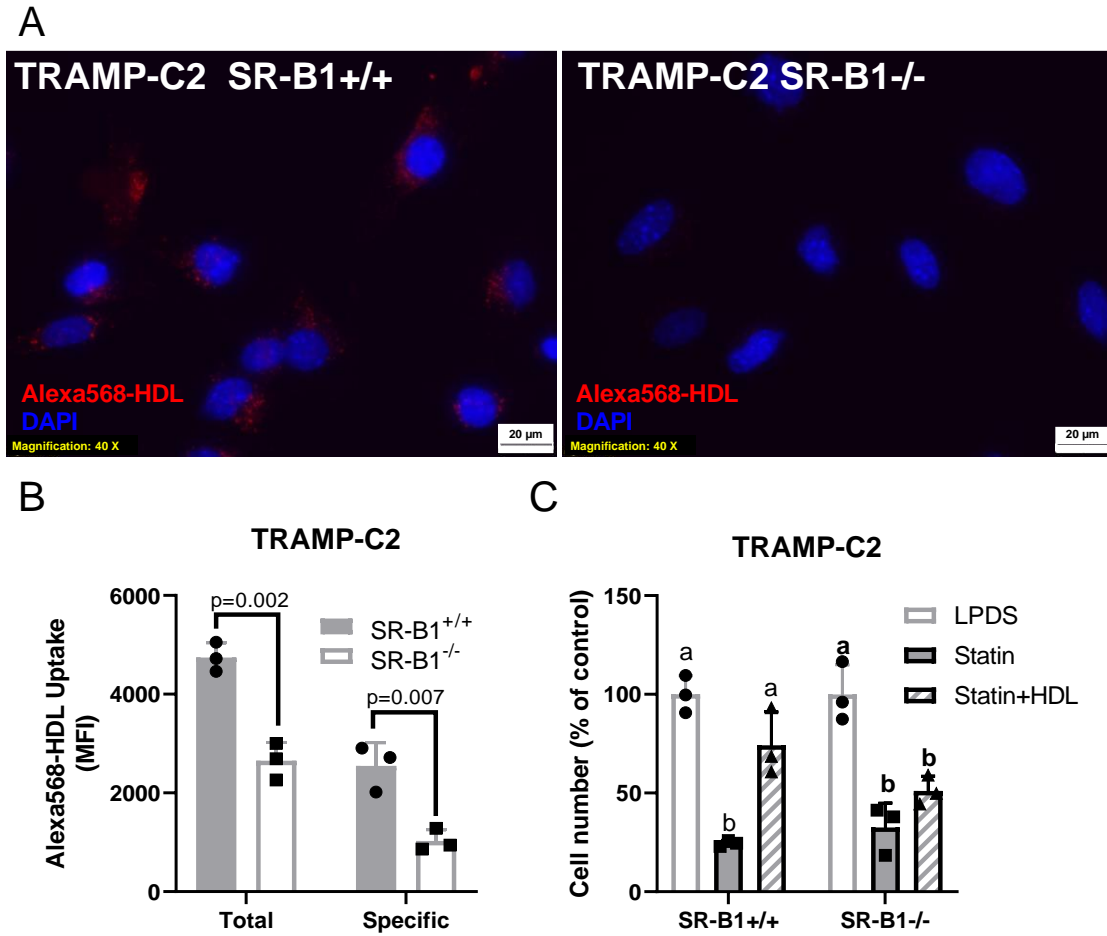


Figure 3.5. HDL uptake and impact on statin treated cells. TRAMP-C2 SR-B1^{+/+} or SR-B1^{-/-} cells were incubated with 20 µg/ml Alexa568-HDL for 90 minutes, then counter stained with DAPI. A) Epifluorescent microscopy. B) Total and specific uptake analysis by flow cytometry with TRAMP-C2 SR-B1^{+/+} and SR-B1^{-/-} cells treated with 20 µg/ml Alexa568-HDL and ± 2mg/ml unlabeled HDL for 90 minutes in serum free media (n=3, mean ± SD; t-test p-values displayed). C) Cell accumulation of TRAMP-C2 SR-B1^{+/+} and SR-B1^{-/-} in LPDS treated with ± 1 µM lovastatin and 100 µg/ml HDL for 4 days normalized to untreated cells (n=3, mean ± SD; different letters represent p<0.05 by ANOVA with Tukey posttest within each cell type).

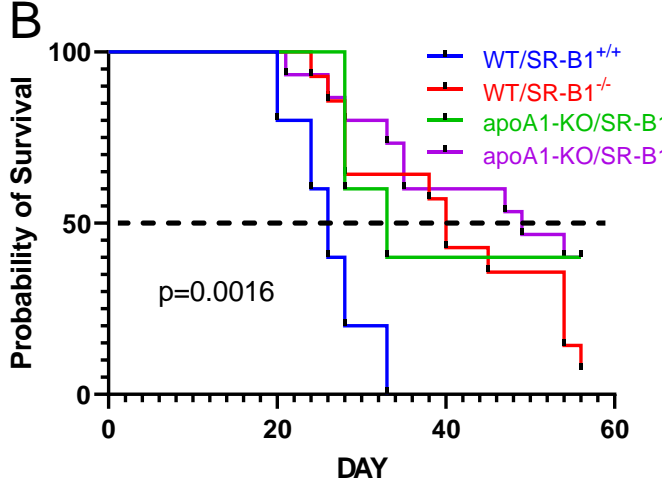
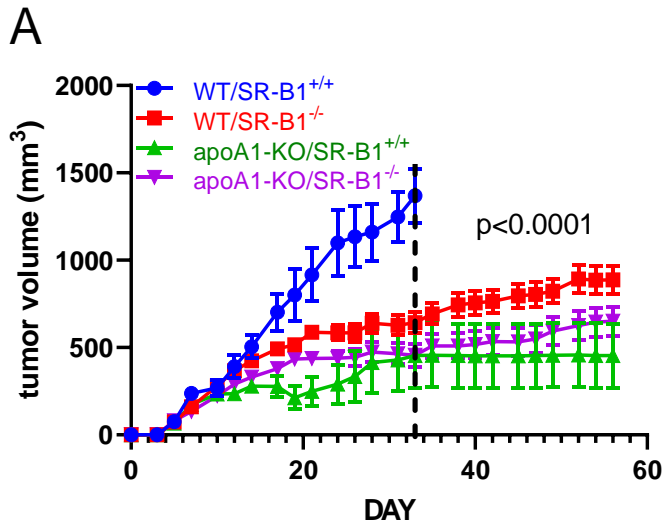
III.3.1 HDL and SR-B1 effects on prostate cancer progression *in vivo*

We hypothesized that elevated HDL levels may promote tumor progression in an SR-B1-dependent manner. To test our hypothesis, we utilized C57BL/6J WT and apoA1-KO mice as high and low HDL models. WT mice had fasting total and HDL cholesterol levels of 97 ± 15 mg/dL and 63 ± 17 mg/dL, respectively. apoA1-KO mice had significantly lower levels of total and HDL-cholesterol (32 ± 8 mg/dL and 18 ± 9 mg/dL, respectively) vs. WT hosts ($p < 0.0001$ for both, **Supplemental Fig 3.11A**). WT mice weighed more than apoA1-KO mice ($p < 0.0001$, **Supplemental Fig 3.11B**); however, there were no differences in testes weights (*Fig. Supplemental Fig 3.11C*). We measured plasma testosterone, and the data was not normally distributed with several outliers. Nonparametric T-tests found no effect on testosterone levels between WT and apoA1-KO mice (**Supplemental Fig. 3.11D**); however, removal of the two outliers in each group, resulted in normally distributed data showing 42% reduced testosterone levels in apoA1-KO mice ($p = 0.009$, **Supplemental Fig. 3.11E**). Dihydrotestosterone levels were undetectable in most mice (not shown).

To test our central hypothesis of the effects of host HDL and tumoral SR-B1 status on tumor progression, we performed a four-arm study using 2×10^6 syngeneic TRAMP-C2 SR-B1^{+/+} or SR-B1^{-/-} cells that were subcutaneously injected into WT or apoA1-KO mice on the C57BL/6J background. Over an 8-week time course SR-B1^{+/+} and SR-B1^{-/-} cells formed solid tumors in WT and apoA1-KO mice. Histology of H&E stained tumors from all study arms showed unorganized sheets of cells with irregular shaped nuclei (**Supplemental Fig. 3.12**). Tumors from all group were characterized as aggressive by a clinical pathologist. Tumor volume ($p < 0.0001$, **Fig. 3.6A**) and survival ($p = 0.0016$, **Fig. 3.6B**) were significantly different in the treatment arms.

First examining the host mouse effects (shown in the rows in **Fig. 3.6C**) using SR-B1^{+/+} cells, WT mice injected with SR-B1^{+/+} cells (WT/SR-B1^{+/+}) had significantly larger tumors vs. apoA1-KO mice injected with SR-B1^{+/+} cells (apoA1-KO/SR-B1^{+/+}) ($p < 0.0001$, **Fig. 3.6A, C**). Additionally, the WT/SR-B1^{+/+} group all reached their human endpoint by day 33 with median survival of 26 days, and their log-rank survival was significantly shorter vs. the apoA1-KO/SR-B1^{+/+} group (median survival of 33 days, $p = 0.049$, **Fig. 3.6B,C**). Examining the host effects using SR-B1^{-/-} cells, WT mice injected with KO cells (WT/SR-B1^{-/-}) had significantly larger tumors vs. apoA1-KO mice injected with SR-B1^{-/-} cells (apoA1-KO/SR-B1^{-/-}) ($p < 0.0001$, **Fig. 3.6A, C**). The WT/ SR-B1^{-/-} group (median survival of 40 days) trended towards shorter log-rank survival vs. the apoA1-KO/SR-B1^{-/-} group (median survival of 49 days, $p = 0.13$, **Fig. 3.6B, C**). Thus the host effect was clear, mice with higher HDL levels promoted more rapid tumor progression, with shorter survival.

Next examining the SR-B1 receptor effects in WT hosts (shown in the columns in **Fig. 3.6C**), the WT/SR-B1^{+/+} group had significantly larger tumors vs. WT mice injected with SR-B1^{-/-} cells (WT/SR-B1^{-/-}) ($p < 0.0001$, **Fig. 3.6A, C**). Log-rank survival for the WT/SR-B1^{+/+} group was significantly shorter vs. the WT/SR-B1^{-/-} group ($p = 0.004$, **Fig. 3.6B,C**). Examining the SR-B1 receptor effects in apoA1-KO mice, apoA1-KO mice injected with SR-B1^{+/+} cells (apoA1-KO/SR-B1^{+/+}) had similar rates of tumor progression and survival compared to the apoA1-KO mice injected with SR-B1^{-/-} cells (apoA1-KO/SR-B1^{-/-}) (NS, **Fig. 3.6**). Thus the SR-B1 receptor effect was only evident in WT mice, where receptor expression promoted more rapid tumor progression and shorter survival.



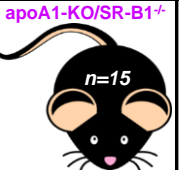
		C57BL/6J Mice		HOST EFFECT	
		WT	apoA1-KO		
TRAMP-C2 Cells	SR-B1 WT (SR-B1 ^{+/+})	 WT/SR-B1 ^{+/+} n=5	 apoA1-KO/SR-B1 ^{+/+} n=5	TUMOR $p=0.0011$	SURVIVAL $p=0.0487$
	SR-B1 KO (SR-B1 ^{-/-})	 WT/SR-B1 ^{-/-} n=14	 apoA1-KO/SR-B1 ^{-/-} n=15	TUMOR $p=0.011$	SURVIVAL $p=0.13$
RECEPTOR EFFECT		TUMOR $p=0.0002$	TUMOR $p=0.42$	Median Survival	
		SURVIVAL $p=0.004$	SURVIVAL $p=0.81$	WT/ SR-B1 ^{+/+} 26d	apoA1-KO/ SR-B1 ^{+/+} 33d
				WT/ SR-B1 ^{-/-} 40d	apoA1-KO/ SR-B1 ^{-/-} 49d

Figure 3.6. Tumor progression study in vivo. A) Tumor volumes of mice injected with 2×10^6 cells in left and right flanks, then followed for 8 weeks. Tumor volume is expressed as mean \pm SEM; WT mice SR-B1^{+/+} cells (WT/SR-B1^{+/+}, blue) n=5; WT mice SR-B1^{-/-} cells (WT/SR-B1^{-/-}, red) n=14; apoA1-KO mice SR-B1^{+/+} cells (apoA1-KO/SR-B1^{+/+}, green) n=5; apoA1-KO mice SR-B1^{-/-} cells (apoA1-KO/SR-B1^{-/-}, purple) n=15. Two-way ANOVA up to day 33 when all groups survived demonstrated group effects, time effects, and interaction effects all with $p < 0.0001$. B) Kaplan Meier survival plot ($p=0.0016$ by Mantel Cox Log Rank Sum test for all four groups). C) Summary of study design and pairwise statistical analysis of host mouse genotype and injected cell genotype effects tumor progression and survival. Tumor volume analyses involving WT/SR-B1^{+/+} group, only used data up to day 33. Pairwise two-way ANOVA group effect on tumor volumes p-values are displayed. Pairwise survival Mantel Cox Log Rank Sum group effect p-values are displayed.

III.4 Discussion

The effects of HDL are mixed on the prevalence of many cancers including, prostate, breast, endometrial, gynecologic, colorectal, biliary tract, lung, and hematological cancers (reviewed in (165)). Prostate cancer is a disease typically driven by androgens in which surgical and chemical castration have proven to slow progression of the disease (2,11). However, prostate cancer often becomes resistant to such treatments (14). The effects of HDL on prostate cancer development and progression are controversial, with both positive and inverse associations found in various studies (66,87,88,150). A meta-analysis of 14 large prospective studies found no significant effect of HDL-cholesterol on the risk of prostate cancer (89). Additionally, a Mendelian randomization study showed that the 35 SNPs associated with HDL-cholesterol did not generate a genetic risk score for prostate cancer (166). Thus, HDL levels may not affect the development of prostate cancer, but may still influence its progression.

HDL-cholesterol is sexually dimorphic, being ~10 mg/dl higher in adult women vs. men (62). However, before puberty, boys and girls have similar (high) HDL, which drop as boys go through puberty and stay unchanged as girls go through puberty (64,65). Androgens lower HDL in humans, and this is thought to be mediated by androgen induction of hepatic SR-B1(158). Thus, the effect of androgens on lowering HDL-cholesterol may partially obscure a potential positive association between HDL and prostate cancer, as androgens drive the early stages of prostate cancer.

HDL is synthesized from lipid-poor apoA1 by ABCA1; and, HDL cellular uptake is mediated by SR-B1 (47,94). Lee et al. found that ABCA1 expression was lower and ABCA1 promoter had higher DNA methylation in more vs. less advanced prostate cancer, and that ABCA1 gene expression was epigenetically silenced by DNA methylation in the LNCaP cell line (126). Schörghofer et al. demonstrated that SR-B1 mRNA expression was

higher in high grade vs. low grade prostate cancer biopsies, and also higher in metastatic vs. primary prostate cancer (112). In contrast, this study reported no difference in LDLR expression in these tissues (112). Gordon et al. also reported increased SR-B1 mRNA expression, but lower LDLR mRNA expression, in prostate cancer vs. normal prostatic tissue (111). Our TCGA data analysis showed that SR-B1 and ABCG1 mRNAs were upregulated, LDLR mRNA was decreased, and ABCA1 mRNA was unchanged in prostate cancer vs. normal tissue.

We found that HDL treatment of cells cultured in LPDS led to an increase in cell number and proliferation in both a human and a mouse prostate cancer cell line. A similar growth promoting effect of HDL was observed by Sekine et al., using prostate cancer cell lines cultured in 1% FBS. This HDL effect was associated with increased phospho-ERK1 and phospho-AKT after 30 minutes of HDL incubation (125). In both TRAMP-C2 and DU145 cells, we found that SR-B1 knockout abolished the growth promoting effects of HDL. However, Sekine et al. showed that siRNA-mediated knockdown of SR-B1 in PC3 cells did not abolish the growth promoting effects of HDL, which they attributed to ABCA1 expression (125). Gordon et al. reported that the growth of C4-2 human prostate cancer cell line in 10% FBS is inhibited by SR-B1 siRNA or by the anti-SR-B1 drug BLT-1, agreeing with our finding that SR-B1 is growth promoting in the presence of HDL.

Sekine et al. demonstrated that HDL promotes cholesterol uptake by PC3 prostate cancer cells, yet 100 µg/ml HDL in 1% FBS for 24h it did not promote an increase in total cholesterol levels in PC3, DU145, or LNCaP cell lines (125). However, we demonstrated that 200 µg/ml HDL in LPDS for 48h increased total cholesterol in DU145 and TRAMP-C2 cells (**Fig. 3.2A, B**). Furthermore, we showed that Alexa568-HDL uptake by TRAMP-C2 cells was in part mediated by SR-B1 (**Fig. 3.5A, B**), a finding that was demonstrated by Gordon et al., in C4-2 prostate cancer cells in which Dil-HDL uptake was partially reduced

upon SR-B1 knock down or chemical inhibition by BLT-1 (111). We found that inhibiting *de novo* cholesterol synthesis in TRAMP-C2 cells by lovastatin led to reduced cell accumulation, which was rescued by HDL treatment in an SR-B1 dependent fashion, suggesting that the cholesterol content of HDL may play a role in the recovery of cell accumulation (**Fig. 3.5C**). Additionally, various statins were found to promote cell cycle arrest of PC3 cells, also indicating the need for *de novo* cholesterol biosynthesis to drive prostate cancer cell proliferation (167). Four meta-analyses of human observational studies on statin use and prostate cancer incidence, progression, and mortality have been published in 2016 or later, with three finding beneficial effects of statins (168-171). For example, prostate cancer specific mortality was significantly reduced in statin users pre- and post-diagnosis with prostate cancer (HR =0.53 and 0.64, respectively) (168). Thus, cholesterol metabolism may play an important role in prostate cancer therapeutics.

A large meta-analysis demonstrated that increased HDL-cholesterol was associated with lower incidence of cancer; although this study did not examine different types of cancer (172). This finding was corroborated in C57BL/6J mice using syngeneic B16F10 melanoma and Lewis Lung carcinoma cells injected into (going from low to high HDL-cholesterol levels) apoA1-KO, WT, and human apoA1 transgenic mice; and, for both of these cancer types higher HDL leads to smaller tumors (90). The protective effect of HDL was associated with increased tumor associated macrophages, cytotoxic CD8 T-cells, and decreased recruitment of myeloid derived suppressor cells (90,173). In addition, B16F10 melanoma tumor progression was slower in *Scarb1* KO mice, another model of high plasma HDL (173). In C57BL/6J WT and apoA1-KO mice, we found an opposite effect of host HDL on syngeneic TRAMP-C2 prostate cancer cells, where higher HDL led to larger tumors, and decreased survival.

Why do the TRAMP-C2 cells respond differently than the B16F10 and Lewis Lung cells? Perhaps it is due to the relative expression levels of SR-B1 and the role of HDL in providing lipids required for cell cycling. Llaverias et al., reported that feeding a western-type vs. chow diet to C57BL/6J TRAMP transgenic mice, which are prone to spontaneously develop prostate tumors, results in increased total and HDL-cholesterol, and a higher prostatic tumor incidence with larger tumors (91). The tumors from western type vs. chow diet-fed TRAMP mice also have higher levels of SR-B1 expression (91). The SNP rs4765623, intronic in the *SCARB1* gene, is associated with clear cell renal cell carcinoma (ccRCC), a cancer characterized by excessive lipid loading (115). This same SNP is associated with *SCARB1* expression levels in human left ventricle, with the T allele associated with increased expression (19). rs4765623 is in linkage disequilibrium with rs12582221 ($d'=1$, $r^2=0.39$) (164), and this SNP is highly associated with SR-B1 expression in testes (19). SR-B1 expression is increased in ccRCC tissue vs normal kidney tissue (114,174), similar to what we and others observed in prostate cancer vs. normal prostate. Also in alignment with our SR-B1 KO findings in prostate cancer cells, Velagapudi et al., showed that antibodies against SR-B1 reduce cellular uptake of ^{125}I -HDL into, and HDL-induced proliferation of, a ccRCC cells line (113). Thus, SR-B1 and HDL may drive proliferation of other lipid accumulating cancers. Whether HDL promotes or inhibits tumor progression may depend on tumor lipid delivery vs. host immune effects.

Our analysis and two other studies found higher SR-B1 mRNA levels in prostate cancer vs. normal prostate tissue, in high grade vs. low grade prostate cancer, and in metastatic vs. primary prostate cancer (111,112). Some prostate cancer cells may be able take up HDL-cholesterol via SR-B1 to synthesize *de novo* androgens (111,175). In general, SR-B1 expression is highest in the major HDL metabolizing organ, the liver, and in steroidogenic tissues. In humans SR-B1 expression is highest in adrenals, liver, and

ovary (19). In 9 tested tissues of C57BL/6J mice, the liver and testes had the highest expression of SR-B1 (176). The role of HDL uptake to support CE storage for steroidogenic tissue was demonstrated in apoA1-KO mice, where adrenal and ovarian CE stores, as well as stress-induced plasma corticosteroid levels, are significantly reduced (177). Although total testes CE storage was not different between WT and apoA1-KO mice, histological analysis showed markedly reduced neutral lipid loading in the Leydig cells, the site of *de novo* androgen biosynthesis (177). We measured plasma testosterone levels in 2 cages each of WT and apoA1-KO mice, and in each cage, there was one high outlier, which may be due to the well-known effect of higher testosterone levels in the socially dominant male of group-housed mice (178,179). Excluding these outliers, we found 42% higher plasma testosterone in the WT vs. apoA1-KO mice, which is a confounder for the pro-tumor effect of HDL in our study.

We found that SR-B1^{-/-} vs. SR-B1^{+/+} TRAMP-C2 cells injected into WT hosts with high HDL-cholesterol led to reduced tumor progression and increased survival, without the caveat of decreased androgen levels observed in apoA1-KO mice. Thus, SR-B1 promotes prostate cancer tumor growth *in vivo*, similar to SR-B1's growth-promoting effects we observed in cell culture. However, SR-B1 is a multi-ligand receptor that can also mediate uptake of non-HDL ligands such as LDL and fat-soluble vitamins (96,97,180). Thus, it is possible that the loss of SR-B1 in TRAMP-C2 cells reduced tumor progression due to decreased uptake of these other ligands. It appears that the growth promoting effects of SR-B1 in TRAMP-C2 cells may be primarily mediated by its ligand HDL, as SR-B1 status (KO vs. WT) has no effect on tumor progression in apoA1-KO mice; but, we cannot exclude the role of other SR-B1 ligands that may play a role in tumor progression in WT mice. Our findings on the role of SR-B1 in prostate cancer are similar to the findings of Gordon et al. who showed that treatment of mice with the SR-B1 inhibitor BLT-1 led to

reduced human PC3 cell xenograft progression (111). These findings also align well with our TCGA analysis and prior analyses showing that SR-B1 expression is higher in prostate cancer vs. controls, higher in high grade vs low-grade prostate cancer, and higher in metastatic vs. localized prostate cancer (111,112).

In conclusion, our findings are in alignment with Llaverias et al. where a high fat diet increased autochthonous tumor prevalence and burden in the TRAMP transgenic mouse model, associated with increased HDL levels (91). Additionally, our findings corroborated the *in vivo* findings of Gordon et al. who demonstrated that treatment with an SR-B1 inhibitor decreased prostate cancer progression (111). Our study was more specific and could differentiate cancer cell vs. host effects due to genetic ablation of SR-B1 in the cancer cells, whereas Gordon et al. used a chemical inhibitor of SR-B1, having specific and non-specific effects on the host as well as the xenograft cancer cells. Our study employed immunocompetent mice, which may be a better model to study HDL effects on prostate cancer since HDL has been shown to modulate tumor infiltrating leukocytes (90)

III.5 Supplemental

III.5.1 Experimental Procedures

III.5.1.1 Cholesterol Mass

To evaluate cholesterol mass, prostate cancer cells were plated on a 6-well plate and incubated overnight in the medium, 10% FBS containing media. Cells were incubated in serum free media for 30 minutes and treated with or 200 $\mu\text{g/ml}$ HDL or 50 $\mu\text{g/ml}$ HDL for 2 days. Cholesterol concentrations were measured through by an enzymatic fluorescent assay and normalized to protein as described by (162).

III.5.1.2 Cell Accumulation

For cell accumulation cells were seeded into a 24-well at densities of 10,000 cells/well for PC3 and DU145 and 20,000 cells/well for TRAMP-C2 in 10% FBS containing media

overnight, then incubated with serum free media for 30 minutes. Cells were then incubated in 10% LPDS or treated with 200 μ g/ml HDL with or without 0.5 μ M BLT-4 for 4 days. Thereafter, cells were lifted by trypsin and counted using the automated cell counter (Z series) by Beckman Coulter

III.5.1.3 HDL lipid uptake

For HDL uptake assays, approximately 100,000 cells/well were seeded onto a 24-well plate and incubated overnight in 10% FBS containing media. Cells were then incubated with serum free media for 30 minutes and then treated DU145 cells were treated with HDL labeled with 3[H]-Cholesterol Ester, 3[H]-cholesterol or dual-labeled with 3[H]-PIP2 and 14[C]-cholesterol in the absence or presence of SR-B1 inhibitor, BLT-1 (1 μ M), for 4 hours. Extracted cellular radiolabeled lipids were counted in scintillation and normalized total cell protein.

III.5.1.4 Mouse Cohort

12 and 18-week age-matched, male, WT and apoA1-KO mice that were not subjected to subcutaneous prostate cancer cells injections were assessed for plasma total and HDL cholesterol levels, body weight, testes weight, and plasma testosterone levels.

III.5.1.5 Quantification of mouse serum total and HDL cholesterol

Total and HDL cholesterol from the plasma fraction was then quantified using the Stanbio Cholesterol LiquiColor (Cat. No. 1010) enzymatic-colorimetric assay according to manufacturer's instructions and adapted to a 96-well plate format. In brief, plasma treated with or without the Stanbio precipitating reagent for HDL assay (Cat. No. 0599) was combined with Stanbio liquicolor reagent (1011) for 10 minutes at room temperature, then absorbance at 500 nm was acquired and cholesterol levels calculated versus a standard curve.

III.5.1.6 Quantification of mouse plasma testosterone

Freshly collected plasma was stored at -80°C until LC/MS/MS analysis. 60 µl of plasma was spiked with 10 µl of internal standard [25ng/ml, Androstene-3, 17-dione-2, 3, 4-¹³C₃]. Samples were extracted twice with 2 mL of methyl-tert-butyl ether (MTBE, Across). MTBE extracts were dried under nitrogen gas and then reconstituted in 120ul of 50% methanol/water (v/v). The extracted testosterone was quantified using liquid chromatography tandem mass spectrometry (LC/ MS/MS). Briefly, the extracted steroids were injected onto a Shimadzu UHPLC system (Shimadzu Corporation), and separated on a C18 column (Zorbax Eclipse Plus C18 column, 150 mm x 2.1 mm, 3.5 µm, Agilent) using a gradient starting from 20% solvent B [acetonitrile/methanol (90/10, v/v) containing 0.2% formic acid] for 4 min and then to 75% solvent B for 10 min, followed by 95% solvent B for 3 min. Testosterone was quantified on a Qtrap 5500 mass Spectrometer (AB Sciex) using ESI in positive ion mode and multiple reaction monitoring using characteristic parent → daughter ion transitions for the specific molecular species monitored. Data acquisition and processing were performed using MultiQuant software (AB Sciex; version 3.0.1). The peak area ratio of the analyte over the internal standard was used for quantification. Each sample run included a calibration curve with standards for data quantification using the analyte/internal standard peak area ratio.

III.5.1.7 H&E Staining of tumors

Formalin fixed tumors were paraffin embedded and sectioned. Sections were deparaffinized and stained with hematoxylin and eosin.

IV.5.1.8 Statistical Analysis

Cholesterol levels, body weight, and testes weight data are expressed as the mean ± SD. Differences between the values were evaluated by either the Student T-test. Hormone

levels were not normally distributed and a non-parametric t-test was performed for the testosterone and dihydrotestosterone levels. An additional parametric Student T-test analysis was performed after removing outliers greater than 2 standard deviations from the mean, normalizing the distribution of the data. Statistics were performed using GraphPad Prism V.8.1.1 software.

III.5.2 Results

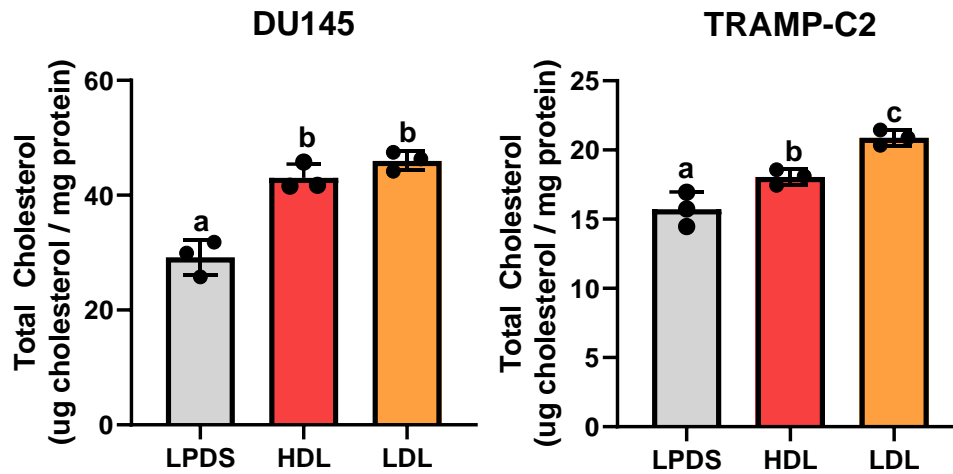


Figure 3.7. HDL and LDL effects on total cholesterol levels in prostate cancer cells. A) human DU145 and B) human PC3, and C) mouse TRAMP-C2 cells were incubated with $\pm 200 \mu\text{g/ml}$ HDL or $\pm 50\mu\text{g/ml}$ LDL for 2 days in LPDS and total cholesterol levels normalized to cell protein determined (N=3; mean \pm SD; significant difference determined by ANOVA $p < 0.05$. between groups with different lettering).

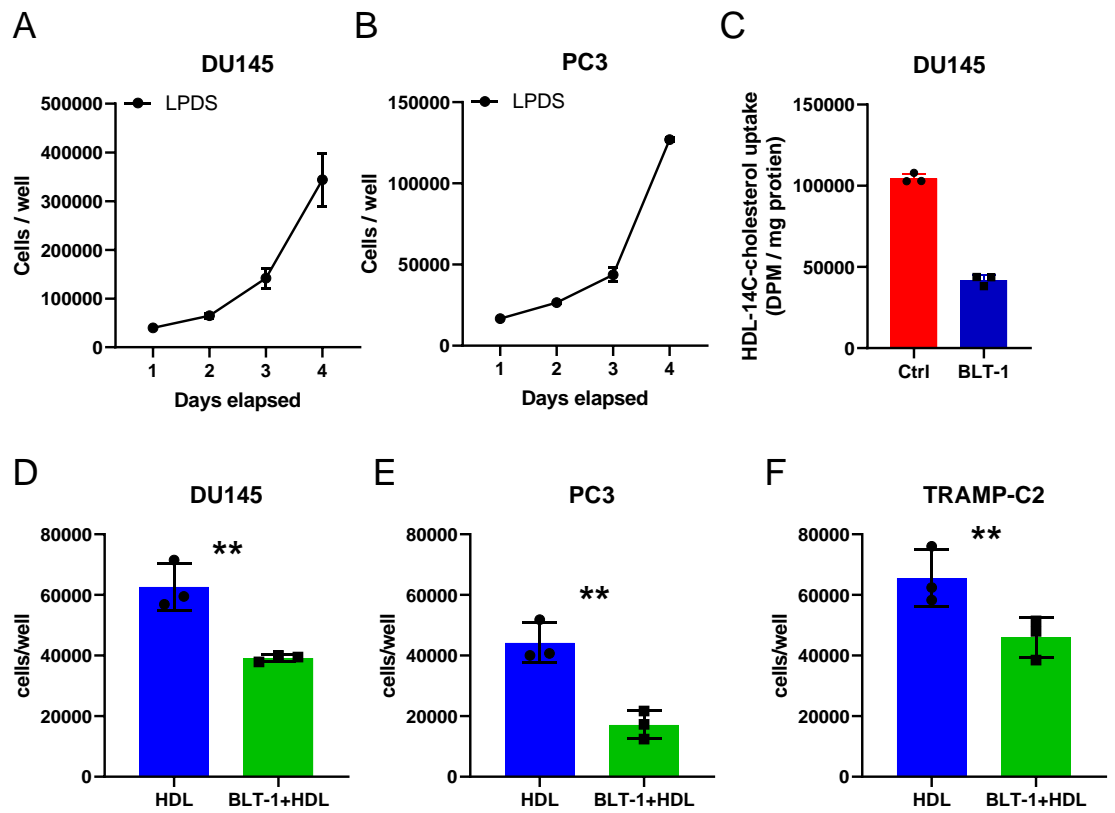


Figure 3.8 Prostate cancer cell number and lipid uptake upon SR-B1 inhibition. (A) DU145 and (B) PC3 cell growth in LPDS over 4 days. (C) DU145 cells were treated with HDL labeled with ^{14}C -cholesterol in the absence or presence of SR-B1 inhibitor, BLT-1 ($1\ \mu\text{M}$), for 4 hours. Extracted cellular radiolabeled lipids were counted in scintillation and normalized total cell protein. $N=3$, T-test; $***p<0.001$. (D) DU145, (E) PC3, and (F) TRAMP-C2 Prostate cancer cells were treated with $200\ \mu\text{g/ml}$ HDL protein and/or $0.5\ \mu\text{M}$ BLT-1 for 4d, $N=3$. T-test; $**p<0.01$, $***p<0.001$.

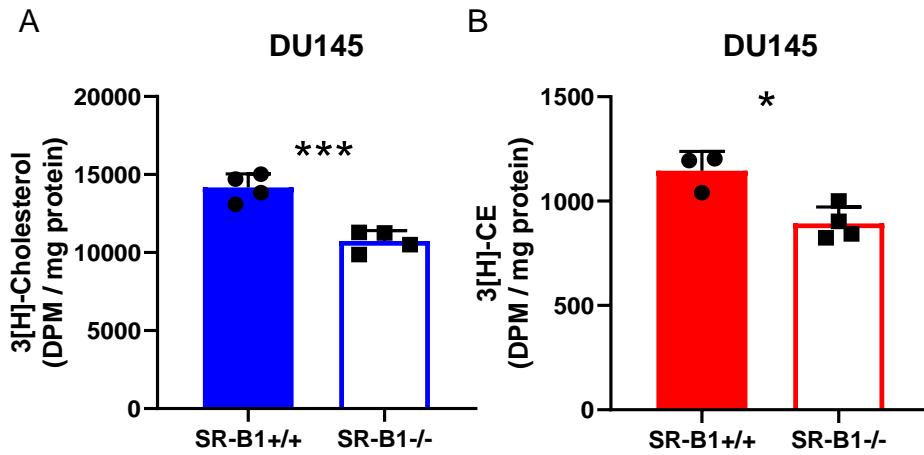


Figure 3.9. HDL lipid uptake upon with SR-B1 KO. DU145 SR-B1^{+/+} and SR-B1^{-/-} cells were treated with HDL labeled with (A) 3[H]-Cholesterol or (B) 3[H]-Cholesterol ester. Extracted cellular radiolabeled lipids were counted in scintillation and normalized total cell protein. N=3, T-test; *p<0.05, ***p<0.001.

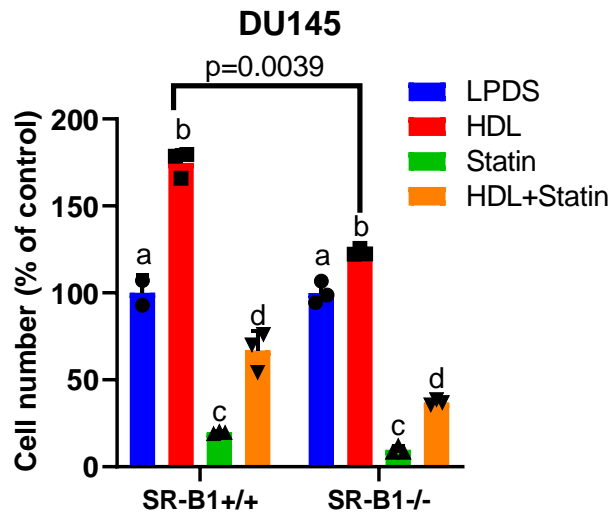


Figure 3.10 .Cell accumulation assay for DU145 WT and SR-B1 KO. Cells incubated \pm 300 μ g/ml HDL and \pm lovastatin in LPDS for 3 days (N=3; mean \pm SD; ANOVA $p < 0.05$ for analyses in each cell line).

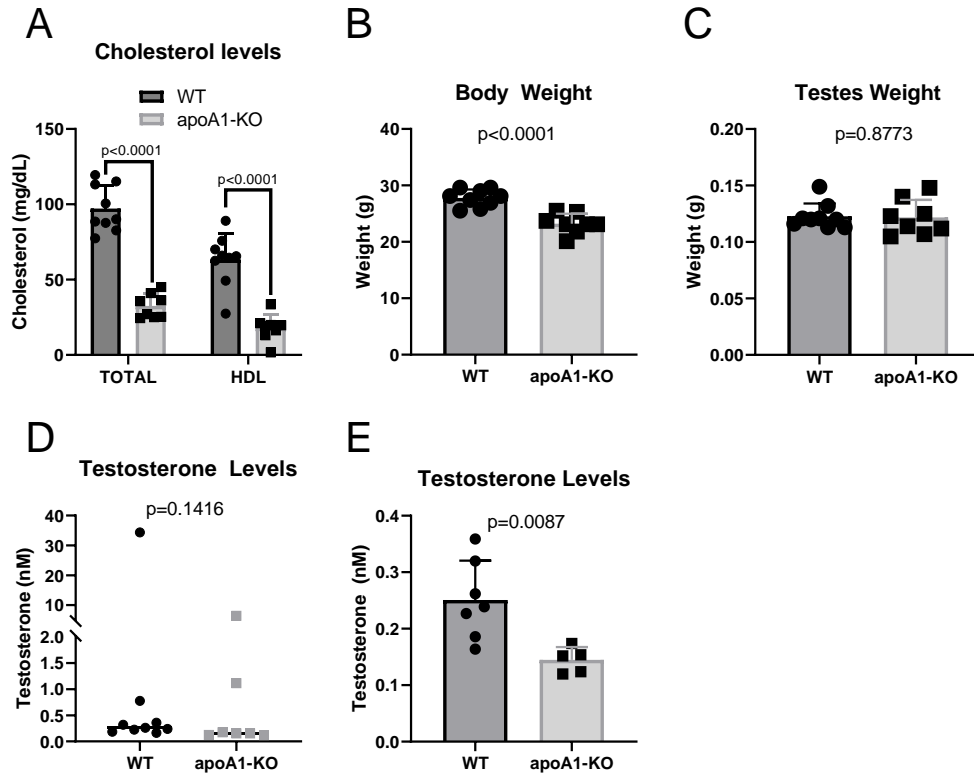


Figure 3.11. Characterization of WT and apoA1-KO mice. Total- and HDL-cholesterol levels (A), body weight (B), and testes weight (C) in 12 and 18 week old aged matched WT (n=9) and apoA1-KO (n=8) mice (mean \pm SD; t-test p-values displayed). D) Serum testosterone levels were not normally distributed (median values; not significant by non-parametric Mann-Whitney t-test). E) Serum testosterone levels after removal of outlier value from each cage were normally distributed (mean \pm SD; t-test p=0.0087).

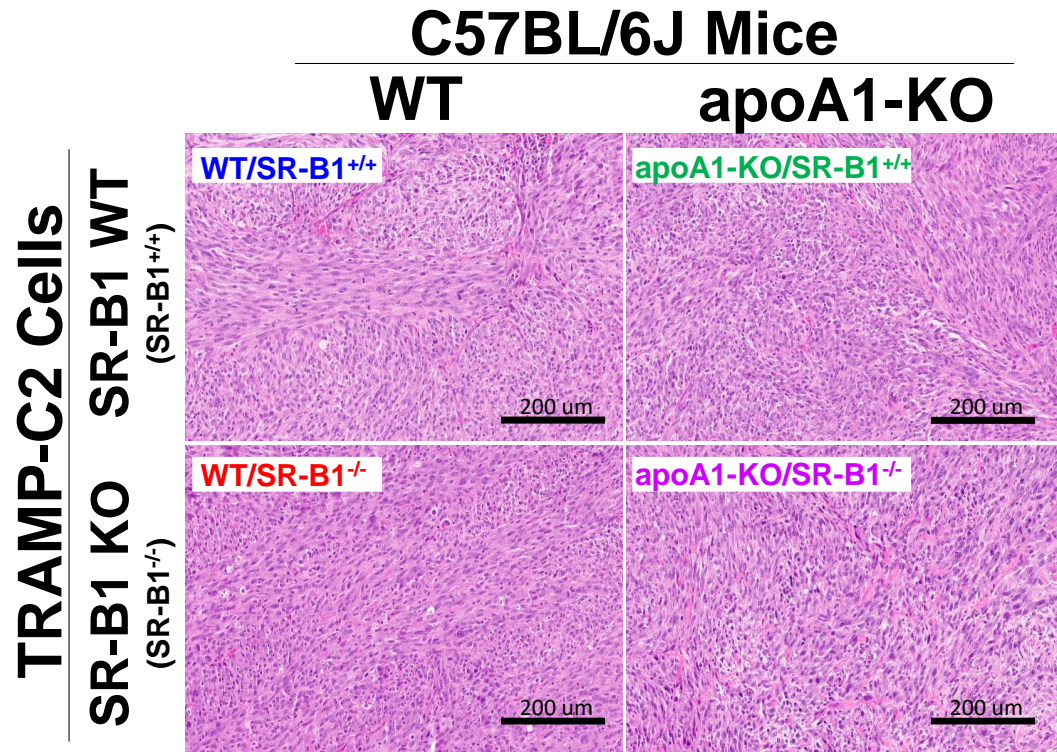


Figure 3.12. Histology of subcutaneous tumors from study arms. Hematoxylin and Eosin stained tumors from WT/SR-B1^{+/+}, WT/SR-B1^{-/-}, apoA1-KO/SR-B1^{+/+}, and apoA1-KO/SR-B1^{-/-} at 20x magnification.

CHAPTER IV

CRISPR use for additional projects

IV.1 CRISPR/Cas9 Gene Editing Work Flow and example of Generation of SR-B1 KO in clear cell renal cell carcinoma cell lines.

IV.1.1 Introduction

Renal disease ranks as the sixth and eighth most frequently diagnosed cancer in men and women, respectively, in the United States (181). Of the subtypes of kidney cancers, clear cell renal cell carcinoma (ccRCC) is the dominant form, accounting for as much as 75% of all kidney cancer cases. Histologically, ccRCC is characterized by its large clear cytoplasm, due to accumulation of lipids (182), mainly cholesterol ester (CE). This lipid accumulation was reduced by knocking down upregulated HIF-1 α and the very-low density lipoprotein receptor (VLDL-R) (183). Recently, genome-wide association studies have discovered single-nucleotide polymorphism (SNP) rs4765623 in ccRCC, which increases susceptibility to the disease(115). This SNP maps to the *SCARB1* gene that encodes for the high-density lipoprotein receptor SR-B1 (115). Studies have reported that SR-B1 is upregulated in ccRCC tissue compared to controls. Furthermore upregulated expression correlates with decreases survival, increased HDL uptake, with subsequent increases in cellular cholesterol ester (113,114,174). Though VLDLR is upregulated in ccRCC and its knockdown decreased lipid accumulation (183), another study showed that knockdown of VLDL-R and LDLR did not influence lipid accumulation in ccRCC cells. However, knockdown of SR-B1 did influence lipid accumulation in ccRCC lines (113). Due to the *SCARB1* SNP, we hypothesized that lipid accumulation could be a result of HDL

uptake through SR-B1, and that knockout of the receptor could reduce lipid accumulation and proliferation of these cells. To evaluate the role of SR-B1 in this disease, we were tasked to knockout SR-B1 in ccRCC line Caki-1 and papillary renal cell carcinoma line Caki-2. I performed this project along with Chase Neumann in the lab of J. Mark Brown.

IV.1.2 Materials and Methods

Bioinformatics of *SCARB1* expression in 73 paired normal adjacent and ccRCC tumor tissue from the TCGA KIRC dataset (19) was viewed by The UCSC Xena browser (163). For qPCR of *SCARB1* in normal adjacent versus different grades of ccRCC, ccRCC patient biopsy samples were acquired from Cleveland Clinic. Samples were stratified based on histological severity compared to a normal adjacent tissue (NAT). RNA was isolated by RNeasy kit according to manufacturer's instruction (Qiagen and Thermo Fisher). qPCR was performed using the Applied Biosystems 7500 Real-Time PCR System on RNA with SR-B1 specific primers. mRNA expression levels were calculated based on the $\Delta\Delta$ -CT method.

Caki-1 and Caki-2 renal cell lines were acquired from American Type Culture Collection (ATCC). Cells were cultured in McCoy's 5A medium with 10% FBS and 1% Penicillin/Streptomycin. In order to generate SR-B1 KO cell lines, 1×10^6 cells were co-transfected via nucleofection (Amaxa) with 0.6 nM human SR-B1 sgRNA (**Table 4.1**) complexed with 0.07nM Cas9 protein (Synthego) targeting exon 4. Transfected cells were plated in 96-well dishes to approximately 1 cell/well then clonally expanded and screened via PCR-Sanger sequencing to detect targeted sequence disruptions using PCR screening primers (**Table 4.1**). SR-B1 status of individual clones was determined by Western blot using SR-B1 rabbit polyclonal antibody (NB400-104) by Novus Biologicals.

Loading control GAPDH rabbit polyclonal antibody (sc-25778) was purchased from Santa Cruz.

sgRNAs	Sequence
<i>husg</i> SCARB1	CAUGAAGGCACGUUCGCCGA
PCR Screening Primers	Sequence
<i>husg</i> SCARB1-Fwd	CCAGTGGGTTCTGAGTTTCCCA
<i>husg</i> SCARB1-Rev	GATCCCCAGCCAGCTACAAAGC

Table 4.1 sgRNA and screening primers for human *SCARB1*

To assess cell growth, we performed cell accumulation assays in which cells were seeded into a 24-well plate at 20,000 cells/well in 10% FBS containing media overnight, then incubated with serum free media for 30 minutes. Cells were then incubated in 10% lipoprotein deficient serum (LPDS) media with or without 100 µg/ml HDL for 3 days. Thereafter, cells were lifted by trypsin and counted using the automated cell counter (Z series) by Beckman Coulter. Statistical analyses were performed using GraphPad Prism V.8.1.1 software: T-test for bioinformatics and One-Way ANOVA for cell accumulation study.

IV.1.3 Results

Our analysis of independent normal kidney tissue and ccRCC tissue samples showed SR-B1 was upregulated in various grades of ccRCC (**Fig. 4.1A, unpublished**). We validated SR-B1 upregulation using the paired normal and ccRCC tissue SR-B1 mRNA expression data from TCGA kidney clear cell carcinoma (KIRC) dataset (**Fig. 4.1B, unpublished**).

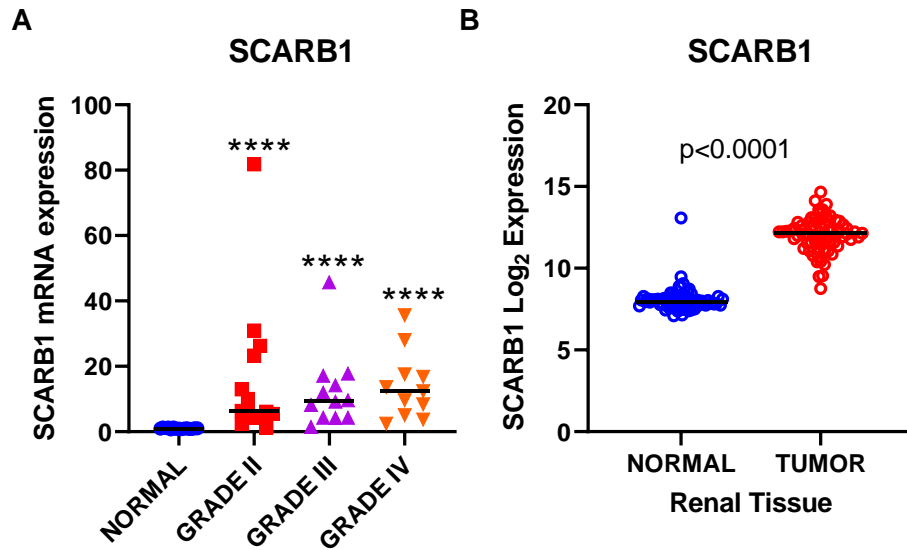


Figure 4.1 SCARB1 Expression in Renal Tissue A) SCARB1 mRNA expression from normal kidney (n=15) and grade II (n=14), grade III (n=12), and grade IV (n=11) ccRCC tissue. Statistical analysis by ANOVA with Dunnett's post-test; ****p<0.0001. B) SCARB1 mRNA expression data from TCGA KIRC data set (n=73 paired tumor and normal adjacent tissue). Significance determined via T-test; p-value displayed.

We next utilized CRISPR/Cas9 system to knockout SR-B1 in renal cell carcinoma lines. To begin, an appropriate guide RNA was determined using open source software CRISPOR, in which coding exon nucleotides are input, a species genome is selected, in addition to PAM type of choice (dependent upon Cas protein; Cas9 is NGG). Computational analysis is performed in which guide RNAs are produced against the gene input. Guides are ranked based on specificity to the genome(184). Selected guide sequences can be synthesized by companies such as Synthego, in which the guide without can be attached to an 80-mer specific scaffold to create a single guide RNA (sgRNA).

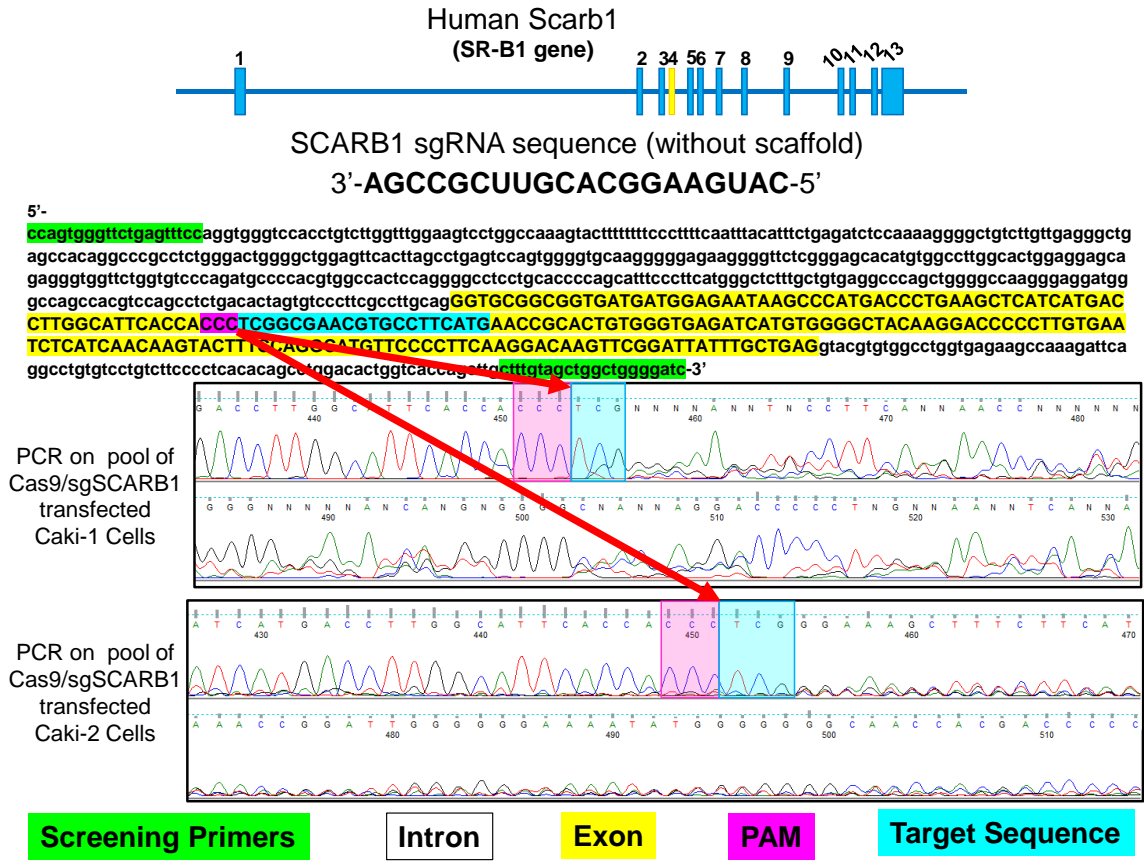


Figure 4.2 CRISPR design and editing of human SCARB1 gene exon 4. The human *SCARB1* gene contains 13 exons. Highlighted in yellow is exon 4. This sequence was analyzed in the CRISPOR software to generate the SCARB1 sgRNA sequence. The sgRNA will complementarily bind to the DNA target sequence highlighted in blue. Next to the target site, in pink, is the sequence 5'-CCC-3'. Thus, the reverse DNA strand possesses the PAM site of 3'-GGG-5' (not depicted). The sgRNA directed Cas9 will recognize the PAM on the reverse strand (not depicted) and induce a double strand break. Screening primers in green will amplify exon 4 and small portions of intronic DNA sequences flanking it (white) in PCR. Below are histograms of the Sanger sequenced DNA PCR products in the forward sense from Caki-1 and Caki-2 cells co-transfected with sgSCARB1 and Cas9. We see that 3 base pairs away from the PAM, our sequence becomes degenerate, indicative of edited genomes of cells in the transfected cell pool. Thus, single-cell derived colonies can be screened via Western blot to find SR-B1 KO clones.

The sgRNA, along with spCas9, were transfected into cells, which were subsequently screened for edits. **Fig 4.2** shows a schematic of a portion of Exon 4 of the human SCARB1 gene, which we targeted with a specific sgRNA. DNA from a pool of sgRNA/Cas9 transfected Caki-1 and Caki-2 cells reveals editing of the gene. In which editing occurs 3 base pairs upstream of the PAM. Single-cell dilution was performed on the pool of cells to isolate individual colonies of SR-B1 KO cells as seen in the western blot below (**Fig. 4.3A**).

Knock out of SR-B1 in the Caki-1 results in inhibition of HDL-mediated cell growth of Caki-1 cells (**Fig 4.3B**). Future work could be performed to evaluate lipid accumulation of these SR-B1 KO cells.

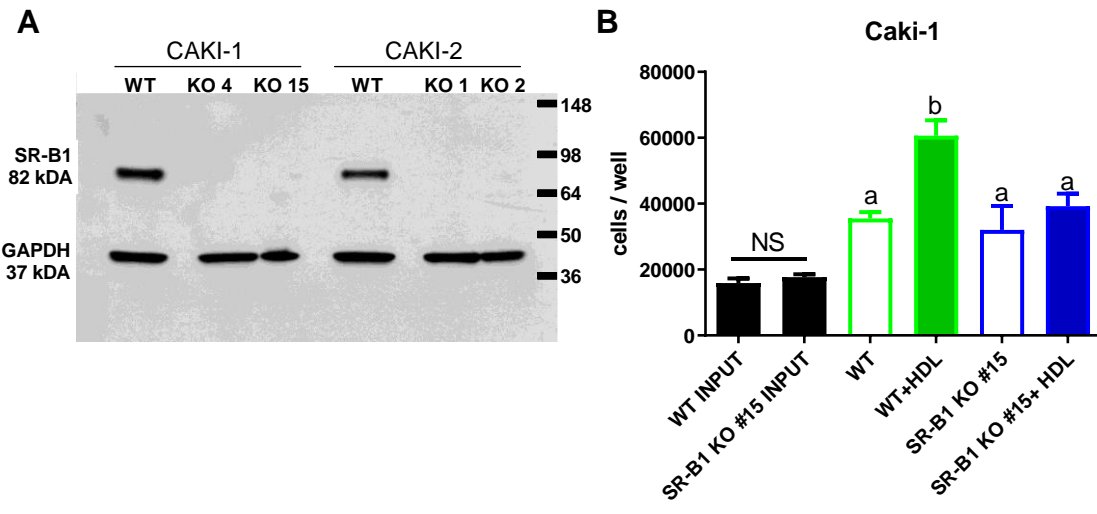


Figure 4.3 SR-B1 KO in Caki-1 Cell Accumulation. A) Western blot of SR-B1 in WT and SR-B1 KO Caki-1 and Caki-2 renal cell carcinoma line. B) Cell accumulation assay in which 20K cells/well were treated with HDL over 4 days.

IV.2 Generation of Gpnmb KO for manuscript: QTL analysis of macrophages from an AKR/JxDBA/2J intercross identified the *Gpnmb* gene as the modifier of lysosome function (185).

IV.2.1 Introduction

Atherosclerosis is the leading cause of death worldwide (186). It is characterized by plaque buildup as a result of lipid laden macrophages known as foam cells. During the process, a host of receptors including LDLR, macrophage scavenger receptor A (MRS1 gene) and CD36 ingest low-density lipoproteins (LDL) in its oxidized (oxLDL) and acetylated (AcLDL) forms. Accumulation and storage of these lipids in lipid droplets promotes an inflammatory response that leads to further macrophage recruitment and dysfunction, thus progressing the disease (187). The way in which macrophages attempt to clear lipid abundance is through a process known as autophagy. Here, autophagosomes ingest accumulated lipids (188), then fuse to lysosomes in which the cholesterol ester (CE) is hydrolyzed to free cholesterol by lysosomal acid lipase, which is subsequently exported out of the cell via ABCA1 (189).

The apoE KO mice has been used as a model to study atherosclerosis. In particular, the DBA/2J and AKR/J mice both develop atherosclerotic plaques. However, the plaque lesion in DBA/2J mice are roughly 11-fold greater than those in the AKR/J mice (190). Subsequent studies have demonstrated that macrophages of DBA/2J mice have lower free cholesterol and greater cholesterol ester storage (191), due to full-length ACAT (enzyme to esterify free cholesterol) as opposed to truncated ACAT in AKR/J mice due to exon deletion in *soat1* gene (192). Additionally, DBA/2J macrophages have reduced cholesterol efflux capacity and delayed autophagolysosome formation compared to AKR/J mice (191). Robinet et al, subsequently demonstrated that DBA/2J mice have reduced lysosomal activity due to differential expression of lysosomal genes *Mflm1* and *Gpnmb*,

identified by quantitative trait locus (QTL) mapping; , however, *Gpnmb* does not appear to regulate cholesterol ester storage or efflux capacity of macrophages based on experiments with siRNA knock down of *Gpnmb* (185).

IV.2.2 Materials and Methods

RAW 264.7 cells were cultured in DMEM supplemented with 10% FBS. In order to generate GPNMB KO cell lines, 1×10^6 cell lines per cell line were co-transfected via nucleofection (Amaxa) with 0.6 nM mouse *Gpnmb* sgRNAs (**Table 4.2**) complexed with 0.07nM Cas9 protein (Synthego). Transfected cells were plated in 96-well dishes to approximately 1 cell/well then clonally expanded and screened Western blot using *Gpnmb* antibody (R&D Systems). To measure lysosome function WT and *Gpnmb* edited RAW cells were incubated with 2 μ g/mL alexa647- labeled DQ-ovalbumin-bodipy (A-DQ-ova) for 1h. Function was evaluated by lysosomal pH as determined by the ratio of Bodipy to Alexa647 fluorescence in flow cytometry. In all experiments, 10,000 cells were analyzed by flow cytometry with a LSRII device (BD) using the following lasers and filters: 488nm excitation and 515/20nm for Bodipy and 639nm excitation and 660/20nm emission for Alexa647.

sgRNA	Sequence
<i>musg</i> GPNMB #1	ACCAACGACCAGGUUUCGUU
<i>musg</i> GPNMB#2	GUGCATCGCCUCAAACUAU

Table 4.2 sgRNA for mouse *Gpnmb*

IV.2.3 Results

Though siRNA significantly reduced AKR Gpnmb expression via PCR and WB compared to control siRNA treated cells, there was residual Gpnmb expression in the knockdown. To confirm that Gpnmb does not regulate efflux and cholesterol ester storage, we were tasked to generate a Gpnmb KO RAW 264.7 macrophage cell line so studies could validate the findings of this paper. Below is a western blot depicting unedited and Gpnmb edited by CRISPR/Cas9 in RAW 264.7 cells (**Fig 4.4A**). Editing of the complete Gpnmb KO clone #24 has recapitulated reduced lysosome function in RAW macrophages, whereas partial Gpnmb KO clones 8 and 13 resembled WT lysosomal function (**Fig. 4.4B**). Though expression of Gpnmb was reduced with CRISPR knockdown, the residual presence may contribute to being enough to effect the cells as seen with incomplete siRNA knockdown in AKR macrophages, thus no differences in efflux or CE levels. Additional testing on Gpnmb KO line is underway.

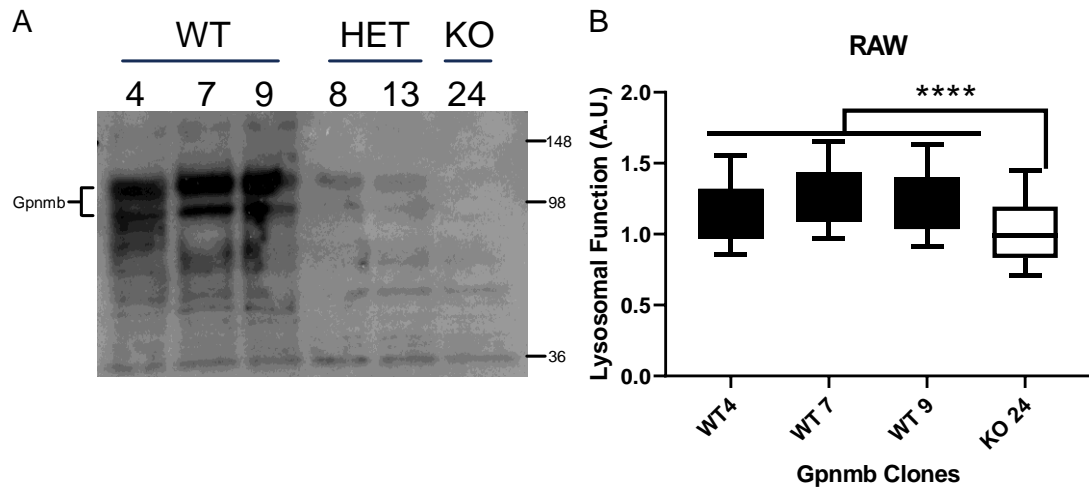


Figure 4.4 Editing of *GPNMB* and Use in Lysosomal Function Assay A) Western blot of Gpnmb in WT and Gpnmb edited cells using B) Lysosomal function assay of WT and Gpnmb edited RAW cells. ANOVA with Dunnett's post-hoc analysis; ****p<0.0001.

IV.3 Preliminary work on the anti-proliferative effects of ABCA1 in prostate cancer using CRISPR/dCas9 activation.

IV.3.1 Introduction

Prostate cancer is the second leading cause of cancer-related death among men in the United States (3). It has been reported that elevated levels of high-density lipoprotein (HDL)-cholesterol, the “good” cholesterol, protect against diseases such as atherosclerosis as well as many types of human cancers (172). The protective effect of HDL on cancer has been confirmed using mouse models with low and elevated levels of HDL (90). An inverse association between HDL in prostate cancer has been observed (88,150), but not in all studies (151,152). HDL biogenesis is mediated by ATP-binding cassette transporter A1 (ABCA1), which assembles cellular lipids with exogenous lipid-poor apoA1 to generate nascent HDL (47). ABCA1, expressed in almost all tissues, is necessary for HDL formation. In cells, upregulation of ABCA1 promotes translocation of phosphatidylserine (PS) from the inner to outer leaflet of the plasma membrane and HDL formation (193) by effluxing phospholipids and cholesterol to apoA1. Additionally, ABCA1 effluxes phosphatidylinositol 4,5-bisphosphate (PIP2) to HDL, and the majority of plasma PIP2 is carried on HDL(58).

It has been demonstrated that ABCA1 mutations and hypermethylation of ABCA1 promoter decreases these activities and leads to cholesterol accumulation (47,126) and ultimately cardiovascular disease. Lee et al, demonstrated that ABCA1 expression is suppressed in prostate cancer, reducing tumor cholesterol efflux capacity (126).

We hypothesize that ABCA1 induction can promote removal of cholesterol and PIP2 that will decrease prostate cancer growth pathways. Preliminarily, we have demonstrated that chemical induction of ABCA1 coincides with reducing some of these processes.

IV.3.2 Materials and Methods

The human prostate cancer cell lines DU145 and PC3 and mouse prostate cancer cell line TRAMP-C2 were used. DU145 and PC3 lines were cultured in RPMI1640 (supplemented with 10 % FBS (Sigma) and TRAMP-C2 was cultured in DMEM supplemented with 10% FBS (Sigma) and 10 nM dihydrotestosterone (Sigma) at 37 °C in 5 % CO₂. AC10 ABCA1 antibodies was from Novus. pan-AKT was fromr Cell Signaling Technologies.

For cell accumulation, proliferation and cell cycle analysis, cells were seeded into a 24-well at densities of 10,000 and 20,000 cells/well respectively in 10% FBS containing medium. Cells were then incubated in 10% FBS with or without 10 µM of the LXR agonist T0901317 (Sigma) for 4 days to induce ABCA1 expression. Thereafter, cells were lifted by trypsin and counted using the automated cell counter (Z series) by Beckman Coulter.

To evaluate cholesterol efflux from prostate cancer cells. Cells were plated in 10% FBS containing serum overnight. Following adherence, cells were rinsed with serum free media, then labeled with 3[H]-cholesterol. Next, cells were treated with or without 10 µM T0901317 in serum free media overnight. The following day cells were treated with or without 10 µM T0901317 and chased with or without 5 µg/ml apoA1 in absence or presence of T0901317 for 6 hours in serum free media.

To determine changes in AKT activation, adherent cells were serum starved overnight in the absence or presence of 10 µM T0901317, then treated with full serum for 2 hours. Cells were harvested for protein then subjected to SDS-PAGE and Western blot.

To generate ABCA1 over expressing DU145 cells (DU145 ABCA1) we used the deadCas9-transcriptional activator (CRISPRa) method. DU145 cells were transfected with addgene plasmid SP-dCas9-VPR (#63798) and selected for with G418 to express dCas9. dCas9 expressing DU145 cells were then transfected addgene plasmid pGL3-U6-sgRNA-PGK-puromycin(#51133), in which ABCA1 oligos (**Table 4.3**) were annealed and then ligated into Bsal cut sites.

Cloning Primers	Sequence
<i>hu</i> ABCA1-Fwd	AAACAGGCAGTAGGTCGCCTATCA
<i>hu</i> ABCA1-Rev	TAGGTGATAGGCGACCTACTGCCT

Table 4.3 cloning primers for human ABCA1

IV.3.3 Results

Lipoprotein receptors in prostate cancers have been widely studied and may serve as targetable entities to counter prostate cancer (111,112,117,126). We decided to evaluate how ABCA1 induction influence prostate cancer cell number. We hypothesize that induction of ABCA1 expression will promote efflux of cellular lipids, thus reducing proliferation and progression of prostate cancer. T0901317 is a liver x receptor (LXR) agonist that can promote induction of ABCA1 expression, which is shown for 3 prostate cancer cell lines. T0901317 induces ABCA1 expression in both human prostate cancer cell line DU145 and PC3, but ABCA1 is expression is nearly negligible in the mouse TRAMP-C2 cell line (**Fig 4.5 A-C**). However, treatment with the LXR agonist was able to reduce cell number compared to non-treated cells (**Fig. 4.5 D-F**).

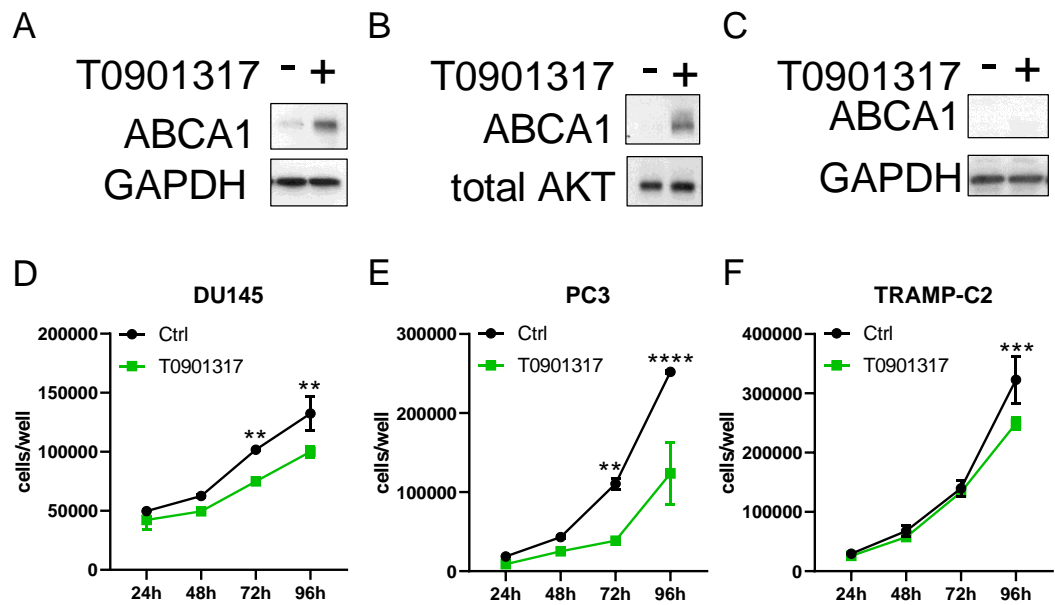


Figure 4.5 LXR effects on ABCA1 expression and cell number in prostate cancer cells. A) human DU145 and B) human PC3 and C) mouse TRAMP-C2 cells were incubated with \pm 10 μ M T0901317 overnight and then lysates were run in SDS-PAGE and probed for ABCA1. D,E,F) human and mouse prostate cancer cell were treated with 10 μ M T0901317 in FBS media for 4 days (N=3; mean \pm SD; **, $p < 0.01$; ***, $p < 0.001$, **** $p < 0.0001$ by t-test).

Next, we evaluated if LXR treatment promoted increased cholesterol efflux to apoA1. We hypothesized that if LXR-induced ABCA1 expression would promote efflux of cholesterol from prostate cancer cells. As expected induction of ABCA1 via LXR increased cholesterol efflux by 1.9-fold for both DU145 and PC3 lines and by 1.6-fold in the TRAMP-C2 (**Fig 4.6 A-C**). It is known that ABCA1 has the capacity to promote efflux of PIP2 from BHK cells. PIP2, a precursor lipid to the PI3K/AKT activation pathway. We hypothesize that LXR treatment, promoting ABCA1 could efflux PIP2 from prostate cancer cells limiting AKT activation. Western blot analysis of PC3 cells treated with LXR agonist revealed reduced AKT activation, but did not reach significant (**Fig. 4.7**).

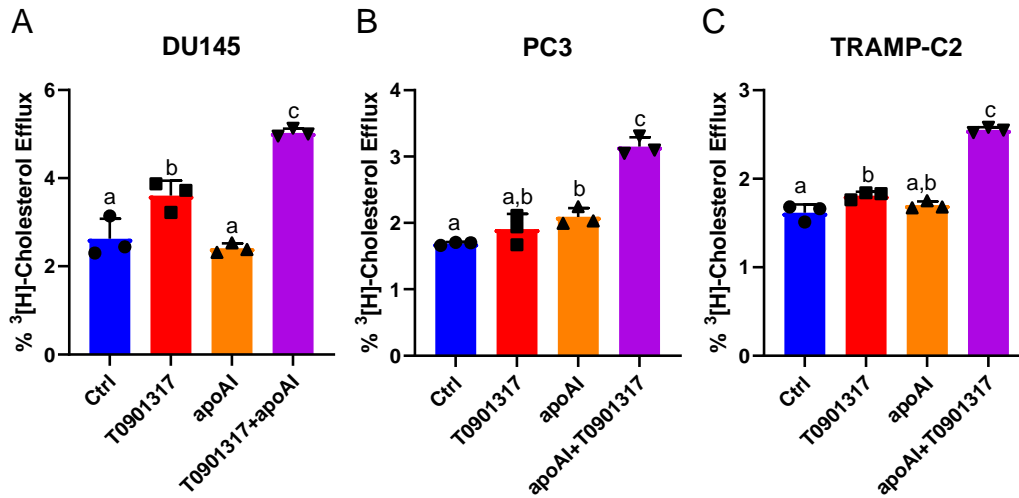


Figure 4.6 Cholesterol efflux to apoA1 in LXR treated prostate cancer cells. A) human DU145 and B) human PC3 and C) mouse TRAMP-C2 cells were labeled with ³[H]-cholesterol, incubated with ± 10 μM T0901317, and chased to 5μg/ml apoA1 in absence or presence of 10μM T0901317. (N=3; mean ± SD; p<0.05 by ANOVA).

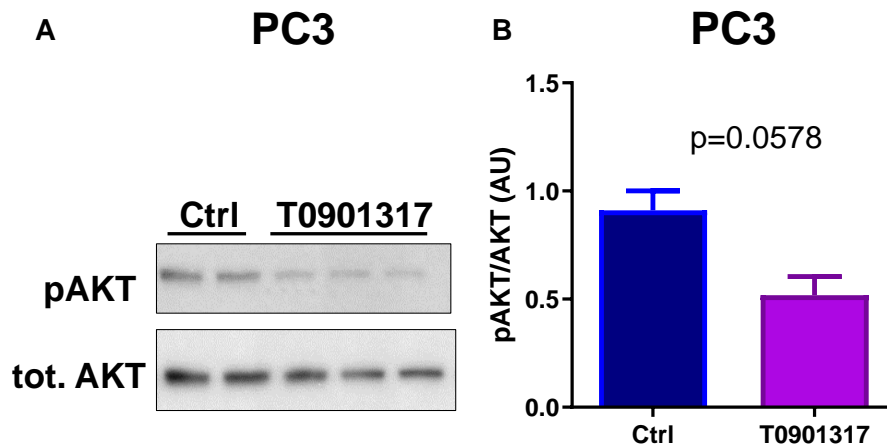
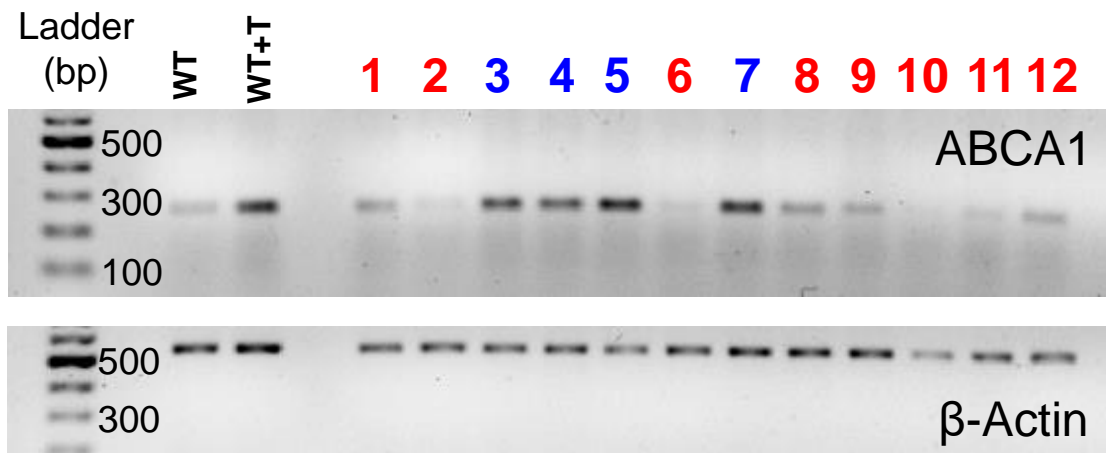


Figure 4.7 LXR activation reduces AKT activity in prostate cancer cells. A) Western blot phosphor-AKT and total AKT in PC3 cells treated with or without 10 μM T0901317. B) Quantification of western blot. T-test with p-value displayed N= 2 to 3 sample.

We believe it is ABCA1 induction that is mediating these effects. In order to evaluate if the T0901317 effects are due to induction of ABCA1, we attempted to utilize the CRISPR/dCas9-transcriptional activation (CRISPRa) method to promote ABCA1 expression. We engineered DU145 to stably express dCas9 using addgene plasmid SP-dCas9-VPR as well as to introduce human-specific ABCA1 targeted guide RNA that would be expressed by addgene plasmid, pGL3-U6-sgRNA-PGK-puromycin, in which ABCA1 oligos were annealed and then ligated into Bsal cut sites. A PCR assay on cDNA revealed generation of ABCA1 upregulation in some clones (**Fig. 4.8**). However, further testing is needed to evaluate if CRISPRa of ABCA1 in DU145 cells can recapitulate the same effects as LXR agonist T0901317.



T: T0901317 LXR agonist #: Failed CRISPRa #: Successful CRISPRa of ABCA1

Figure 4.8 CRISPRa of ABCA1 in DU145 cells. A) PCR of DU145 ABCA1 clones generated with SP-VPR-dCas9 and pGL3-U-sgABCA1-PGK-puromycin.

CHAPTER V

General discussion and future directions

Our data demonstrate the pro-proliferative effects of HDL by SR-B1, suggesting that anti-SR-B1 therapies could be beneficial due HDL uptake. Studies by Gordon demonstrating reduced tumor rate in response to BLT-1 (111) and regression of tumors in response to ITX5061 in the Patel study (118) affirm the relevance of the bulk of this work. Our dual hypothesis focused on HDL driving proliferation and progression through SR-B1, whereas ABCA1 mediated HDL generation reduces proliferation and progress. However

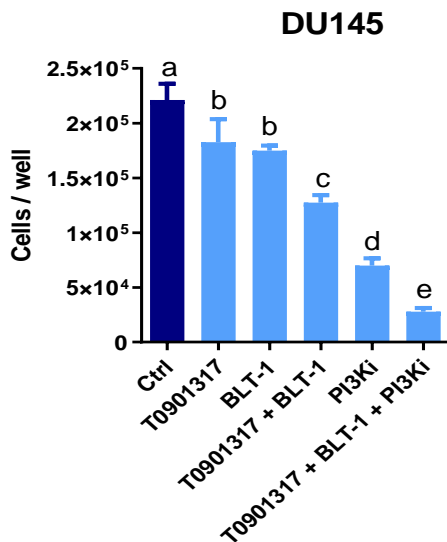


Figure 5.1 Combinatorial treatment for ABCA1 induction, SR-B1 inhibition, and PI3K inhibition additively decrease prostate cancer cell growth. Cells were treated with 10 μ M T0901317, 1 μ M BLT-1, and/or 1 μ M ZSTK474 for 4d in 10% FBS media. Beckman Coulter Counter was used to quantify cell proliferation. Significance by ANOVA; $p < 0.05$ between groups with different letters.

it is of interest of us to integrate knowledge of SR-B1 knockout with the preliminary evidence of ABCA1 induction mediating decreases in prostate cancer cells. Continuing work on generating stable ABCA1 expression in TRAMP-C2 cells would be of interest to test our hypothesis of its anti-proliferative of and anti-tumorigenic in vitro and in vivo similar to our study design for SR-B1 KO.

We have preliminary evidence that inhibition of SR-B1 and T0901317-induced ABCA1 synergistically reduce growth of DU145 cells (**Fig. 5.1**). Since, we have established SR-B1 KO cells for both DU145 and TRAMP-C2 cells it would be interesting to see if we could

recapitulate the finding in the cells with the SR-B1 and T0901317 or with cell additionally engineered to overexpress ABCA1.

Additionally, It is known that PIP2 is a phospholipid primarily sequestered on the inner leaflet of the plasma membrane, where it can be converted to PIP3 via PI-3 kinase with subsequent recruitment and activation of AKT (Reviewed in (21)). Semenas et al. showed that inhibition of PI-4-phosphate 5 kinase 1 alpha (PIP5K1 α), which produces PIP2, reduced prostate cancer tumor growth, androgen receptor (AR) expression, and prostate specific antigen (PSA) levels (194). Our lab has previously shown that phosphatidylinositol 4,5-bisphosphate (PIP2) can be trafficked in and out of cells via SR-B1 and ABCA1 and that the majority of circulating PIP2 is carried on HDL (58). Thus, HDL-PIP2 uptake via SR-B1 into prostate cancer cells may also promote cell proliferation. Our preliminary results demonstrate that this is a plausible event in that could occur in prostate

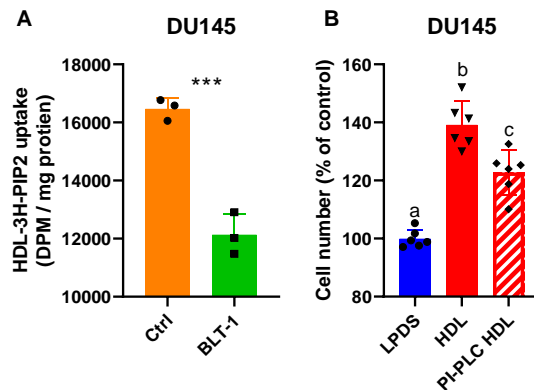


Figure 5.2 HDL-PIP2 in DU145 cells. DU145 cells were treated with HDL labeled with 3[H]-PIP2 in the absence or presence of SR-B1 inhibitor, BLT-1 (1 μ M), for 4 hours. Extracted cellular radiolabeled lipids were counted in scintillation and normalized total cell protein. N=3, T-test; ***p<0.001. B) DU145 cells treated HDL or PI-PLC pre-treated HDL for 4 days.

cancer cells. In DU145 cells we demonstrated that HDL-PIP2 uptake is partially facilitated by SR-B1, using SR-B1 inhibitor BLT-1 (**Fig. 5.2A**). Furthermore, HDL pre-treated with phosphatidylinositol phospholipase C (PI-PLC), which cleaves PIPs, proved to moderately decrease HDL-mediated cell accumulation of DU145 cells (**Fig.5.2B**).

This could potentially complement the preliminary finding that combined therapy of SR-B1 inhibition, ABCA1 induction, and PI3K inhibition work together to diminish prostate cancer cell growth as observed in (**Fig 5.1**) However, we have not demonstrated ABCA1 mediated removal of PIP2 from prostate cancer cells as demonstrated by Gulshan et al. (58).

Moreover, several studies have conferred its anti-cancer activity of ABCA1 in glioblastoma (195), breast cancer (196), and colon cancer (197) cells. In these studies LXR treatment, which mediates ABCA1 transcriptional activation, has shown to promote cell death, reduce PIP3 accumulation, and/or lower AKT activation, and in *in vivo* models cause smaller tumors (195). Again this highlights the potential role that PIP2 may play in the cancer, along with a potential role to regulate PIP2 levels being transported into cells by SR-B1 or exported by ABCA1.

There is much literature that has looked at statins or cholesterol levels with respect to prostate cancer risk. As with HDL and prostate cancer risk, the data on statin use and prostate cancer risk is inconsistent. Several studies supporting statins and reducing risk (53,70,73,75,77,78,168,169), whereas, other did not (82-85). However a more recent meta-analysis of multiple statins overall did not show that statins reduced risk of prostate cancer (171). With this in mind, it would be of interest to look at multiple statins on HDL transporters like SR-B1 and ABCA1 to evaluate if this statin association is due the effects on these receptors. Statins have been shown to decrease macrophage ABCA1 expression (198) and increase SR-B1 expression in both macrophages and endothelial cells (199,200). This is of interest since it has also been demonstrated that ABCA1 expression is reduced in prostate cancer as it advances due to hypermethylation (126), even though TCGA analysis was not stratified by severity to observe a similar finding (**Fig 3.1**).

Lastly, if therapies to promote ABCA1 expression and inhibit SR-B1 are to be developed, it is necessary to consider what impacts this will have in increasing risks for other morbidities, namely cardiovascular disease. As androgens are a primary driver of prostate cancer (2,11), it is only natural to treat patients with androgen deprivation therapies ADT. It is known that, ABCA1 is suppressed by androgens (124,125), whereas in human hepatic cells SR-B1 is induced by androgens, which most likely is the reason that men have lower HDL levels than women (94,98,156). However, it has not been well characterized as to how ADT influences both SR-B1 as well as ABCA1 with respect to prostate cancer or cardiovascular disease. However one study demonstrated downregulation of ABCA1 in response to ADT with Enzalutamide in LAPC-4 prostate cancer cells, but not LNCaP, VCaP, or CWR-R1 cell lines. Additionally SR-B1 expression was not demonstrated to be altered in micro array analysis in response to this treatment (201). ***What was interesting about the Patel et al, study was that use of SR-B1 inhibitor sensitized cancer to androgen deprivation therapy and statins.***

However it has been consistently demonstrated that ADT with standard of care drugs such as Enzalutamide, Abiraterone, or gonadotropin-releasing hormone (GnRH) analogues, increases risk or worsening of a cardiovascular disease (202-205), worsening of diabetes (205) and/or development of a new comorbidity, such as obesity and hypertension (205). Therefore, it would be interesting to evaluate how these drugs, which lower androgens, by multiple pathways, impact cholesterol transporters like SR-B1 and ABCA1, to gain a greater understanding of prostate cancer progression and treatment in addition to evaluating the consequences toward development of other comorbidities, that also might involve HDL metabolizing receptors SR-B1 and ABCA1.

CHAPTER VI

Appendix

Permission of use: DIAGENODE, Inc



Cynthia Traughber <cat73@case.edu>

Cas9 antibody image use request, services info

5 messages

David Greenberg <david.greenberg@diagenode.com> Tue, Apr 7, 2020 at 4:23 PM

To: "cat73@case.edu" <cat73@case.edu>

Cc: "michelle.fosler@diagenode.com" <michelle.fosler@diagenode.com>, "bindu.sundaresan@diagenode.com" <bindu.sundaresan@diagenode.com>

Hi Michelle and Bindu-

I spoke with Cynthia on Chat today. She is interested in using our Cas9 webpage art in her dissertation.

They need permission to include it. I am checking with our team on this.

<https://www.diagenode.com/en/categories/crispr-cas9-genome-editing>

She will be continuing research and is considering services for big data and seq approaches to compliment her own experiments. Would you mind connecting with her about any relevant services? She's busy for the next few weeks writing, but I sent her the link to our data mining webinar in the event that it is a welcome distraction to thesis writing!

I think for her samples, Cas9 edited prostate samples could benefit from scATACseq, RNA_seq, and CHIP-seq for Cas9 potentially.

I will let you know if I hear anything about how to go about using the artwork for your thesis. In my opinion if you cite the source, it should be fine, but her committee requires getting permission.

Thanks,

David Greenberg, Ph.D
Inside Sales and Technical Support Specialist
Diagenode, Inc.
Cell: (213) 929-0337
<https://www.diagenode.com/en/p/single-cell-atac-seq-service>

David Greenberg <david.greenberg@diagenode.com> Wed, Apr 8, 2020 at 10:41 AM

To: Michelle Fosler <michelle.fosler@diagenode.com>, cat73@case.edu, c.alicia1208@gmail.com

Cc: bindu.sundaresan@diagenode.com

Hi Cynthia,

We heard back from our marketing team in charge of the artwork. They said

"Cynthia is more than welcome to use our graphics if she cites the name of our company in the source. "

Best,

David

CHAPTER VII

Bibliography

1. Verze, P., Cai, T., and Lorenzetti, S. (2016) The role of the prostate in male fertility, health and disease. *Nat Rev Urol* **13**, 379-386
2. Huggins, C., Stevens, R. E., and Hodges, C. V. (1941) Studies on Prostatic Cancer: II. The Effects of Castration on Advanced Carcinoma of the Prostate Gland. *Arch Surg* **43**, 209-223
3. Siegel, R. L., Miller, K. D., and Jemal, A. (2019) Cancer statistics, 2019. *CA Cancer J Clin* **69**, 7-34
4. Georgantopoulos, P., Eberth, J. M., Cai, B., Emrich, C., Rao, G., Bennett, C. L., Haddock, K. S., and Hebert, J. R. (2020) Patient- and area-level predictors of prostate cancer among South Carolina veterans: a spatial analysis. *Cancer Causes Control*
5. Xu, Y., Huang, D., Wu, Y., Ye, D., Zhang, N., Gao, Y., Xu, D., Na, R., and Xu, J. (2019) Family history is significantly associated with prostate cancer and its early onset in Chinese population. *Prostate* **79**, 1762-1766
6. Barber, L., Gerke, T., Markt, S. C., Peisch, S. F., Wilson, K. M., Ahearn, T., Giovannucci, E., Parmigiani, G., and Mucci, L. A. (2018) Family History of Breast or Prostate Cancer and Prostate Cancer Risk. *Clin Cancer Res* **24**, 5910-5917
7. Grönberg, H. (2003) Prostate cancer epidemiology. *The Lancet* **361**, 859-864
8. Rawla, P. (2019) Epidemiology of Prostate Cancer. *World J Oncol* **10**, 63-89
9. Colli, J. L., and Colli, A. (2006) International comparisons of prostate cancer mortality rates with dietary practices and sunlight levels. *Urol Oncol* **24**, 184-194

10. Howlander, N., Noone, A. M., Krapcho, M., Miller, D., Brest, A., Yu, M., Ruhl, J., Tatalovich, Z., Mariotto, A., Lewis, D. R., Chen, H. S., Feuer, E. J., and Cronin, K. A. SEER Cancer Statistics Review, 1975-2016.
11. Huggins, C., and Hodges, C. V. (1941) Studies on Prostatic Cancer: I. The Effect of Castation of Estrogen and of Androgen Injection on Serum Phosphatases in Metastatic Carcinoma of the Prostate. *Cancer Res* **1**, 293-297
12. Gurung, P., and Jialal, I. (2019) Physiology, Male Reproductive System. in *StatPearls*, Treasure Island (FL). pp
13. Heindel, J. J., and Treinen, K. A. (1989) Physiology of the male reproductive system: endocrine, paracrine and autocrine regulation. *Toxicol Pathol* **17**, 411-445
14. Debes, J. D., and Tindall, D. J. (2004) Mechanisms of androgen-refractory prostate cancer. *N Engl J Med* **351**, 1488-1490
15. Gao, W., Bohl, C. E., and Dalton, J. T. (2005) Chemistry and structural biology of androgen receptor. *Chem Rev* **105**, 3352-3370
16. Heinlein, C. A., and Chang, C. (2004) Androgen receptor in prostate cancer. *Endocr Rev* **25**, 276-308
17. Hussain, M., Daignault-Newton, S., Twardowski, P. W., Albany, C., Stein, M. N., Kunju, L. P., Siddiqui, J., Wu, Y. M., Robinson, D., Lonigro, R. J., Cao, X., Tomlins, S. A., Mehra, R., Cooney, K. A., Montgomery, B., Antonarakis, E. S., Shevrin, D. H., Corn, P. G., Whang, Y. E., Smith, D. C., Caram, M. V., Knudsen, K. E., Stadler, W. M., Feng, F. Y., and Chinnaiyan, A. M. (2018) Targeting Androgen Receptor and DNA Repair in Metastatic Castration-Resistant Prostate Cancer: Results From NCI 9012. *J Clin Oncol* **36**, 991-999

18. Poelaert, F., Kumps, C., Lumen, N., Verschuere, S., Libbrecht, L., Praet, M., Rottey, S., Claeys, T., Ost, P., Decaestecker, K., De Meerleer, G., and Van Praet, C. (2017) Androgen Receptor Gene Copy Number and Protein Expression in Treatment-Naive Prostate Cancer. *Urol Int* **99**, 222-228
19. Consortium, G. T. (2013) The Genotype-Tissue Expression (GTEx) project. *Nat Genet* **45**, 580-585
20. Nishiyama, T., Hashimoto, Y., and Takahashi, K. (2004) The influence of androgen deprivation therapy on dihydrotestosterone levels in the prostatic tissue of patients with prostate cancer. *Clin Cancer Res* **10**, 7121-7126
21. Czech, M. P. (2000) PIP2 and PIP3: complex roles at the cell surface. *Cell* **100**, 603-606
22. Chalhoub, N., and Baker, S. J. (2009) PTEN and the PI3-kinase pathway in cancer. *Annu Rev Pathol* **4**, 127-150
23. Zhang, S., and Yu, D. (2010) PI(3)king apart PTEN's role in cancer. *Clin Cancer Res* **16**, 4325-4330
24. Wang, S., Gao, J., Lei, Q., Rozengurt, N., Pritchard, C., Jiao, J., Thomas, G. V., Li, G., Roy-Burman, P., Nelson, P. S., Liu, X., and Wu, H. (2003) Prostate-specific deletion of the murine Pten tumor suppressor gene leads to metastatic prostate cancer. *Cancer Cell* **4**, 209-221
25. Kwabi-Addo, B., Giri, D., Schmidt, K., Podsypanina, K., Parsons, R., Greenberg, N., and Ittmann, M. (2001) Haploinsufficiency of the Pten tumor suppressor gene promotes prostate cancer progression. *Proc Natl Acad Sci U S A* **98**, 11563-11568

26. Liu, R., Zhou, J., Xia, S., and Li, T. (2019) The impact of PTEN deletion and ERG rearrangement on recurrence after treatment for prostate cancer: a systematic review and meta-analysis. *Clin Transl Oncol*
27. Barry, M. J. (2001) Clinical practice. Prostate-specific-antigen testing for early diagnosis of prostate cancer. *N Engl J Med* **344**, 1373-1377
28. Fleshner, K., Tin, A., Benfante, N., Carlsson, S., and Vickers, A. J. (2018) Comparison of Physician-Documented Versus Patient-Reported Collection of Comorbidities Among Patients With Prostate Cancer Upon First Visit to the Urology Clinic. *JCO Clin Cancer Inform* **2**, 1-10
29. Stamey, T. A., Yang, N., Hay, A. R., McNeal, J. E., Freiha, F. S., and Redwine, E. (1987) Prostate-specific antigen as a serum marker for adenocarcinoma of the prostate. *N Engl J Med* **317**, 909-916
30. Pentylala, S. N., Lee, J., Hsieh, K., Waltzer, W. C., Trocchia, A., Musacchia, L., Rebecchi, M. J., and Khan, S. A. (2000) Prostate cancer: a comprehensive review. *Med Oncol* **17**, 85-105
31. Gann, P. H., Hennekens, C. H., and Stampfer, M. J. (1995) A prospective evaluation of plasma prostate-specific antigen for detection of prostatic cancer. *JAMA* **273**, 289-294
32. Draisma, G., Boer, R., Otto, S. J., van der Crujisen, I. W., Damhuis, R. A., Schroder, F. H., and de Koning, H. J. (2003) Lead times and overdetection due to prostate-specific antigen screening: estimates from the European Randomized Study of Screening for Prostate Cancer. *J Natl Cancer Inst* **95**, 868-878
33. Albertsen, P. C., Hanley, J. A., Gleason, D. F., and Barry, M. J. (1998) Competing risk analysis of men aged 55 to 74 years at diagnosis managed conservatively for clinically localized prostate cancer. *JAMA* **280**, 975-980

34. Borley, N., and Feneley, M. R. (2009) Prostate cancer: diagnosis and staging. *Asian J Androl* **11**, 74-80
35. Gleason, D. F., and Mellinger, G. T. (1974) Prediction of prognosis for prostatic adenocarcinoma by combined histological grading and clinical staging. *J Urol* **111**, 58-64
36. Ikonen, E. (2008) Cellular cholesterol trafficking and compartmentalization. *Nat Rev Mol Cell Biol* **9**, 125-138
37. Ikonen, E. (2006) Mechanisms for cellular cholesterol transport: defects and human disease. *Physiol Rev* **86**, 1237-1261
38. van Meer, G., Voelker, D. R., and Feigenson, G. W. (2008) Membrane lipids: where they are and how they behave. *Nat Rev Mol Cell Biol* **9**, 112-124
39. Pike, L. J. (2003) Lipid rafts: bringing order to chaos. *J Lipid Res* **44**, 655-667
40. Buhaescu, I., and Izzedine, H. (2007) Mevalonate pathway: a review of clinical and therapeutical implications. *Clin Biochem* **40**, 575-584
41. Goldstein, J. L., and Brown, M. S. (1990) Regulation of the mevalonate pathway. *Nature* **343**, 425-430
42. Burg, J. S., and Espenshade, P. J. (2011) Regulation of HMG-CoA reductase in mammals and yeast. *Prog Lipid Res* **50**, 403-410
43. Cyster, J. G., Dang, E. V., Reboldi, A., and Yi, T. (2014) 25-Hydroxycholesterols in innate and adaptive immunity. *Nat Rev Immunol* **14**, 731-743
44. Goldstein, J. L., DeBose-Boyd, R. A., and Brown, M. S. (2006) Protein sensors for membrane sterols. *Cell* **124**, 35-46
45. Costet, P., Luo, Y., Wang, N., and Tall, A. R. (2000) Sterol-dependent transactivation of the ABC1 promoter by the liver X receptor/retinoid X receptor. *J Biol Chem* **275**, 28240-28245

46. Edwards, P. A., Kennedy, M. A., and Mak, P. A. (2002) LXRs; oxysterol-activated nuclear receptors that regulate genes controlling lipid homeostasis. *Vascul Pharmacol* **38**, 249-256
47. Wang, S., and Smith, J. D. (2014) ABCA1 and nascent HDL biogenesis. *Biofactors* **40**, 547-554
48. Feingold, K. R., and Grunfeld, C. (2000) Introduction to Lipids and Lipoproteins. in *Endotext* (Feingold, K. R., Anawalt, B., Boyce, A., Chrousos, G., Dungan, K., Grossman, A., Hershman, J. M., Kaltsas, G., Koch, C., Kopp, P., Korbonits, M., McLachlan, R., Morley, J. E., New, M., Perreault, L., Purnell, J., Rebar, R., Singer, F., Trencle, D. L., Vinik, A., and Wilson, D. P. eds.), South Dartmouth (MA). pp
49. Srisen, K., Rohrl, C., Meisslitzer-Ruppitsch, C., Ranftler, C., Ellinger, A., Pavelka, M., and Neumuller, J. (2013) Human endothelial progenitor cells internalize high-density lipoprotein. *PLoS One* **8**, e83189
50. Pagler, T. A., Rhode, S., Neuhofer, A., Laggner, H., Strobl, W., Hinterndorfer, C., Volf, I., Pavelka, M., Eckhardt, E. R., van der Westhuyzen, D. R., Schutz, G. J., and Stangl, H. (2006) SR-BI-mediated high density lipoprotein (HDL) endocytosis leads to HDL resecretion facilitating cholesterol efflux. *J Biol Chem* **281**, 11193-11204
51. Acton, S., Rigotti, A., Landschulz, K. T., Xu, S., Hobbs, H. H., and Krieger, M. (1996) Identification of scavenger receptor SR-BI as a high density lipoprotein receptor. *Science* **271**, 518-520
52. Reaven, E., Leers-Sucheta, S., Nomoto, A., and Azhar, S. (2001) Expression of scavenger receptor class B type 1 (SR-BI) promotes microvillar channel

- formation and selective cholesteryl ester transport in a heterologous reconstituted system. *Proc Natl Acad Sci U S A* **98**, 1613-1618
53. <Characterization of hCAP cells.pdf>.
54. Ji, Y., Jian, B., Wang, N., Sun, Y., Moya, M. L., Phillips, M. C., Rothblat, G. H., Swaney, J. B., and Tall, A. R. (1997) Scavenger receptor BI promotes high density lipoprotein-mediated cellular cholesterol efflux. *J Biol Chem* **272**, 20982-20985
55. Ji, Y., Wang, N., Ramakrishnan, R., Sehayek, E., Huszar, D., Breslow, J. L., and Tall, A. R. (1999) Hepatic scavenger receptor BI promotes rapid clearance of high density lipoprotein free cholesterol and its transport into bile. *J Biol Chem* **274**, 33398-33402
56. Jian, B., de la Llera-Moya, M., Ji, Y., Wang, N., Phillips, M. C., Swaney, J. B., Tall, A. R., and Rothblat, G. H. (1998) Scavenger receptor class B type I as a mediator of cellular cholesterol efflux to lipoproteins and phospholipid acceptors. *J Biol Chem* **273**, 5599-5606
57. Stangl, H., Hyatt, M., and Hobbs, H. H. (1999) Transport of lipids from high and low density lipoproteins via scavenger receptor-BI. *J Biol Chem* **274**, 32692-32698
58. Gulshan, K., Brubaker, G., Conger, H., Wang, S., Zhang, R., Hazen, S. L., and Smith, J. D. (2016) PI(4,5)P2 Is Translocated by ABCA1 to the Cell Surface Where It Mediates Apolipoprotein A1 Binding and Nascent HDL Assembly. *Circ Res* **119**, 827-838
59. Urban, S., Zieseniss, S., Werder, M., Hauser, H., Budzinski, R., and Engelmann, B. (2000) Scavenger receptor BI transfers major lipoprotein-associated phospholipids into the cells. *J Biol Chem* **275**, 33409-33415

60. Stoffel, W. (1984) Synthesis, transport, and processing of apolipoproteins of high density lipoproteins. *J Lipid Res* **25**, 1586-1592
61. Khera, A. V., and Rader, D. J. (2010) Future therapeutic directions in reverse cholesterol transport. *Curr Atheroscler Rep* **12**, 73-81
62. Davis, C. E., Williams, D. H., Oganov, R. G., Tao, S. C., Rywik, S. L., Stein, Y., and Little, J. A. (1996) Sex difference in high density lipoprotein cholesterol in six countries. *Am J Epidemiol* **143**, 1100-1106
63. Gordon, D. J., Probstfield, J. L., Garrison, R. J., Neaton, J. D., Castelli, W. P., Knoke, J. D., Jacobs, D. R., Jr., Bangdiwala, S., and Tyroler, H. A. (1989) High-density lipoprotein cholesterol and cardiovascular disease. Four prospective American studies. *Circulation* **79**, 8-15
64. Eissa, M. A., Mihalopoulos, N. L., Holubkov, R., Dai, S., and Labarthe, D. R. (2016) Changes in Fasting Lipids during Puberty. *J Pediatr* **170**, 199-205
65. Kirkland, R. T., Keenan, B. S., Probstfield, J. L., Patsch, W., Lin, T. L., Clayton, G. W., and Insull, W., Jr. (1987) Decrease in plasma high-density lipoprotein cholesterol levels at puberty in boys with delayed adolescence. Correlation with plasma testosterone levels. *JAMA* **257**, 502-507
66. Jamnagerwalla, J., Howard, L. E., Allott, E. H., Vidal, A. C., Moreira, D. M., Castro-Santamaria, R., Andriole, G. L., Freeman, M. R., and Freedland, S. J. (2018) Serum cholesterol and risk of high-grade prostate cancer: results from the REDUCE study. *Prostate Cancer Prostatic Dis* **21**, 252-259
67. Magura, L., Blanchard, R., Hope, B., Beal, J. R., Schwartz, G. G., and Sahmoun, A. E. (2008) Hypercholesterolemia and prostate cancer: a hospital-based case-control study. *Cancer Causes Control* **19**, 1259-1266

68. Mondul, A. M., Weinstein, S. J., Virtamo, J., and Albanes, D. (2011) Serum total and HDL cholesterol and risk of prostate cancer. *Cancer Causes Control* **22**, 1545-1552
69. Murtola, T. J., Kasurinen, T. V. J., Talala, K., Taari, K., Tammela, T. L. J., and Auvinen, A. (2019) Serum cholesterol and prostate cancer risk in the Finnish randomized study of screening for prostate cancer. *Prostate Cancer Prostatic Dis* **22**, 66-76
70. Breau, R. H., Karnes, R. J., Jacobson, D. J., McGree, M. E., Jacobsen, S. J., Nehra, A., Lieber, M. M., and St Sauver, J. L. (2010) The association between statin use and the diagnosis of prostate cancer in a population based cohort. *J Urol* **184**, 494-499
71. Wang, K., Gerke, T. A., Chen, X., and Prosperi, M. (2019) Association of statin use with risk of Gleason score-specific prostate cancer: A hospital-based cohort study. *Cancer Med* **8**, 7399-7407
72. Jacobs, E. J., Rodriguez, C., Bain, E. B., Wang, Y., Thun, M. J., and Calle, E. E. (2007) Cholesterol-lowering drugs and advanced prostate cancer incidence in a large U.S. cohort. *Cancer Epidemiol Biomarkers Prev* **16**, 2213-2217
73. Platz, E. A., Leitzmann, M. F., Visvanathan, K., Rimm, E. B., Stampfer, M. J., Willett, W. C., and Giovannucci, E. (2006) Statin drugs and risk of advanced prostate cancer. *J Natl Cancer Inst* **98**, 1819-1825
74. Boudreau, D. M., Yu, O., Buist, D. S., and Miglioretti, D. L. (2008) Statin use and prostate cancer risk in a large population-based setting. *Cancer Causes Control* **19**, 767-774

75. Tan, N., Klein, E. A., Li, J., Moussa, A. S., and Jones, J. S. (2011) Statin use and risk of prostate cancer in a population of men who underwent biopsy. *J Urol* **186**, 86-90
76. Flick, E. D., Habel, L. A., Chan, K. A., Van Den Eeden, S. K., Quinn, V. P., Haque, R., Orav, E. J., Seeger, J. D., Sadler, M. C., Quesenberry, C. P., Jr., Sternfeld, B., Jacobsen, S. J., Whitmer, R. A., and Caan, B. J. (2007) Statin use and risk of prostate cancer in the California Men's Health Study cohort. *Cancer Epidemiol Biomarkers Prev* **16**, 2218-2225
77. Farwell, W. R., D'Avolio, L. W., Scranton, R. E., Lawler, E. V., and Gaziano, J. M. (2011) Statins and prostate cancer diagnosis and grade in a veterans population. *J Natl Cancer Inst* **103**, 885-892
78. Shannon, J., Tewoderos, S., Garzotto, M., Beer, T. M., Derenick, R., Palma, A., and Farris, P. E. (2005) Statins and prostate cancer risk: a case-control study. *Am J Epidemiol* **162**, 318-325
79. Fowke, J. H., Motley, S. S., Barocas, D. A., Cookson, M. S., Concepcion, R., Byerly, S., and Smith, J. A., Jr. (2011) The associations between statin use and prostate cancer screening, prostate size, high-grade prostatic intraepithelial neoplasia (PIN), and prostate cancer. *Cancer Causes Control* **22**, 417-426
80. Jacobs, E. J., Newton, C. C., Thun, M. J., and Gapstur, S. M. (2011) Long-term use of cholesterol-lowering drugs and cancer incidence in a large United States cohort. *Cancer Res* **71**, 1763-1771
81. Friedman, G. D., Flick, E. D., Udaltsova, N., Chan, J., Quesenberry, C. P., Jr., and Habel, L. A. (2008) Screening statins for possible carcinogenic risk: up to 9 years of follow-up of 361,859 recipients. *Pharmacoepidemiol Drug Saf* **17**, 27-36

82. Coogan, P. F., Kelly, J. P., Strom, B. L., and Rosenberg, L. (2010) Statin and NSAID use and prostate cancer risk. *Pharmacoepidemiol Drug Saf* **19**, 752-755
83. Platz, E. A., Tangen, C. M., Goodman, P. J., Till, C., Parnes, H. L., Figg, W. D., Albanes, D., Neuhauser, M. L., Klein, E. A., Lucia, M. S., Thompson, I. M., Jr., and Kristal, A. R. (2014) Statin drug use is not associated with prostate cancer risk in men who are regularly screened. *J Urol* **192**, 379-384
84. Chan, J. M., Litwack-Harrison, S., Bauer, S. R., Daniels, N. A., Wilt, T. J., Shannon, J., and Bauer, D. C. (2012) Statin use and risk of prostate cancer in the prospective Osteoporotic Fractures in Men (MrOS) Study. *Cancer Epidemiol Biomarkers Prev* **21**, 1886-1888
85. Agalliu, I., Salinas, C. A., Hansten, P. D., Ostrander, E. A., and Stanford, J. L. (2008) Statin use and risk of prostate cancer: results from a population-based epidemiologic study. *Am J Epidemiol* **168**, 250-260
86. Kantor, E. D., Lipworth, L., Fowke, J. H., Giovannucci, E. L., Mucci, L. A., and Signorello, L. B. (2015) Statin use and risk of prostate cancer: Results from the Southern Community Cohort Study. *Prostate* **75**, 1384-1393
87. Kok, D. E., van Roermund, J. G., Aben, K. K., den Heijer, M., Swinkels, D. W., Kampman, E., and Kiemeny, L. A. (2011) Blood lipid levels and prostate cancer risk; a cohort study. *Prostate Cancer Prostatic Dis* **14**, 340-345
88. Van Hemelrijck, M., Walldius, G., Jungner, I., Hammar, N., Garmo, H., Binda, E., Hayday, A., Lambe, M., and Holmberg, L. (2011) Low levels of apolipoprotein A-I and HDL are associated with risk of prostate cancer in the Swedish AMORIS study. *Cancer Causes Control* **22**, 1011-1019
89. YuPeng, L., YuXue, Z., PengFei, L., Cheng, C., YaShuang, Z., DaPeng, L., and Chen, D. (2015) Cholesterol Levels in Blood and the Risk of Prostate Cancer: A

- Meta-analysis of 14 Prospective Studies. *Cancer Epidemiol Biomarkers Prev* **24**, 1086-1093
90. Zamanian-Daryoush, M., Lindner, D., Tallant, T. C., Wang, Z., Buffa, J., Klipfell, E., Parker, Y., Hatala, D., Parsons-Wingerter, P., Rayman, P., Yusufshaq, M. S., Fisher, E. A., Smith, J. D., Finke, J., DiDonato, J. A., and Hazen, S. L. (2013) The cardioprotective protein apolipoprotein A1 promotes potent anti-tumorigenic effects. *J Biol Chem* **288**, 21237-21252
91. Llaverias, G., Danilo, C., Wang, Y., Witkiewicz, A. K., Daumer, K., Lisanti, M. P., and Frank, P. G. (2010) A Western-type diet accelerates tumor progression in an autochthonous mouse model of prostate cancer. *Am J Pathol* **177**, 3180-3191
92. Babitt, J., Trigatti, B., Rigotti, A., Smart, E. J., Anderson, R. G., Xu, S., and Krieger, M. (1997) Murine SR-BI, a high density lipoprotein receptor that mediates selective lipid uptake, is N-glycosylated and fatty acylated and colocalizes with plasma membrane caveolae. *J Biol Chem* **272**, 13242-13249
93. Vinals, M., Xu, S., Vasile, E., and Krieger, M. (2003) Identification of the N-linked glycosylation sites on the high density lipoprotein (HDL) receptor SR-BI and assessment of their effects on HDL binding and selective lipid uptake. *J Biol Chem* **278**, 5325-5332
94. Rigotti, A., Miettinen, H. E., and Krieger, M. (2003) The role of the high-density lipoprotein receptor SR-BI in the lipid metabolism of endocrine and other tissues. *Endocr Rev* **24**, 357-387
95. Shen, W. J., Azhar, S., and Kraemer, F. B. (2018) SR-B1: A Unique Multifunctional Receptor for Cholesterol Influx and Efflux. *Annu Rev Physiol* **80**, 95-116

96. Calvo, D., Gomez-Coronado, D., Lasuncion, M. A., and Vega, M. A. (1997) CLA-1 is an 85-kD plasma membrane glycoprotein that acts as a high-affinity receptor for both native (HDL, LDL, and VLDL) and modified (OxLDL and AcLDL) lipoproteins. *Arterioscler Thromb Vasc Biol* **17**, 2341-2349
97. Gillotte-Taylor, K., Boullier, A., Witztum, J. L., Steinberg, D., and Quehenberger, O. (2001) Scavenger receptor class B type I as a receptor for oxidized low density lipoprotein. *J Lipid Res* **42**, 1474-1482
98. Rigotti, A., Edelman, E. R., Seifert, P., Iqbal, S. N., DeMattos, R. B., Temel, R. E., Krieger, M., and Williams, D. L. (1996) Regulation by adrenocorticotrophic hormone of the in vivo expression of scavenger receptor class B type I (SR-BI), a high density lipoprotein receptor, in steroidogenic cells of the murine adrenal gland. *J Biol Chem* **271**, 33545-33549
99. Danilo, C., Gutierrez-Pajares, J. L., Mainieri, M. A., Mercier, I., Lisanti, M. P., and Frank, P. G. (2013) Scavenger receptor class B type I regulates cellular cholesterol metabolism and cell signaling associated with breast cancer development. *Breast Cancer Res* **15**, R87
100. Yuhanna, I. S., Zhu, Y., Cox, B. E., Hahner, L. D., Osborne-Lawrence, S., Lu, P., Marcel, Y. L., Anderson, R. G., Mendelsohn, M. E., Hobbs, H. H., and Shaul, P. W. (2001) High-density lipoprotein binding to scavenger receptor-BI activates endothelial nitric oxide synthase. *Nat Med* **7**, 853-857
101. Trigatti, B., Rayburn, H., Vinals, M., Braun, A., Miettinen, H., Penman, M., Hertz, M., Schrenzel, M., Amigo, L., Rigotti, A., and Krieger, M. (1999) Influence of the high density lipoprotein receptor SR-BI on reproductive and cardiovascular pathophysiology. *Proc Natl Acad Sci U S A* **96**, 9322-9327

102. Cao, G., Garcia, C. K., Wyne, K. L., Schultz, R. A., Parker, K. L., and Hobbs, H. H. (1997) Structure and localization of the human gene encoding SR-BI/CLA-1. Evidence for transcriptional control by steroidogenic factor 1. *J Biol Chem* **272**, 33068-33076
103. Martin, G., Pilon, A., Albert, C., Valle, M., Hum, D. W., Fruchart, J. C., Najib, J., Clavey, V., and Staels, B. (1999) Comparison of expression and regulation of the high-density lipoprotein receptor SR-BI and the low-density lipoprotein receptor in human adrenocortical carcinoma NCI-H295 cells. *Eur J Biochem* **261**, 481-491
104. Sun, Y., Wang, N., and Tall, A. R. (1999) Regulation of adrenal scavenger receptor-BI expression by ACTH and cellular cholesterol pools. *J Lipid Res* **40**, 1799-1805
105. Malerod, L., Sporstol, M., Juvet, L. K., Mousavi, A., Gjoen, T., and Berg, T. (2003) Hepatic scavenger receptor class B, type I is stimulated by peroxisome proliferator-activated receptor gamma and hepatocyte nuclear factor 4alpha. *Biochem Biophys Res Commun* **305**, 557-565
106. Malerod, L., Juvet, L. K., Hanssen-Bauer, A., Eskild, W., and Berg, T. (2002) Oxysterol-activated LXRAalpha/RXR induces hSR-BI-promoter activity in hepatoma cells and preadipocytes. *Biochem Biophys Res Commun* **299**, 916-923
107. Lopez, D., Shea-Eaton, W., Sanchez, M. D., and McLean, M. P. (2001) DAX-1 represses the high-density lipoprotein receptor through interaction with positive regulators sterol regulatory element-binding protein-1a and steroidogenic factor-1. *Endocrinology* **142**, 5097-5106
108. Sporstol, M., Tapia, G., Malerod, L., Mousavi, S. A., and Berg, T. (2005) Pregnane X receptor-agonists down-regulate hepatic ATP-binding cassette

- transporter A1 and scavenger receptor class B type I. *Biochem Biophys Res Commun* **331**, 1533-1541
109. Hu, Z., Shen, W. J., Kraemer, F. B., and Azhar, S. (2012) MicroRNAs 125a and 455 repress lipoprotein-supported steroidogenesis by targeting scavenger receptor class B type I in steroidogenic cells. *Mol Cell Biol* **32**, 5035-5045
110. Wang, L., Jia, X. J., Jiang, H. J., Du, Y., Yang, F., Si, S. Y., and Hong, B. (2013) MicroRNAs 185, 96, and 223 repress selective high-density lipoprotein cholesterol uptake through posttranscriptional inhibition. *Mol Cell Biol* **33**, 1956-1964
111. Gordon, J. A., Noble, J. W., Midha, A., Derakhshan, F., Wang, G., Adomat, H. H., Tomlinson Guns, E. S., Lin, Y. Y., Ren, S., Collins, C. C., Nelson, P. S., Morrissey, C., Wasan, K. M., and Cox, M. E. (2019) Upregulation of Scavenger Receptor B1 Is Required for Steroidogenic and Nonsteroidogenic Cholesterol Metabolism in Prostate Cancer. *Cancer Res* **79**, 3320-3331
112. Schorghofer, D., Kinslechner, K., Preitschopf, A., Schutz, B., Rohrl, C., Hengstschlager, M., Stangl, H., and Mikula, M. (2015) The HDL receptor SR-BI is associated with human prostate cancer progression and plays a possible role in establishing androgen independence. *Reprod Biol Endocrinol* **13**, 88
113. Velagapudi, S., Schraml, P., Yalcinkaya, M., Bolck, H. A., Rohrer, L., Moch, H., and von Eckardstein, A. (2018) Scavenger receptor BI promotes cytoplasmic accumulation of lipoproteins in clear-cell renal cell carcinoma. *J Lipid Res* **59**, 2188-2201
114. Xu, G. H., Lou, N., Shi, H. C., Xu, Y. C., Ruan, H. L., Xiao, W., Liu, L., Li, X., Xiao, H. B., Qiu, B., Bao, L., Yuan, C. F., Zhou, Y. L., Hu, W. J., Chen, K., Yang, H. M., and Zhang, X. P. (2018) Up-regulation of SR-BI promotes progression and

serves as a prognostic biomarker in clear cell renal cell carcinoma. *BMC Cancer* **18**, 88

115. Purdue, M. P., Johansson, M., Zelenika, D., Toro, J. R., Scelo, G., Moore, L. E., Prokhortchouk, E., Wu, X., Kiemenev, L. A., Gaborieau, V., Jacobs, K. B., Chow, W. H., Zaridze, D., Matveev, V., Lubinski, J., Trubicka, J., Szeszenia-Dabrowska, N., Lissowska, J., Rudnai, P., Fabianova, E., Bucur, A., Bencko, V., Foretova, L., Janout, V., Boffetta, P., Colt, J. S., Davis, F. G., Schwartz, K. L., Banks, R. E., Selby, P. J., Harnden, P., Berg, C. D., Hsing, A. W., Grubb, R. L., 3rd, Boeing, H., Vineis, P., Clavel-Chapelon, F., Palli, D., Tumino, R., Krogh, V., Panico, S., Duell, E. J., Quiros, J. R., Sanchez, M. J., Navarro, C., Ardanaz, E., Dorronsoro, M., Khaw, K. T., Allen, N. E., Bueno-de-Mesquita, H. B., Peeters, P. H., Trichopoulos, D., Linseisen, J., Ljungberg, B., Overvad, K., Tjonneland, A., Romieu, I., Riboli, E., Mukeria, A., Shangina, O., Stevens, V. L., Thun, M. J., Diver, W. R., Gapstur, S. M., Pharoah, P. D., Easton, D. F., Albanes, D., Weinstein, S. J., Virtamo, J., Vatten, L., Hveem, K., Njolstad, I., Tell, G. S., Stoltenberg, C., Kumar, R., Koppova, K., Cussenot, O., Benhamou, S., Oosterwijk, E., Vermeulen, S. H., Aben, K. K., van der Marel, S. L., Ye, Y., Wood, C. G., Pu, X., Mazur, A. M., Boulygina, E. S., Chekanov, N. N., Foglio, M., Lechner, D., Gut, I., Heath, S., Blanche, H., Hutchinson, A., Thomas, G., Wang, Z., Yeager, M., Fraumeni, J. F., Jr., Skryabin, K. G., McKay, J. D., Rothman, N., Chanock, S. J., Lathrop, M., and Brennan, P. (2011) Genome-wide association study of renal cell carcinoma identifies two susceptibility loci on 2p21 and 11q13.3. *Nat Genet* **43**, 60-65
116. de Gonzalo-Calvo, D., Lopez-Vilaro, L., Nasarre, L., Perez-Olabarria, M., Vazquez, T., Escuin, D., Badimon, L., Barnadas, A., Lerma, E., and Llorente-

- Cortes, V. (2015) Intratumor cholesteryl ester accumulation is associated with human breast cancer proliferation and aggressive potential: a molecular and clinicopathological study. *BMC Cancer* **15**, 460
117. Yue, S., Li, J., Lee, S. Y., Lee, H. J., Shao, T., Song, B., Cheng, L., Masterson, T. A., Liu, X., Ratliff, T. L., and Cheng, J. X. (2014) Cholesteryl ester accumulation induced by PTEN loss and PI3K/AKT activation underlies human prostate cancer aggressiveness. *Cell Metab* **19**, 393-406
118. Patel, R., Fleming, J., Mui, E., Loveridge, C., Repiscak, P., Blomme, A., Harle, V., Salji, M., Ahmad, I., Teo, K., Hamdy, F. C., Hedley, A., van den Broek, N., Mackay, G., Edwards, J., Sansom, O. J., and Leung, H. Y. (2018) Sprouty2 loss-induced IL6 drives castration-resistant prostate cancer through scavenger receptor B1. *EMBO Mol Med* **10**
119. Trasino, S. E., Kim, Y. S., and Wang, T. T. (2009) Ligand, receptor, and cell type-dependent regulation of ABCA1 and ABCG1 mRNA in prostate cancer epithelial cells. *Mol Cancer Ther* **8**, 1934-1945
120. Vaidya, M., Jentsch, J. A., Peters, S., Keul, P., Weske, S., Graler, M. H., Mladenov, E., Iliakis, G., Heusch, G., and Levkau, B. (2019) Regulation of ABCA1-mediated cholesterol efflux by sphingosine-1-phosphate signaling in macrophages. *J Lipid Res* **60**, 506-515
121. Dufour, J., Pommier, A., Alves, G., De Boussac, H., Lours-Calet, C., Volle, D. H., Lobaccaro, J. M., and Baron, S. (2013) Lack of liver X receptors leads to cell proliferation in a model of mouse dorsal prostate epithelial cell. *PLoS One* **8**, e58876
122. Chuu, C. P., Hiipakka, R. A., Kokontis, J. M., Fukuchi, J., Chen, R. Y., and Liao, S. (2006) Inhibition of tumor growth and progression of LNCaP prostate cancer

- cells in athymic mice by androgen and liver X receptor agonist. *Cancer Res* **66**, 6482-6486
123. Leon, C. G., Locke, J. A., Adomat, H. H., Etinger, S. L., Twiddy, A. L., Neumann, R. D., Nelson, C. C., Guns, E. S., and Wasan, K. M. (2010) Alterations in cholesterol regulation contribute to the production of intratumoral androgens during progression to castration-resistant prostate cancer in a mouse xenograft model. *Prostate* **70**, 390-400
124. Fukuchi, J., Hiipakka, R. A., Kokontis, J. M., Hsu, S., Ko, A. L., Fitzgerald, M. L., and Liao, S. (2004) Androgenic suppression of ATP-binding cassette transporter A1 expression in LNCaP human prostate cancer cells. *Cancer Res* **64**, 7682-7685
125. Sekine, Y., Demosky, S. J., Stonik, J. A., Furuya, Y., Koike, H., Suzuki, K., and Remaley, A. T. (2010) High-density lipoprotein induces proliferation and migration of human prostate androgen-independent cancer cells by an ABCA1-dependent mechanism. *Mol Cancer Res* **8**, 1284-1294
126. Lee, B. H., Taylor, M. G., Robinet, P., Smith, J. D., Schweitzer, J., Sehayek, E., Falzarano, S. M., Magi-Galluzzi, C., Klein, E. A., and Ting, A. H. (2013) Dysregulation of cholesterol homeostasis in human prostate cancer through loss of ABCA1. *Cancer Res* **73**, 1211-1218
127. Hajj, K. A., and Whitehead, K. A. (2017) Tools for translation: non-viral materials for therapeutic mRNA delivery. *Nat. Rev. Mater.* **2**
128. Gaj, T., Gersbach, C. A., and Barbas, C. F., 3rd. (2013) ZFN, TALEN, and CRISPR/Cas-based methods for genome engineering. *Trends Biotechnol* **31**, 397-405

129. Zhang, H. X., Zhang, Y., and Yin, H. (2019) Genome Editing with mRNA Encoding ZFN, TALEN, and Cas9. *Mol Ther* **27**, 735-746
130. Cong, L., Ran, F. A., Cox, D., Lin, S., Barretto, R., Habib, N., Hsu, P. D., Wu, X., Jiang, W., Marraffini, L. A., and Zhang, F. (2013) Multiplex genome engineering using CRISPR/Cas systems. *Science* **339**, 819-823
131. Makarova, K. S., Grishin, N. V., Shabalina, S. A., Wolf, Y. I., and Koonin, E. V. (2006) A putative RNA-interference-based immune system in prokaryotes: computational analysis of the predicted enzymatic machinery, functional analogies with eukaryotic RNAi, and hypothetical mechanisms of action. *Biol Direct* **1**, 7
132. Ishino, Y., Shinagawa, H., Makino, K., Amemura, M., and Nakata, A. (1987) Nucleotide sequence of the iap gene, responsible for alkaline phosphatase isozyme conversion in *Escherichia coli*, and identification of the gene product. *J Bacteriol* **169**, 5429-5433
133. Loureiro, A., and da Silva, G. J. (2019) CRISPR-Cas: Converting A Bacterial Defence Mechanism into A State-of-the-Art Genetic Manipulation Tool. *Antibiotics (Basel)* **8**
134. Makarova, K. S., Haft, D. H., Barrangou, R., Brouns, S. J., Charpentier, E., Horvath, P., Moineau, S., Mojica, F. J., Wolf, Y. I., Yakunin, A. F., van der Oost, J., and Koonin, E. V. (2011) Evolution and classification of the CRISPR-Cas systems. *Nat Rev Microbiol* **9**, 467-477
135. Wright, A. V., Nunez, J. K., and Doudna, J. A. (2016) Biology and Applications of CRISPR Systems: Harnessing Nature's Toolbox for Genome Engineering. *Cell* **164**, 29-44

136. Gleditzsch, D., Pausch, P., Muller-Esparza, H., Ozcan, A., Guo, X., Bange, G., and Randau, L. (2019) PAM identification by CRISPR-Cas effector complexes: diversified mechanisms and structures. *RNA Biol* **16**, 504-517
137. Deveau, H., Barrangou, R., Garneau, J. E., Labonte, J., Fremaux, C., Boyaval, P., Romero, D. A., Horvath, P., and Moineau, S. (2008) Phage response to CRISPR-encoded resistance in *Streptococcus thermophilus*. *J Bacteriol* **190**, 1390-1400
138. Mojica, F. J. M., Diez-Villasenor, C., Garcia-Martinez, J., and Almendros, C. (2009) Short motif sequences determine the targets of the prokaryotic CRISPR defence system. *Microbiology* **155**, 733-740
139. Makarova, K. S., Aravind, L., Wolf, Y. I., and Koonin, E. V. (2011) Unification of Cas protein families and a simple scenario for the origin and evolution of CRISPR-Cas systems. *Biol Direct* **6**, 38
140. Jinek, M., Chylinski, K., Fonfara, I., Hauer, M., Doudna, J. A., and Charpentier, E. (2012) A programmable dual-RNA-guided DNA endonuclease in adaptive bacterial immunity. *Science* **337**, 816-821
141. Sander, J. D., and Joung, J. K. (2014) CRISPR-Cas systems for editing, regulating and targeting genomes. *Nat Biotechnol* **32**, 347-355
142. Sternberg, S. H., Redding, S., Jinek, M., Greene, E. C., and Doudna, J. A. (2014) DNA interrogation by the CRISPR RNA-guided endonuclease Cas9. *Nature* **507**, 62-67
143. Anders, C., Niewoehner, O., Duerst, A., and Jinek, M. (2014) Structural basis of PAM-dependent target DNA recognition by the Cas9 endonuclease. *Nature* **513**, 569-573

144. Chang, H. H. Y., Pannunzio, N. R., Adachi, N., and Lieber, M. R. (2017) Non-homologous DNA end joining and alternative pathways to double-strand break repair. *Nat Rev Mol Cell Biol* **18**, 495-506
145. Popp, M. W., and Maquat, L. E. (2016) Leveraging Rules of Nonsense-Mediated mRNA Decay for Genome Engineering and Personalized Medicine. *Cell* **165**, 1319-1322
146. Song, J., Yang, D., Xu, J., Zhu, T., Chen, Y. E., and Zhang, J. (2016) RS-1 enhances CRISPR/Cas9- and TALEN-mediated knock-in efficiency. *Nat Commun* **7**, 10548
147. Li, G., Zhang, X., Zhong, C., Mo, J., Quan, R., Yang, J., Liu, D., Li, Z., Yang, H., and Wu, Z. (2017) Small molecules enhance CRISPR/Cas9-mediated homology-directed genome editing in primary cells. *Sci Rep* **7**, 8943
148. Yu, C., Liu, Y., Ma, T., Liu, K., Xu, S., Zhang, Y., Liu, H., La Russa, M., Xie, M., Ding, S., and Qi, L. S. (2015) Small molecules enhance CRISPR genome editing in pluripotent stem cells. *Cell Stem Cell* **16**, 142-147
149. Chavez, A., Tuttle, M., Pruitt, B. W., Ewen-Campen, B., Chari, R., Ter-Ovanesyan, D., Haque, S. J., Cecchi, R. J., Kowal, E. J. K., Buchthal, J., Housden, B. E., Perrimon, N., Collins, J. J., and Church, G. (2016) Comparison of Cas9 activators in multiple species. *Nat Methods* **13**, 563-567
150. Hammarsten, J., and Hogstedt, B. (2004) Clinical, haemodynamic, anthropometric, metabolic and insulin profile of men with high-stage and high-grade clinical prostate cancer. *Blood Press* **13**, 47-55
151. Jacobs, E. J., Stevens, V. L., Newton, C. C., and Gapstur, S. M. (2012) Plasma total, LDL, and HDL cholesterol and risk of aggressive prostate cancer in the

- Cancer Prevention Study II Nutrition Cohort. *Cancer Causes Control* **23**, 1289-1296
152. Martin, R. M., Vatten, L., Gunnell, D., Romundstad, P., and Nilsen, T. I. (2009) Components of the metabolic syndrome and risk of prostate cancer: the HUNT 2 cohort, Norway. *Cancer Causes Control* **20**, 1181-1192
153. Acton, S. L., Scherer, P. E., Lodish, H. F., and Krieger, M. (1994) Expression cloning of SR-BI, a CD36-related class B scavenger receptor. *J Biol Chem* **269**, 21003-21009
154. Calvo, D., and Vega, M. A. (1993) Identification, primary structure, and distribution of CLA-1, a novel member of the CD36/LIMP-II gene family. *J Biol Chem* **268**, 18929-18935
155. de la Llera-Moya, M., Rothblat, G. H., Connelly, M. A., Kellner-Weibel, G., Sakr, S. W., Phillips, M. C., and Williams, D. L. (1999) Scavenger receptor BI (SR-BI) mediates free cholesterol flux independently of HDL tethering to the cell surface. *J Lipid Res* **40**, 575-580
156. Langer, C., Gansz, B., Goepfert, C., Engel, T., Uehara, Y., von Dehn, G., Jansen, H., Assmann, G., and von Eckardstein, A. (2002) Testosterone up-regulates scavenger receptor BI and stimulates cholesterol efflux from macrophages. *Biochem Biophys Res Commun* **296**, 1051-1057
157. Tilly-Kiesi, M., Lichtenstein, A. H., Joven, J., Vilella, E., Cheung, M. C., Carrasco, W. V., Ordovas, J. M., Dolnikowski, G., and Schaefer, E. J. (1997) Impact of gender on the metabolism of apolipoprotein A-I in HDL subclasses LpAI and LpAI:All in older subjects. *Arterioscler Thromb Vasc Biol* **17**, 3513-3518
158. Wu, F. C., and von Eckardstein, A. (2003) Androgens and coronary artery disease. *Endocr Rev* **24**, 183-217

159. Li, K., Wong, D. K., Luk, F. S., Kim, R. Y., and Raffai, R. L. (2018) Isolation of Plasma Lipoproteins as a Source of Extracellular RNA. *Methods Mol Biol* **1740**, 139-153
160. Lowry, O. H., Rosebrough, N. J., Farr, A. L., and Randall, R. J. (1951) Protein measurement with the Folin phenol reagent. *J Biol Chem* **193**, 265-275
161. Haeussler, M., Schonig, K., Eckert, H., Eschstruth, A., Mianne, J., Renaud, J. B., Schneider-Maunoury, S., Shkumatava, A., Teboul, L., Kent, J., Joly, J. S., and Concordet, J. P. (2016) Evaluation of off-target and on-target scoring algorithms and integration into the guide RNA selection tool CRISPOR. *Genome Biol* **17**, 148
162. Robinet, P., Wang, Z., Hazen, S. L., and Smith, J. D. (2010) A simple and sensitive enzymatic method for cholesterol quantification in macrophages and foam cells. *J Lipid Res* **51**, 3364-3369
163. Goldman, M., Craft, B., Hastie, M., Repečka, K., McDade, F., Kamath, A., Banerjee, A., Luo, Y., Rogers, D., Brooks, A. N., Zhu, J., and Haussler, D. (2019) The UCSC Xena platform for public and private cancer genomics data visualization and interpretation. *bioRxiv*, 326470
164. Machiela, M. J., and Chanock, S. J. (2018) LDassoc: an online tool for interactively exploring genome-wide association study results and prioritizing variants for functional investigation. *Bioinformatics* **34**, 887-889
165. Pirro, M., Ricciuti, B., Rader, D. J., Catapano, A. L., Sahebkar, A., and Banach, M. (2018) High density lipoprotein cholesterol and cancer: Marker or causative? *Prog Lipid Res* **71**, 54-69
166. Bull, C. J., Bonilla, C., Holly, J. M., Perks, C. M., Davies, N., Haycock, P., Yu, O. H., Richards, J. B., Eeles, R., Easton, D., Kote-Jarai, Z., Amin Al Olama, A.,

- Benlloch, S., Muir, K., Giles, G. G., MacInnis, R. J., Wiklund, F., Gronberg, H., Haiman, C. A., Schleutker, J., Nordestgaard, B. G., Travis, R. C., Neal, D., Pashayan, N., Khaw, K. T., Stanford, J. L., Blot, W. J., Thibodeau, S., Maier, C., Kibel, A. S., Cybulski, C., Cannon-Albright, L., Brenner, H., Park, J., Kaneva, R., Batra, J., Teixeira, M. R., Micheal, A., Pandha, H., Smith, G. D., Lewis, S. J., Martin, R. M., and consortium, P. (2016) Blood lipids and prostate cancer: a Mendelian randomization analysis. *Cancer Med* **5**, 1125-1136
167. Sivaprasad, U., Abbas, T., and Dutta, A. (2006) Differential efficacy of 3-hydroxy-3-methylglutaryl CoA reductase inhibitors on the cell cycle of prostate cancer cells. *Mol Cancer Ther* **5**, 2310-2316
168. Meng, Y., Liao, Y. B., Xu, P., Wei, W. R., and Wang, J. (2016) Statin use and mortality of patients with prostate cancer: a meta-analysis. *Onco Targets Ther* **9**, 1689-1696
169. Murtola, T. J., Peltomaa, A. I., Talala, K., Maattanen, L., Taari, K., Tammela, T. L. J., and Auvinen, A. (2017) Statin Use and Prostate Cancer Survival in the Finnish Randomized Study of Screening for Prostate Cancer. *Eur Urol Focus* **3**, 212-220
170. Raval, A. D., Thakker, D., Negi, H., Vyas, A., Kaur, H., and Salkini, M. W. (2016) Association between statins and clinical outcomes among men with prostate cancer: a systematic review and meta-analysis. *Prostate Cancer Prostatic Dis* **19**, 151-162
171. Tan, P., Zhang, C., Wei, S. Y., Tang, Z., Gao, L., Yang, L., and Wei, Q. (2017) Effect of statins type on incident prostate cancer risk: a meta-analysis and systematic review. *Asian J Androl* **19**, 666-671

172. Jafri, H., Alsheikh-Ali, A. A., and Karas, R. H. (2010) Baseline and on-treatment high-density lipoprotein cholesterol and the risk of cancer in randomized controlled trials of lipid-altering therapy. *J Am Coll Cardiol* **55**, 2846-2854
173. Zamanian-Daryoush, M., Lindner, D. J., DiDonato, J. A., Wagner, M., Buffa, J., Rayman, P., Parks, J. S., Westerterp, M., Tall, A. R., and Hazen, S. L. (2017) Myeloid-specific genetic ablation of ATP-binding cassette transporter ABCA1 is protective against cancer. *Oncotarget* **8**, 71965-71980
174. Kim, J., Thompson, B., Han, S., Lotan, Y., McDonald, J. G., and Ye, J. (2019) Uptake of HDL-cholesterol contributes to lipid accumulation in clear cell renal cell carcinoma. *Biochim Biophys Acta Mol Cell Biol Lipids* **1864**, 158525
175. Dillard, P. R., Lin, M. F., and Khan, S. A. (2008) Androgen-independent prostate cancer cells acquire the complete steroidogenic potential of synthesizing testosterone from cholesterol. *Mol Cell Endocrinol* **295**, 115-120
176. Petryszak, R., Keays, M., Tang, Y. A., Fonseca, N. A., Barrera, E., Burdett, T., Fullgrabe, A., Fuentes, A. M., Jupp, S., Koskinen, S., Mannion, O., Huerta, L., Megy, K., Snow, C., Williams, E., Barzine, M., Hastings, E., Weisser, H., Wright, J., Jaiswal, P., Huber, W., Choudhary, J., Parkinson, H. E., and Brazma, A. (2016) Expression Atlas update--an integrated database of gene and protein expression in humans, animals and plants. *Nucleic Acids Res* **44**, D746-752
177. Plump, A. S., Erickson, S. K., Weng, W., Partin, J. S., Breslow, J. L., and Williams, D. L. (1996) Apolipoprotein A-I is required for cholesteryl ester accumulation in steroidogenic cells and for normal adrenal steroid production. *J Clin Invest* **97**, 2660-2671

178. Machida, T., Yonezawa, Y., and Noumura, T. (1981) Age-associated changes in plasma testosterone levels in male mice and their relation to social dominance or subordination. *Horm Behav* **15**, 238-245
179. Williamson, C. M., Lee, W., Romeo, R. D., and Curley, J. P. (2017) Social context-dependent relationships between mouse dominance rank and plasma hormone levels. *Physiol Behav* **171**, 110-119
180. Witt, W., Kolleck, I., Fechner, H., Sinha, P., and Rustow, B. (2000) Regulation by vitamin E of the scavenger receptor BI in rat liver and HepG2 cells. *J Lipid Res* **41**, 2009-2016
181. Siegel, R. L., Miller, K. D., and Jemal, A. (2020) Cancer statistics, 2020. *CA Cancer J Clin* **70**, 7-30
182. Shuch, B., Amin, A., Armstrong, A. J., Eble, J. N., Ficarra, V., Lopez-Beltran, A., Martignoni, G., Rini, B. I., and Kutikov, A. (2015) Understanding pathologic variants of renal cell carcinoma: distilling therapeutic opportunities from biologic complexity. *Eur Urol* **67**, 85-97
183. Sundelin, J. P., Stahlman, M., Lundqvist, A., Levin, M., Parini, P., Johansson, M. E., and Boren, J. (2012) Increased expression of the very low-density lipoprotein receptor mediates lipid accumulation in clear-cell renal cell carcinoma. *PLoS One* **7**, e48694
184. Concordet, J. P., and Haeussler, M. (2018) CRISPOR: intuitive guide selection for CRISPR/Cas9 genome editing experiments and screens. *Nucleic Acids Res* **46**, W242-W245
185. Robinet, P., Ritchey, B., Alzayed, A. M., DeGeorgia, S., Schodowski, E., Lorkowski, S. W., and Smith, J. D. (2019) QTL analysis of macrophages from an

AKR/JxDBA/2J intercross identified the *Gpnmb* gene as a modifier of lysosome function. *bioRxiv*

186. Barquera, S., Pedroza-Tobias, A., Medina, C., Hernandez-Barrera, L., Bibbins-Domingo, K., Lozano, R., and Moran, A. E. (2015) Global Overview of the Epidemiology of Atherosclerotic Cardiovascular Disease. *Arch Med Res* **46**, 328-338
187. Moore, K. J., Sheedy, F. J., and Fisher, E. A. (2013) Macrophages in atherosclerosis: a dynamic balance. *Nat Rev Immunol* **13**, 709-721
188. Singh, R., Kaushik, S., Wang, Y., Xiang, Y., Novak, I., Komatsu, M., Tanaka, K., Cuervo, A. M., and Czaja, M. J. (2009) Autophagy regulates lipid metabolism. *Nature* **458**, 1131-1135
189. Ouimet, M., Franklin, V., Mak, E., Liao, X., Tabas, I., and Marcel, Y. L. (2011) Autophagy regulates cholesterol efflux from macrophage foam cells via lysosomal acid lipase. *Cell Metab* **13**, 655-667
190. Smith, J. D., James, D., Dansky, H. M., Wittkowski, K. M., Moore, K. J., and Breslow, J. L. (2003) In silico quantitative trait locus map for atherosclerosis susceptibility in apolipoprotein E-deficient mice. *Arterioscler Thromb Vasc Biol* **23**, 117-122
191. Robinet, P., Ritchey, B., and Smith, J. D. (2013) Physiological difference in autophagic flux in macrophages from 2 mouse strains regulates cholesterol ester metabolism. *Arterioscler Thromb Vasc Biol* **33**, 903-910
192. Hai, Q., Ritchey, B., Robinet, P., Alzayed, A. M., Brubaker, G., Zhang, J., and Smith, J. D. (2018) Quantitative Trait Locus Mapping of Macrophage Cholesterol Metabolism and CRISPR/Cas9 Editing Implicate an ACAT1 Truncation as a Causal Modifier Variant. *Arterioscler Thromb Vasc Biol* **38**, 83-91

193. Wang, S., Gulshan, K., Brubaker, G., Hazen, S. L., and Smith, J. D. (2013) ABCA1 mediates unfolding of apolipoprotein AI N terminus on the cell surface before lipidation and release of nascent high-density lipoprotein. *Arterioscler Thromb Vasc Biol* **33**, 1197-1205
194. Semenas, J., Hedblom, A., Miftakhova, R. R., Sarwar, M., Larsson, R., Shcherbina, L., Johansson, M. E., Harkonen, P., Sterner, O., and Persson, J. L. (2014) The role of PI3K/AKT-related PIP5K1alpha and the discovery of its selective inhibitor for treatment of advanced prostate cancer. *Proc Natl Acad Sci U S A* **111**, E3689-3698
195. Guo, D., Reinitz, F., Youssef, M., Hong, C., Nathanson, D., Akhavan, D., Kuga, D., Amzajerdi, A. N., Soto, H., Zhu, S., Babic, I., Tanaka, K., Dang, J., Iwanami, A., Gini, B., Dejesus, J., Lisiero, D. D., Huang, T. T., Prins, R. M., Wen, P. Y., Robins, H. I., Prados, M. D., Deangelis, L. M., Mellinshoff, I. K., Mehta, M. P., James, C. D., Chakravarti, A., Cloughesy, T. F., Tontonoz, P., and Mischel, P. S. (2011) An LXR agonist promotes glioblastoma cell death through inhibition of an EGFR/AKT/SREBP-1/LDLR-dependent pathway. *Cancer Discov* **1**, 442-456
196. Hassan, T. S., Paniccia, A., Russo, V., and Steffensen, K. R. (2015) LXR Inhibits Proliferation of Human Breast Cancer Cells through the PI3K-Akt Pathway. *Nuclear Receptor Research* **2**
197. Smith, B., and Land, H. (2012) Anticancer activity of the cholesterol exporter ABCA1 gene. *Cell Rep* **2**, 580-590
198. Zhang, H., Lamon, B. D., Moran, G., Sun, T., Gotto, A. M., Jr., and Hajjar, D. P. (2016) Pitavastatin Differentially Modulates MicroRNA-Associated Cholesterol Transport Proteins in Macrophages. *PLoS One* **11**, e0159130

199. Han, J., Parsons, M., Zhou, X., Nicholson, A. C., Gotto, A. M., Jr., and Hajjar, D. P. (2004) Functional interplay between the macrophage scavenger receptor class B type I and pitavastatin (NK-104). *Circulation* **110**, 3472-3479
200. Kimura, T., Mogi, C., Tomura, H., Kuwabara, A., Im, D. S., Sato, K., Kurose, H., Murakami, M., and Okajima, F. (2008) Induction of scavenger receptor class B type I is critical for simvastatin enhancement of high-density lipoprotein-induced anti-inflammatory actions in endothelial cells. *J Immunol* **181**, 7332-7340
201. Kregel, S., Chen, J. L., Tom, W., Krishnan, V., Kach, J., Brechka, H., Fessenden, T. B., Isikbay, M., Paner, G. P., Szmulewitz, R. Z., and Vander Griend, D. J. (2016) Acquired resistance to the second-generation androgen receptor antagonist enzalutamide in castration-resistant prostate cancer. *Oncotarget* **7**, 26259-26274
202. Liang, Z., Zhu, J., Chen, L., Xu, Y., Yang, Y., Hu, R., Zhang, W., Song, Y., Lu, Y., Ou, N., and Liu, X. (2019) Is Androgen Deprivation Therapy for Prostate Cancer Associated with Cardiovascular disease ? A Meta-Analysis and systematic review. *Andrology*
203. Margel, D., Peer, A., Ber, Y., Shavit-Grievink, L., Tabachnik, T., Sela, S., Witberg, G., Baniel, J., Kedar, D., Duivenvoorden, W. C. M., Rosenbaum, E., and Pinthus, J. H. (2019) Cardiovascular Morbidity in a Randomized Trial Comparing GnRH Agonist and GnRH Antagonist among Patients with Advanced Prostate Cancer and Preexisting Cardiovascular Disease. *J Urol* **202**, 1199-1208
204. Moustsen, I. R., Larsen, S. B., Duun-Henriksen, A. K., Tjonneland, A., Kjaer, S. K., Brasso, K., Johansen, C., and Dalton, S. O. (2019) Risk of cardiovascular events in men treated for prostate cancer compared with prostate cancer-free men. *Br J Cancer* **120**, 1067-1074

205. Tsao, P. A., Estes, J. P., Griggs, J. J., Smith, D. C., and Caram, M. E. V. (2019) Cardiovascular and Metabolic Toxicity of Abiraterone in Castration-resistant Prostate Cancer: Post-marketing Experience. *Clin Genitourin Cancer* **17**, e592-e601